

بِسْمِ اللَّهِ الرَّحْمَنِ الرَّحِيمِ

In the Name of Allah (God), Most Gracious, Most Merciful

**Modeling of Phase Equilibria
Containing Associating Fluids**

Samer Omar Derawi

Ph.D. Dissertation, July 2002

Centre for Phase Equilibria and Separation Processes (IVC-SEP)

Department of Chemical Engineering

Technical University of Denmark

DK-2800 Lyngby, Denmark

Copyright © Samer O. Derawi, 2002

Printed by Book Partner, Nørhaven Digital, Copenhagen, Denmark

ISBN 87-90142-86-1

Preface

This thesis is submitted in partial fulfilment of the requirements for the Ph.D. degree at the Technical University of Denmark (Danmarks Tekniske Universitet).

This work has been conducted at the Department of Chemical Engineering (Institut for Kemiteknik) from May 1999 to June 2002 under the supervision of professor Erling H. Stenby and associate professor Georgios M. Kontogeorgis.

The project has been financed by grants from the Centre for Phase Equilibria and Separation Processes (IVC-SEP), the Statoil Research Centre in Trondheim (Norway), and the Nordic Energy Research Fund. The author gratefully acknowledges their financial support.

I would like to thank professor Stenby for providing me the opportunity to work with such a scientifically interesting and challenging project in the IVC-SEP group, and would like to express my sincere gratitude for his help and guidance throughout this project. Special and countless thanks go to professor Kontogeorgis for his continuous help and support, his inspiring discussions, and his huge enthusiasm during the time we worked together. Also in this regard, I would like to thank professor Michael Michelsen for his contribution and suggestions in the CPA-part of the project. Additionally, I greatly appreciate the help from professors Peter Rasmussen and Jørgen Møllerup for their suggestions and fruitful discussions. Dr. Henk Meijer and Dr. Eric Hendriks from Shell are acknowledged for their help and useful discussions. I would like to thank Dr. Arne Fredheim and Dr. Per Grini for making my stay in Trondheim very pleasant and provided me with any help needed. Also I would like thank all the colleagues as well as friends in the IVC-SEP group for the nice time we had together. My gratitude and appreciation go also to Mrs. Annelise Kofod and Mrs. Anne Louise Biede for being very supportive and helpful with the administrative work.

Last -but definitely not least- I would like to express my deepest gratitude to my beloved family, especially my father and my mother, for their endless moral support, patience and understanding.

Kongens Lyngby, July 2002

Samer Omar Derawi
(Author)

Contents

Preface	i
Synopsis	vii
Dansk Resumé	ix
1 THESIS BACKGROUND	1
2 APPLICATION OF GROUP-CONTRIBUTION MODELS TO THE CALCULATION OF OCTANOL-WATER PARTITION COEFFICIENT	3
2.1 INTRODUCTION	3
2.2 BACKGROUND.....	5
2.3 GROUP CONTRIBUTION MODELS FOR ESTIMATING P_{ow}	8
2.3.1 UNIFAC Models.....	8
2.3.2 The AFC Correlation Model.....	11
2.4 RESULTS AND DISCUSSION.....	12
2.4.1 Data Base	12
2.4.2 The Partitioning of Hydrocarbons.....	20
2.4.3 The Partitioning of Oxygenated Compounds.....	20
2.4.4 The Partitioning of Amines, Aromatics, and Complex Compounds.....	21
2.4.5 Summary.....	22
2.5 CONCLUSIONS.....	23
References.....	24
3 LIQUID-LIQUID EQUILIBRIA FOR GLYCOLS + HYDROCARBONS: DATA AND CORRELATION	27
3.1 INTRODUCTION	27
3.2 EXPERIMENTAL SECTION	29
3.2.1 Chemicals.....	29
3.2.2 Experimental Procedure.....	29
3.2.3 Sampling and Analysis.....	30
3.3 RESULTS AND DATA CORRELATION.....	34
3.3.1 Experimental Results.....	34

3.3.2	<i>Data Correlation</i>	36
3.4	CONCLUSIONS	41
	<i>References</i>	42
4	APPLICATION OF THE CPA EQUATION OF STATE TO GLYCOL-HYDROCARBONS LIQUID-LIQUID EQUILIBRIA	43
4.1	INTRODUCTION	43
4.2	THE CPA EQUATION OF STATE - MODEL DESCRIPTION	44
4.3	DATABASE USED IN THE PARAMETER ESTIMATION	48
4.4	CORRELATION OF LLE - CHOICE OF THE ASSOCIATION SCHEME FOR GLYCOLS	53
4.5	CORRELATION OF LLE FOR GLYCOL - HYDROCARBON SYSTEMS	60
4.5.1	<i>The Case of Tetraethylene Glycol (Tetra-EG)</i>	65
4.6	COMPARISON OF THE SRK AND CPA EQUATIONS OF STATE	70
4.6.1	<i>Results</i>	71
4.6.2	<i>An "Alternative" Approach</i>	72
4.7	TEMPERATURE EXTRAPOLATION CAPABILITIES OF CPA	73
4.8	CONCLUSIONS	76
	<i>References</i>	77
5	EXTENSION OF THE CPA EQUATION OF STATE TO GLYCOL-WATER CROSS-ASSOCIATING SYSTEMS	79
5.1	INTRODUCTION	79
5.2	EXTENSION OF CPA TO CROSS-ASSOCIATING SYSTEMS	82
5.3	RESULTS AND DISCUSSION.....	85
5.4	APPLICATION OF CPA TO MULTICOMPONENT ASSOCIATING SYSTEMS.....	94
5.5	CONCLUSIONS	99
	<i>References</i>	100
6	CONCLUSIONS AND RECOMMENDATIONS FOR FUTURE WORK	103
	LIST OF SYMBOLS	107

Appendices

A	DERIVATION OF THE PRESSURE AND CHEMICAL POTENTIAL FROM THE ASSOCIATION HELMHOLTZ ENERGY BASED ON WERTHEIM'S PERTURBATION THEORY	113
B	A THEORETICAL JUSTIFICATION FOR THE CR-1 COMBINING RULE OF CPA	119

Synopsis

In recent years, there has been an increasing interest of the petrochemical industry in modeling of the partitioning of production chemicals e.g. gas hydrate inhibitors, corrosion inhibitors, solvents etc. between the crude oil and water. This requires basically a thermodynamic model either in terms of an activity coefficient model or an equation of state. Our target in this thesis is to review and develop such models capable of describing qualitatively as well as quantitatively phase equilibria in multicomponent multiphase systems containing non-polar, polar, and associating compounds. The background and main targets for this thesis are presented in Chapter 1.

In Chapter 2, a comprehensive review of the application of group contribution (GC) models such as various forms of UNIFAC and the so-called AFC (Atom and Fragment Contributions) correlation model for P_{ow} (octanol-water partition coefficient) calculations has been carried out. UNIFAC is an activity coefficient model while AFC is a model specifically developed for P_{ow} calculations. Five different versions of UNIFAC and the AFC correlation model have been compared with each other and with experimental data. The range of applicability of the GC models to P_{ow} is discussed, and general conclusions are obtained. A thorough analysis of the models was conducted including residual plots and numerical and graphical comparisons. We conclude that the group-contribution concept has possibly exhausted its applicability to account for highly asymmetric systems, especially for aqueous solutions with complex poly-functional chemicals.

In Chapter 3, liquid-liquid equilibrium data for 7 binary glycol-hydrocarbon systems have been measured in the temperature range 32 °C to 80 °C and pressure equal to 1 bar. The measured systems are monoethylene glycol + heptane, methylcyclohexane, hexane, propylene glycol + heptane, diethylene glycol + heptane, triethylene glycol + heptane, and tetraethylene glycol + heptane. The data obtained were correlated with the NRTL model and two different versions of the UNIQUAC equation. The NRTL model and one of the UNIQUAC equations (UQ 4) have a linear temperature-dependent interaction parameter term, while the other UNIQUAC equation (UQ 2) has an interaction parameter that is independent of the temperature. There was a fairly good agreement between the experimental data and the two temperature dependent models

with an average deviation in the composition for both phases of 3 % for both NRTL and UQ 4 while deviation is 15 % for UQ 2. These results indicate the necessity of using the linearly dependent interaction parameters.

The CPA equation of state is a thermodynamic model, which combines the well-known cubic SRK equation of state and the association term proposed by Wertheim, typically employed in models like the various variations of SAFT. CPA has been shown in the past to be a successful model for phase equilibria calculations for systems containing water, hydrocarbons and alcohols.

In Chapter 4, CPA is applied for the first time to liquid-liquid equilibria for systems containing glycols and hydrocarbons. It is shown that excellent correlation is achieved with solely a single interaction parameter per binary system. The correlation procedure as well as the nature of the experimental data play a crucial role in the parameter estimation and they are thus extensively discussed.

In Chapter 5, the application of the CPA equation of state is extended to mixtures containing cross-associating compounds such as glycols and water. In this case, combining rules are required in the association term of CPA for the cross-association energy and volume parameters. Different types of such combining rules have been suggested over the past years for association models such as SAFT.

These are tested in this work for CPA in terms of their correlation and prediction capabilities for vapor-liquid equilibria of glycol-water systems. Comparisons with SRK are also provided.

It was found, that the arithmetic mean combining rule for the cross-association energy parameter and the geometric mean for the cross-association volume parameter provide overall the best results for cross-associating systems containing glycols and water. Moreover, preliminary results show that the CPA model can be used to predict multi-component, multiphase equilibria for glycol/water/hydrocarbon mixtures based solely on binary interaction parameters.

In Chapter 6, conclusions and suggestions for future work are presented.

Dansk Resumé

Der har i den senere tid været en stigende interesse i den petrokemiske industri for at modellere fordelingen af produktionskemikalier, som f.eks. gashydratinhibitorer, korrosionsinhibitorer, opløsningsmidler osv. mellem råolie og vand.

Grundlæggende kræver dette en termodynamisk model enten i form af en aktivitetskoefficientmodel eller en tilstandsligning. Vort mål i denne afhandling er at gennemgå og udvikle sådanne modeller som gør det muligt at beskrive kvalitativt såvel som kvantitativt fase-ligevægte for multikomponent, multifase systemer indeholdende ikke-polære, polære, og associerende komponenter.

I kapitel 1 præsenteres baggrunden og hovedformålet med denne afhandling.

I kapitel 2 udføres en omfattende gennemgang af anvendelsen af gruppebidragsmodeller såsom adskillige UNIFAC versioner samt den såkaldte AFC (forkortelse af: Atom og Fragment Bidrag) korrelationsmodel til P_{ow} (oktanol-vand fordelingskoefficient) beregninger. UNIFAC er en aktivitetskoefficientmodel, medens AFC er en model der specifikt er udviklet til P_{ow} beregning. Fem forskellige udgaver af UNIFAC samt AFC korrelationsmodellen sammenlignes med hinanden og med eksperimentelle data. Omfanget af gruppebidragsmodellernes anvendelighed til P_{ow} forudsigelse diskuteres og der drages generelle konklusioner. Der udføres en grundig analyse af modellerne som indbefatter *residual plot* samt numeriske og grafiske sammenligninger. Det konkluderes, at gruppebidragsbegrebet muligvis ikke er helt egnet til at beskrive stærkt asymmetriske blandinger og specielt vandige opløsninger indeholdende komplekse multifunktionelle kemikalier.

I kapitel 3 diskuteres eksperimentelle målinger af væske-væske ligevægtsdata for 7 binære glykol-kulbrinte blandinger i temperaturområdet 32 °C til 80 °C og med et tryk svarende til 1 bar. De målte systemer er monoethylenglykol + heptan, methylcyclohexan + hexan, propylenglykol + heptan, diethylenglykol + heptan, triethylenglykol + heptan samt tetraethylenglykol + heptan. De opnåede eksperimentelle data blev korreleret med NRTL modellen samt to forskellige udgaver af UNIQUAC ligningen. NRTL modellen samt en af UNIQUAC ligningen (UQ 4) har et lineært temperaturafhængigt interaktionsparameterled, medens den anden UNIQUAC ligning (UQ 2) har et interaktionsparameterled der er temperaturafhængigt. Der var en ganske

god overensstemmelse mellem de eksperimentelle data og de 2 temperaturnafhængige modeller med en afvigelse i sammensætningen i begge faser på 3 % for både NRTL og UQ 4, hvorimod afvigelsen er på 15 % for UQ 2. Disse resultater viser nødvendigheden af temperaturnafhængigheden i modellerne.

CPA tilstandsligningen er en termodynamisk model som kombinerer den velkendte kubiske SRK tilstandsligning med et associationsled foreslået af Wertheim. Dette associationsled er typisk anvendt i de forskellige versioner af SAFT. CPA har vist sig at være en vellykket model for fase-ligevægtsberegninger for blandinger indeholdende vand, kulbrinter og alkoholer.

I kapitel 4 anvendes CPA for første gang til væske-væske ligevægtsberegninger for binære blandinger indeholdende glykoler og kulbrinter. Det vises, at man kan opnå en udmærket korrelation med kun en enkel interaktionsparameter for hvert binært system. Det vises, at korrelationsproceduren såvel som kvaliteten af de eksperimentelle data spiller en afgørende rolle i parameterestimeringsmetoden og er derfor grundigt diskuteret.

I kapitel 5 er anvendelsen af CPA tilstandsligningen blevet udvidet til blandinger som indeholder krydsassocierende komponenter såsom glykoler og vand.

I dette tilfælde har man brug for kombinationsregler i associationsleddet af CPA tilstandsligningen for krydsassociations- energi og volumen parametrene. Forskellige typer af kombinationsregler har været foreslået igennem de sidste år for associationsmodeller såsom SAFT.

Disse er afprøvet i dette arbejde for CPA modellen i form af deres korrelations- og forudsigelsesevne for damp-væske ligevægtsberegninger for glykoler-vand blandinger. Sammenligninger med SRK er også inkluderet.

Det vises, at den aritmetiske kombinationsregel for krydsassociationsenergi parameteren samt den geometriske for krydsassociationsvolumen parameteren overordnet giver de bedste resultater for krydsassocierende blandinger indeholdende glykoler og vand. Ydermere viser indledende resultater at CPA modellen kan anvendes til at forudsige multikomponent, multifase-ligevægte for glykol/vand/kulbrinter systemer udelukkende baseret på binære interaktionsparametre.

I kapitel 6 er konklusioner og forslag for fremtidigt arbejde præsenteret.

Chapter 1

Thesis Background

For the last 25 years, the group contribution (GC) concept has been successfully applied to non-polar as well as to polar systems mainly encountered in the petroleum and chemical industry. Thermodynamic models such as UNIFAC (an activity coefficient model) and the van der Waals type equations of state have been adequate for such systems. In the recent years, however, much interest from the petrochemical industry concerns aqueous solutions and mixtures containing associating and inert (non-associating) compounds. This has emphasized the importance for the development of new thermodynamic models, which could predict satisfactorily the phase equilibria for such systems. Unlike the conventional models such as cubic equations of state and UNIFAC, these novel models should take into account the ‘chemical’ association effect, preferably explicitly.

A particular application is the partitioning of production chemicals such as gas hydrate inhibitors and several types of additives between an organic phase and water at various operation conditions. As a first step, the calculation of the so-called octanol-water partition coefficient, P_{ow} is of importance. P_{ow} can be defined (under some plausible assumptions) as:

$$P_{ow} = 0.151 \times \frac{\gamma_i^{w,\infty}}{\gamma_i^{o,\infty}}$$

where $\gamma_i^{w,\infty}$ and $\gamma_i^{o,\infty}$ are the infinite dilution activity coefficients in the water and octanol phases, respectively.

In the first part of this thesis, the purpose of our work is to employ and compare the performance of various modifications of UNIFAC and the empirical AFC model for octanol-water partition coefficient calculations. Such asymmetric aqueous solutions may be considered to be a very strict test for group contribution models such as UNIFAC, since the model’s interaction parameters are determined from experimental VLE & LLE data at finite concentrations.

Problems are encountered for specific chemicals, which only partly could be attributed to experimental data. Thus, we believe that the group contribution models of this type may have possibly reached their limit for highly asymmetric systems, and in particular aqueous solutions with multi-functional associating chemicals. New thermodynamic concepts and models are thus necessary for obtaining quantitatively correct predictions. Equations of state such as the Peng-Robinson (PR) and Soave-Redlich-Kwong (SRK) EoS have mainly been used for hydrocarbon mixtures, where the association effect has been neglected. Therefore, a new equation of state, the CPA (Cubic-Plus-Association) model, has recently been developed, where the physical term has been taken from SRK EoS and the association term from SAFT which is based on Wertheim's first order perturbation theory.

The CPA EoS was developed in 1996, and since then it has been applied to VLE and LLE calculations for mixtures of hydrocarbons with alcohols and water. Excellent results were obtained from the new model at various conditions including partition of methanol between water and hydrocarbons. In the second part of this thesis, the application of the CPA EoS is extended to glycols and glycol-ethers, which are relevant for the chemical and the petroleum industry. In order to use the CPA EoS to such systems, we must understand the association of these new compounds with each other (self-association) and with other associating compounds (cross-association).

Chapter 2

Application of Group-Contribution Models to the Calculation of Octanol-Water Partition Coefficient

A comprehensive review of the application of group contribution (GC) models such as various forms of UNIFAC and the AFC correlation model for P_{ow} (octanol-water partition coefficient) calculations has been carried out. UNIFAC is an activity coefficient model while AFC is a model specific for P_{ow} calculations. Five different versions of UNIFAC and the AFC correlation model have been compared to each other and to experimental data. The range of applicability of the GC models to P_{ow} is discussed, and general conclusions are obtained. A thorough analysis of the models was conducted including residual plots and numerical and graphical comparisons. We conclude that the group-contribution concept has possibly exhausted its applicability to account for highly asymmetric systems, especially aqueous solutions with complex poly-functional chemicals.

2.1 Introduction

An adequate thermodynamic model describing the chemical and physical nature of aqueous liquid mixtures at infinite dilution is necessary in the chemical industry for the design of separation processes. Such processes involve various applications e.g. modelling of waste and product streams, gas hydrate inhibition and glycol regeneration units as well as special applications such as the use of alcohols as additives in gasoline. In the recent years, there is an increasing interest of the petrochemical industry in the modelling of the partitioning of production chemicals between the crude oil and water. These production chemicals consist of low-molecular weight compounds, which are well defined in structure and high-molecular weight complex molecules such as

inhibitors or antifoaming agents with polyfunctional groups and which are less well defined mixtures. A common characteristic for these production chemicals is that they are very diluted in both phases.

Our target in this work was to apply and investigate the applicability of existing models based on the quasi-chemical theory and the GC concept for aqueous solutions at infinite dilution. In particular, we were interested in the calculation of the octanol-water partition coefficient which is a very important physical property for both industrial and other (environmental, pharmaceutical) applications. This is shown by the extensive amount of octanol-water (P_{ow}) data available in the literature.¹ P_{ow} is defined as:

$$P_{ow} = \frac{C_i^o}{C_i^w} \quad (2.1)$$

where C_i^o and C_i^w are the concentrations of solute i in the octanol phase (o) and the water phase (w), respectively. The unit of the concentration is mol/L or mol/cm³. The concentration variables can be readily converted to activity coefficients so that application of a thermodynamic model is feasible for P_{ow} estimation. Equation (2.1) can therefore be rewritten as²:

$$P_{ow} = 0.151 \times \frac{\gamma_i^{w,\infty}}{\gamma_i^{o,\infty}} \quad (2.2)$$

where $\gamma_i^{w,\infty}$ and $\gamma_i^{o,\infty}$ are the infinite dilution activity coefficients at infinite dilution in the water and octanol phases, respectively. The coefficient in Eq. (2.2) (0.151) and the calculation of the activity coefficients in the octanol phase have been carried out in this work at 25°C. We have assumed that the solubility of water in octanol is 27.5 mole percent, as reported by Apleblat.³ The water phase is assumed to be pure water due to insignificant solubility of octanol in water. Several authors have investigated the solubility of water in 1-octanol and the values are only in moderate agreement with each other ranging from 20.7 to 27.5 mole percent. The majority of the values are close to 27.5 mole percent. The purity of the 1-octanol on which Apleblat³ based his measurement is over 99%.

Up to 15000 experimental P_{ow} data are estimated to be available. The reason for such an abundance of P_{ow} data is due to its extensive use and its adoption by many international

and governmental agencies as a physical property of organic pollutants which is directly related to the uptake in tissue and fat of living species and thus a potential toxicity.

The phase behaviour of multicomponent aqueous systems is, especially in the presence of poly-functional organic chemicals, particularly complex. State of the art models for calculating phase equilibria are the so-called association equations of state such as SAFT and CPA.⁴⁻⁷ These equations are shown to predict satisfactorily multicomponent behaviour based on binary data; however as yet they are not predictive and thus they cannot be generally applied. Moreover, the association scheme of many chemicals of importance to practical applications, e.g. glycols, glycolethers, amines etc., is yet to be determined. For this reason, we presently focused our research on predictive simplified GC models such as the UNIFAC and the AFC correlation model. Association models will be investigated in the next chapters.

The purpose of this work was to establish the optimal GC model(s) with regard to the prediction of the octanol-water partition coefficient for both mono-functional and poly-functional molecules. A critical evaluation and comparison of the GC models is carried out using statistical methods and an extensive database.

2.2 Background

Group-contribution (GC) models have been extensively used for phase equilibrium calculations for the last 25 years. However, there have been attempts to apply GC models such as UNIFAC^{8,9} and ASOG¹⁰ for the calculation of the octanol-water partition coefficient.¹¹⁻¹³ These interesting works are however limited to the original UNIFAC model applied only to some environmentally important compounds. Our work mainly focuses on production chemicals of importance to the oil and petroleum industry.

The applicability of group-contribution models for highly polar and asymmetric systems, in particular aqueous solutions, is rather suspicious for several reasons: The UNIFAC expression for the activity coefficient does not explicitly take into account the association effect (hydrogen-bonding) present in such solutions. Moreover, the group interaction parameters in most cases are based on phase equilibrium (VLE & LLE) data at finite concentrations. However, the UNIFAC concept is under continuous

development. Several new versions of UNIFAC have been proposed the last years for complex phase equilibria, including versions specific for estimating γ^∞ and P_{ow} .^{2,14,15} Thus, a comprehensive analysis of all these models is necessary so that the practical user employs the best model for each situation.

A critical evaluation of several UNIFAC-type models in predicting the activity coefficient at infinite dilution in aqueous solutions has been recently reported.^{16,17} The conclusions from these evaluations can be used for reference purposes in conjunction with our results in this work for P_{ow} . This is because, as observed from Eq. (2.2), the model which best predicts $\gamma_i^{\infty,w}$, is expected to perform best also for P_{ow} . Nevertheless, $\gamma_i^{\infty,w}$ studies are only indirect tests for P_{ow} performance.

Recently, a comparison between four UNIFAC-type models has been carried out directly for P_{ow} .¹⁸ The UNIFAC models have been applied to the prediction of the partition coefficient of approximately 140 mono-functional molecules and some biochemicals between octanol and water. Another interesting recent development is the so-called KOW UNIFAC, which was targeted specifically for the estimation of octanol-water partition coefficients.¹⁵ The KOW UNIFAC is distinguished from other GC models in the sense that the group interaction parameters are entirely based on P_{ow} and γ_i^∞ data. However, the resulting group table is rather limited. Thus, until now KOW UNIFAC has limited application to some environmentally significant compounds.

The group-contribution concept was not originally designed to predict phase equilibria for hydrogen-bonded systems such as those often encountered in calculations of the octanol-water partition coefficient. Numerous empirical correlation methods specifically designed for P_{ow} have been proposed; the methods of Leo & Hansch¹⁹, Rekker²⁰, the AFC correlation model²¹, and the method of Suzuki & Kudo²² are among the most well known. Like UNIFAC, these methods are also based on the fragment or group contribution concept as well; in that sense they are similar to UNIFAC. The fragment contributions to the whole molecule are obtained from experimental P_{ow} data. Unlike UNIFAC, these specific correlations are capable of distinguishing between isomers and also can take into account, to some extent, the proximity and the intramolecular effects.

A third approach, which has been employed for the calculation of octanol – water partition coefficients, is based on specific correlations for activity coefficients at infinite dilution e.g. the MOSCED model^{23,24}. The advantage of such methods, compared to the GC ones, is that they treat strong interactions like hydrogen bonding in a separate way, and thus are much more realistic for highly non-ideal systems. However, a serious shortcoming lies in their application to aqueous systems.²⁵ Consequently, Sherman et al.²⁶ provided a 7-parameter correlation model based on the Linear Solvation Energy Relationship (LSER) which, unlike MOSCED, can estimate activity coefficients in aqueous solutions. However, the parameters of this LSER (the solute solvatochromic parameters α , β , and π^* , solute and solvent molar volume, solute vapour pressure, and the solute gas – liquid partition coefficient between hexadecane and an inert gas phase) are available for only some mono-functional molecules, which limits the applicability of the model. An additional drawback of this LSER model is that it is limited to binary solutions.

The above analysis indicates that a comparison of several general UNIFAC models and a characteristic of the specific P_{ow} models e.g. the AFC correlation model would cover a gap of the existing literature. Especially, if both mono-functional and some poly-functional production chemicals are considered.

2.3 Group Contribution Models for Estimating P_{ow}

2.3.1 UNIFAC Models

UNIFAC is a group contribution method for activity coefficients, which is based on the local composition concept. In principle it can be applied to both LLE (Liquid–Liquid Equilibria) and VLE (Vapor–Liquid Equilibria). In this work, various UNIFAC versions will be employed in order to test the effect on P_{ow} calculations of different parameter tables.

In the UNIFAC model each functional group uniquely contributes to the activity coefficients. The group interaction parameters are determined from binary data; the same parameters will be used in multi-component systems. In the UNIFAC model⁸ the activity coefficient is expressed as a sum of a combinatorial and a residual term:

$$\ln \gamma_i = \ln \gamma_i^{comb} + \ln \gamma_i^{res} \quad (2.3)$$

The combinatorial or entropy term takes into account the differences in molecular size and shape, and the residual term accounts for the molecular interactions. The combinatorial term is a function of the mole fraction of the components in the mixture and also a function of pure–component parameters, the van der Waals (vdW) volume (r_i) and surface area (q_i) parameters shown below. In the original UNIFAC model the combinatorial term is given by the equation:

$$\ln \gamma_i^{comb} = \ln \frac{\Phi_i}{x_i} + 1 - \frac{\Phi_i}{x_i} - \frac{Z}{2} q_i \left(\ln \frac{\Phi_i}{\theta_i} + 1 - \frac{\Phi_i}{\theta_i} \right) \quad (2.4)$$

$$\Phi_i = \frac{x_i r_i^k}{\sum_j x_j r_j^k} \quad \text{and} \quad \theta_i = \frac{x_i q_i}{\sum_j x_j q_j} \quad (2.5)$$

The surface area (q_i) and the vdW volume (r_i) of the components in the mixture are:

$$r_i = \sum_k \nu_k^{(i)} \cdot R_k \quad , \quad q_i = \sum_k \nu_k^{(i)} \cdot Q_k \quad (2.6)$$

where $\nu_k^{(i)}$ is the number of groups of type k in molecule i . R_k and Q_k are the group vdW volume and surface area, respectively, which are readily available in tables for a large variety of groups.

The first three terms in Eq. (2.4) constitute the Flory–Huggins (F–H) expression, and the last one is the Stavermann–Guggenheim correction term. Z is the coordination number as defined in the *lattice theory* and may have a value between 4 and 36 depending on the type of packing. UNIFAC uses $Z = 10$.

The residual term of the activity coefficient is expressed as follows:

$$\ln \gamma_i^{res} = \sum_k \nu_k^{(i)} \cdot (\ln \Gamma_k - \ln \Gamma_k^{(i)}) \quad (2.7)$$

where Γ_k is the group residual activity coefficient in the *actual mixture*, while $\Gamma_k^{(i)}$ is the group residual activity coefficient in a reference group solution containing only molecules of type i .

$$\ln \Gamma_k = Q_k \left[1 - \ln \left(\sum_m \theta_m \cdot \Psi_{mk} \right) - \sum_m \frac{\theta_m \cdot \Psi_{km}}{\sum_n \theta_n \cdot \Psi_{nm}} \right] \quad (2.8)$$

where the group area fraction, θ_m , is given by the equation:

$$\theta_m = \frac{X_m Q_m}{\sum_n X_n Q_n} \quad (2.9)$$

and the group mole fraction is given by:

$$X_m = \frac{\sum_j \nu_m^{(j)} x_j}{\sum_j \sum_n \nu_n^{(j)} x_j} \quad (2.10)$$

The group interaction parameter Ψ_{mn} is, in the original UNIFAC model, given by the equation:

$$\Psi_{mn} = \exp \left(\frac{-a_{mn}}{T} \right) \quad (2.11)$$

where m and n denote the main groups in the UNIFAC table.

We have employed five different UNIFAC versions which are hereafter briefly outlined and also summarized in Table 2.1.

Table 2.1 An overview of the five UNIFAC models

	original UNIFAC VLE-1	UNIFAC LLE	original UNIFAC VLE-2	modified UNIFAC VLE-3	WATER UNIFAC
reference	Hansen et al., 1991 ²⁷	Magnussen et al., 1981 ⁹	Hansen et al., 1992 ²⁸	Larsen et al., 1987 ²⁹	Chen et al., 1993 ²
data used	VLE	LLE	VLE	VLE & H ^E	VLE & $\gamma^{\infty, aq}$
temperature dependency	$a \neq f(T)$ eq. 11	$a \neq f(T)$ eq. 11	Linear eq. 12	Logarithmic eq. 13	$a \neq f(T)$ eq. 11
k factor in Eq. (2.5)	1	1	1	$\frac{2}{3}$	1

The *first* model (VLE-1) is the original UNIFAC with parameters by *Hansen et al.*²⁷ This model is functionally similar to the original UNIFAC by *Fredenslund et al.*⁸ However, some new functional groups have been defined. The interaction parameters, a_{mn} , have been experimentally determined by VLE data and are not temperature dependent (Eq. 2.11)

The *second* model (LLE) is identical to the original UNIFAC (*Hansen et al.*²⁷). However, the interaction parameters have been determined by fitting LLE experimental data. The LLE table was developed by *Magnussen et al.*⁹, and is less extensive than the VLE-based one.

The *third* model (VLE-2) is developed by *Hansen et al.*²⁸ and the equations are identical to VLE-1 and LLE except that the group interaction parameters are linearly temperature dependent.

They are determined from VLE experimental data as in VLE-1:

$$\Psi_{mn} = \exp\left\{-\frac{(a_{mn} + b_{mn}(T - T_0))}{T}\right\} \quad (2.12)$$

where T_0 is an arbitrary reference temperature ($T = 298.15$ K).

In VLE-1, LLE, and VLE-2 the value of k in Eq. (2.5) is equal to 1. The *fourth* model (VLE-3) is a modified version of the original UNIFAC by *Larsen et al.*²⁹ developed at

the Technical University of Denmark. A similar modified UNIFAC model has been developed at the University of Dortmund (Germany). The k -factor in Eq. (2.5) is set to 2/3, and the Stavermann–Guggenheim term in Eq. (2.4) is eliminated. The interaction parameters are temperature dependent and have the following form:

$$\Psi_{mn} = \exp \left\{ - \frac{\left(a_{mn} + b_{mn}(T - T_0) + c_{mn} \left(T \ln \left(\frac{T_0}{T} \right) + T - T_0 \right) \right)}{T} \right\} \quad (2.13)$$

The interaction parameters, a_{mn} , b_{mn} , and c_{mn} are determined from experimental VLE and excess enthalpies (H^E) data.

The *fifth* model is the WATER-UNIFAC model developed by *Chen et al.*² This model is similar to original UNIFAC (VLE-1), but is specifically designed for aqueous systems. New interaction parameters have been determined between the water molecule and other functional groups from experimental infinite dilution activity coefficients in aqueous solutions.

2.3.2 The AFC Correlation Model

The AFC correlation model has been proposed by Meylan & Howard.²¹ It is a group or fragment contribution method specifically for the calculation of the octanol – water partition coefficient. The fragments consist of the well-known organic functional groups such as alcohols, amines etc. as well as of atoms such as halogens. The expression for the calculation of octanol-water partition coefficients is:

$$\log P_{ow} = \sum_i n_i \cdot f_i + \sum_j n_j \cdot c_j + 0.229 \quad (2.14)$$

where n_i is the number of occurrences of the fragment f_i and n_j is the number of occurrences of the correction factor c_j . The fragment constants are determined by regression from reliable experimental $\log P_{ow}$ data. The AFC model will be applied in this work for comparison purposes, being a typical representative of those models specially designed for the calculation of P_{ow} . The Environmental Science Centre (ESC) of Syracuse Research Corporation (SCR) offers computerized form of the AFC method

available on its web page (<http://esc.syrres.com/interkow/kowdemo.htm>). We have employed this public-domain version of the AFC method.

2.4 Results and Discussion

2.4.1 Data Base

The database used in this work is retrieved from the Sangster compilation¹, which contains approximately 600 simple organic compounds. We have investigated here compounds of the following families: alkanes, aromatics, cycloalkanes, ethers, alcohols, aldehydes, ketones, acids, esters, amines, and some poly-functional compounds (production chemicals) in total 137 compounds. Due to uncertainty in the measured octanol-water partition coefficients, Sangster¹ has also provided a recommended P_{ow} value for each listed compound. Most of the data in the Sangster compilation are based on the reliable measurements of Hansch and Leo¹⁹.

No rigorous consistency tests similar to Gibbs-Duhem for VLE can be applied to P_{ow} . However, the reliability of experimental data is investigated in this work by plotting $\log P_{ow}$ versus the carbon number.

The predicted results of octanol-water partition coefficient by the various group-contribution models including the AFC correlation model are compared with the experimental data in Figure 2.1.

The poly-functional compounds are not included in this comparison. In Figures 2.2 – 2.6, the predicted and the experimental octanol-water partition coefficients are plotted against the carbon number for n-alkanes, 1-alkanols, carboxylic acids, aldehydes, and 2-ketones, respectively.

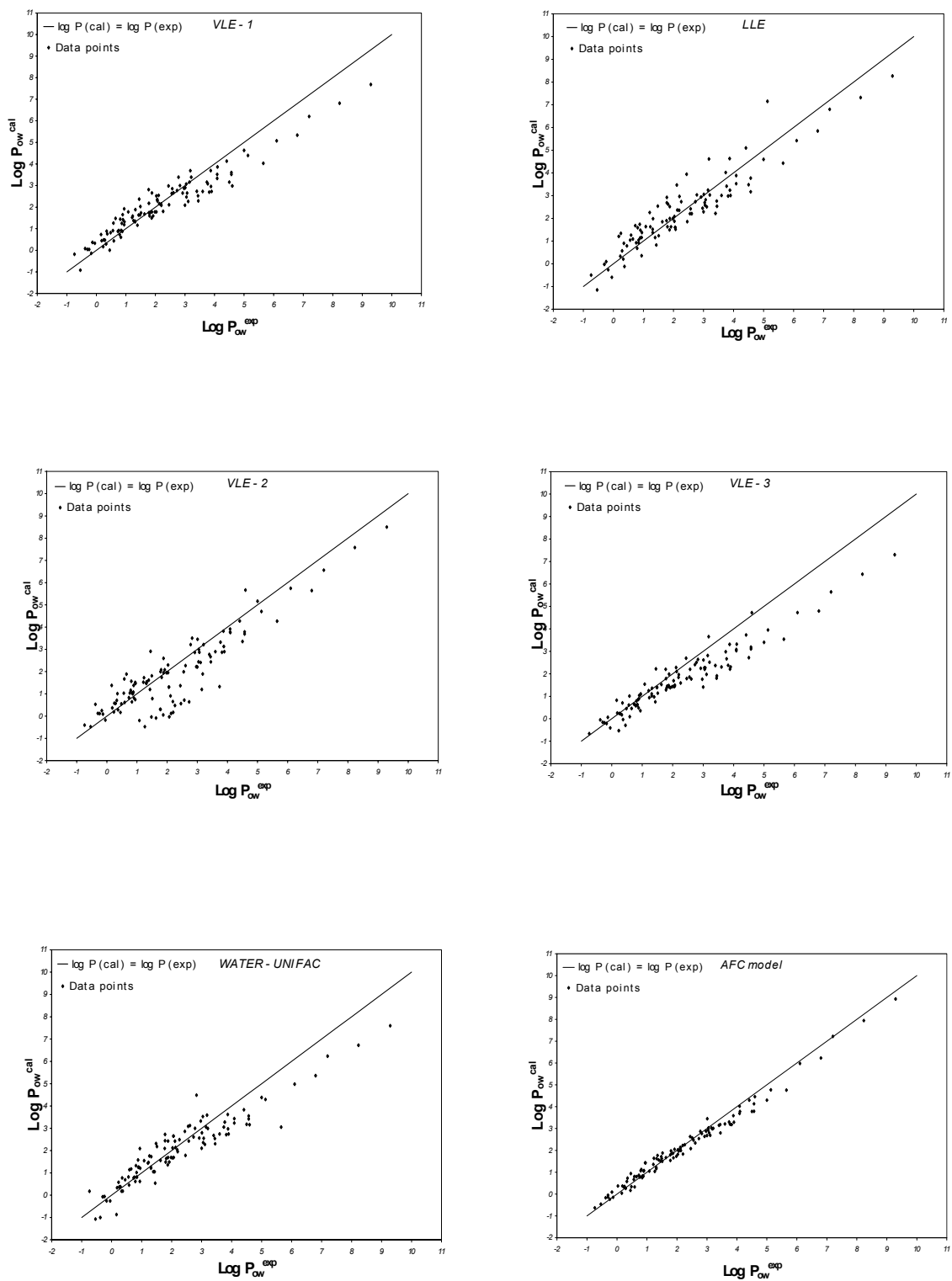


Figure 2.1 $\log P_{ow}$ predicted for mono-functional compounds by the UNIFAC models and the AFC correlation model compared with experimental data (Sangster, 1989) at 298.15 K.

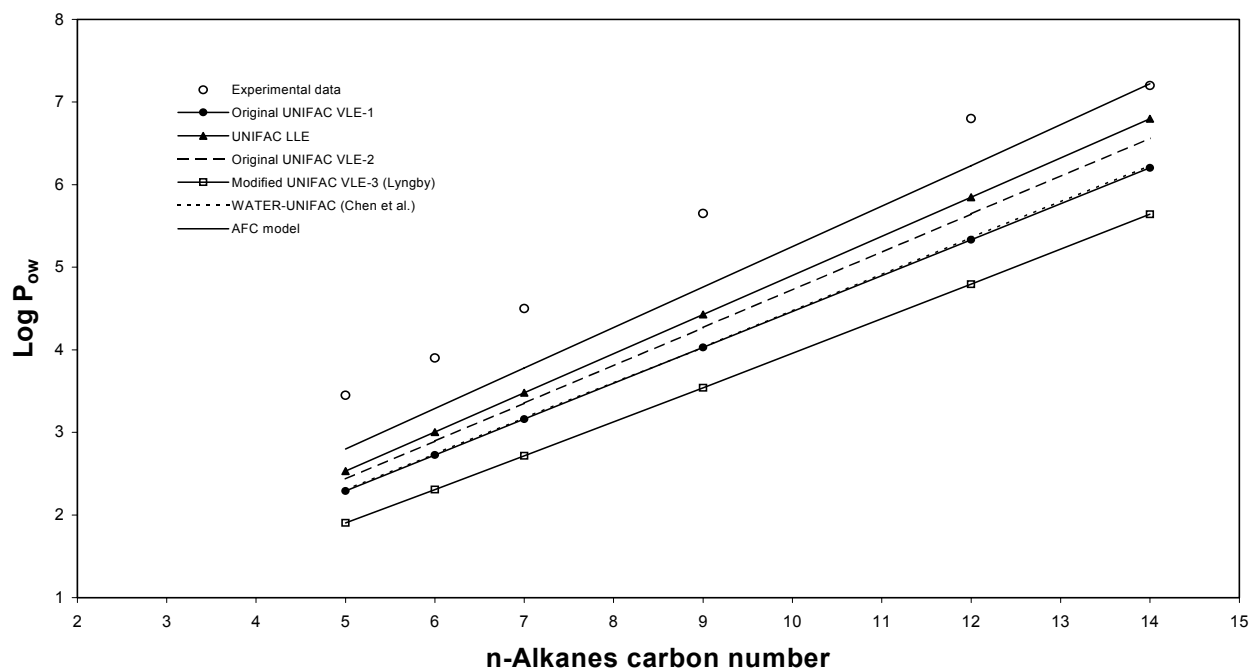


Figure 2.2 Octanol – water partition coefficient for *n-alkanes* predicted from group-contribution models and compared with experimental data at 298.15 K. Experimental data from Sangster (1989).

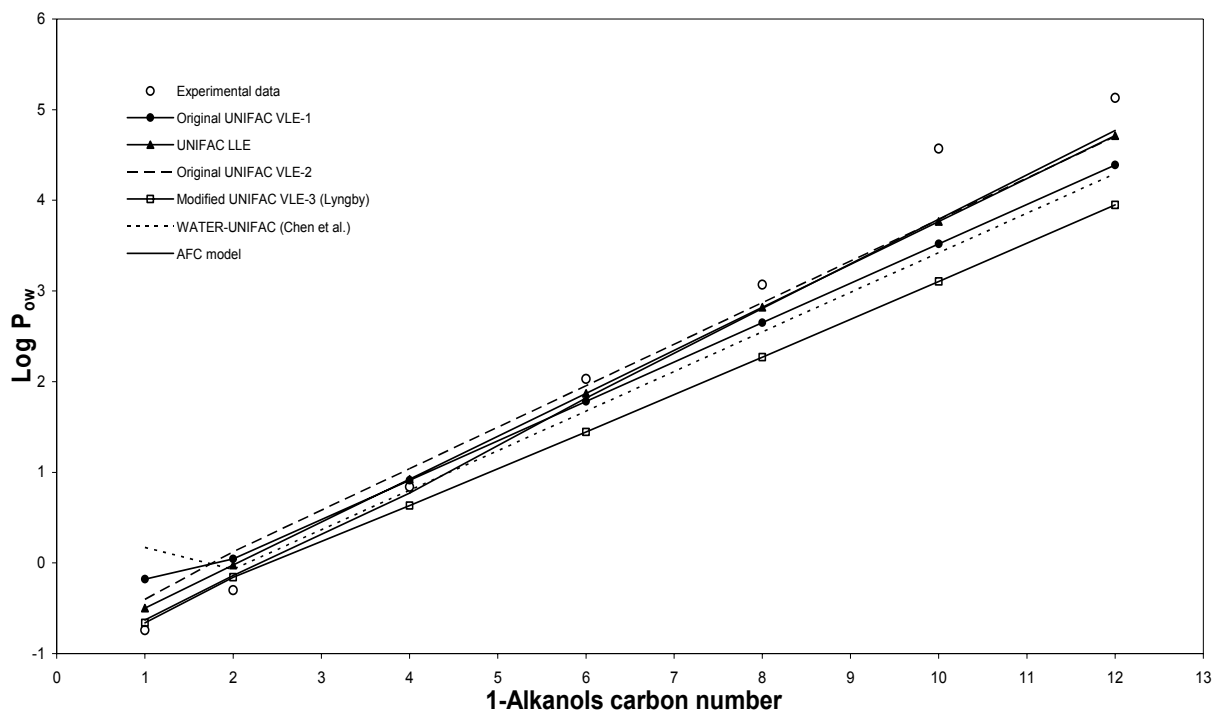


Figure 2.3 Octanol – water partition coefficient for *1-alkanols* predicted from group-contribution models and compared with experimental data at 298.15 K. Experimental data from Sangster (1989).

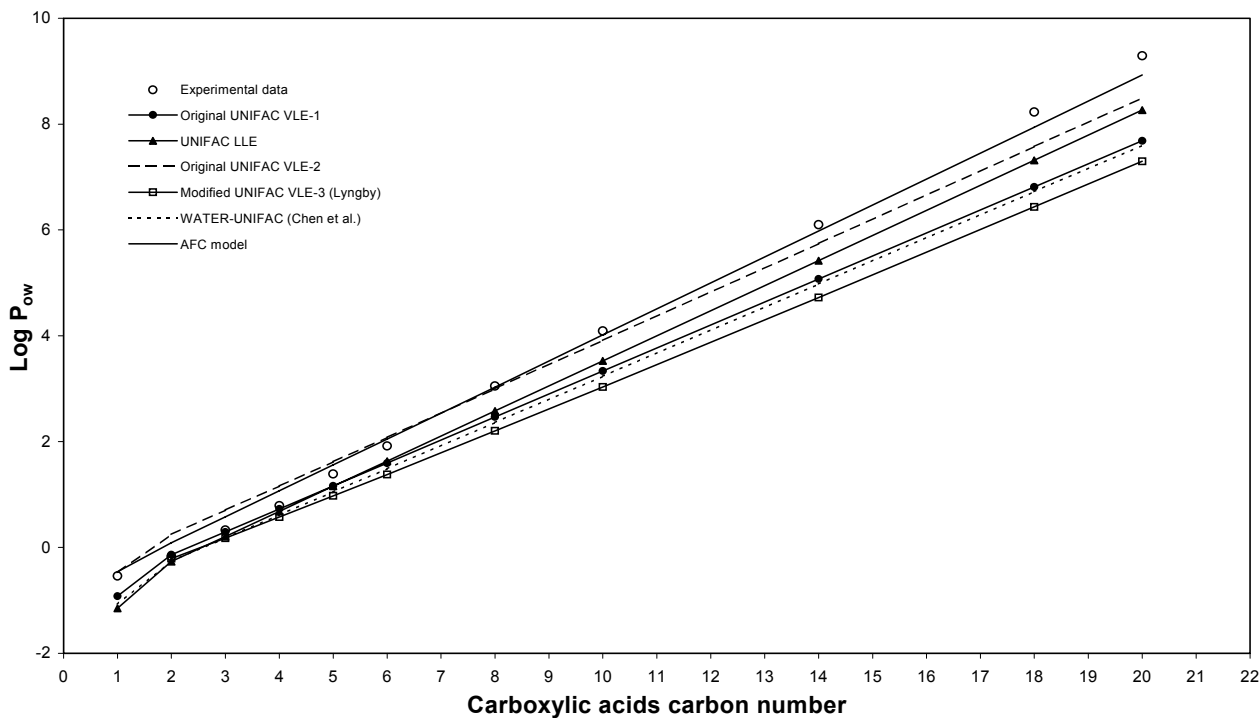


Figure 2.4 Octanol – water partition coefficient for *carboxylic acids* predicted from group-contribution models and compared with experimental data at 298.15 K. Experimental data from Sangster (1989).

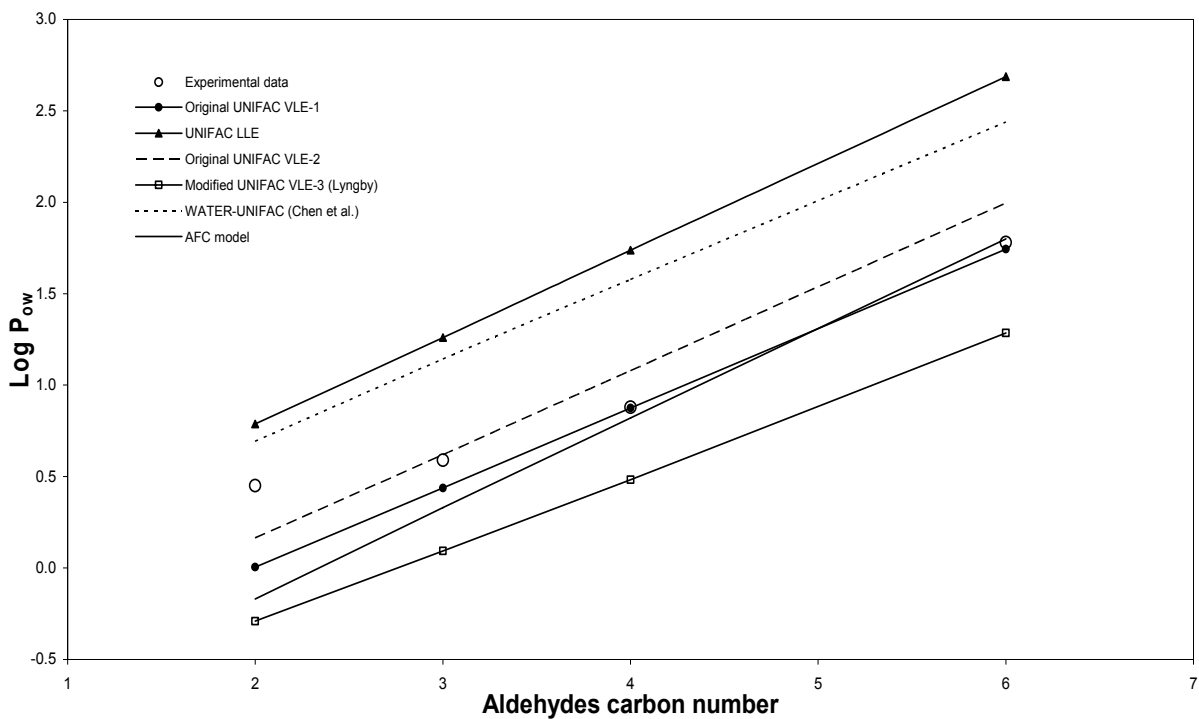


Figure 2.5 Octanol – water partition coefficient for *aldehydes* predicted from group-contribution models and compared with experimental data at 298.15 K. Experimental data from Sangster (1989).

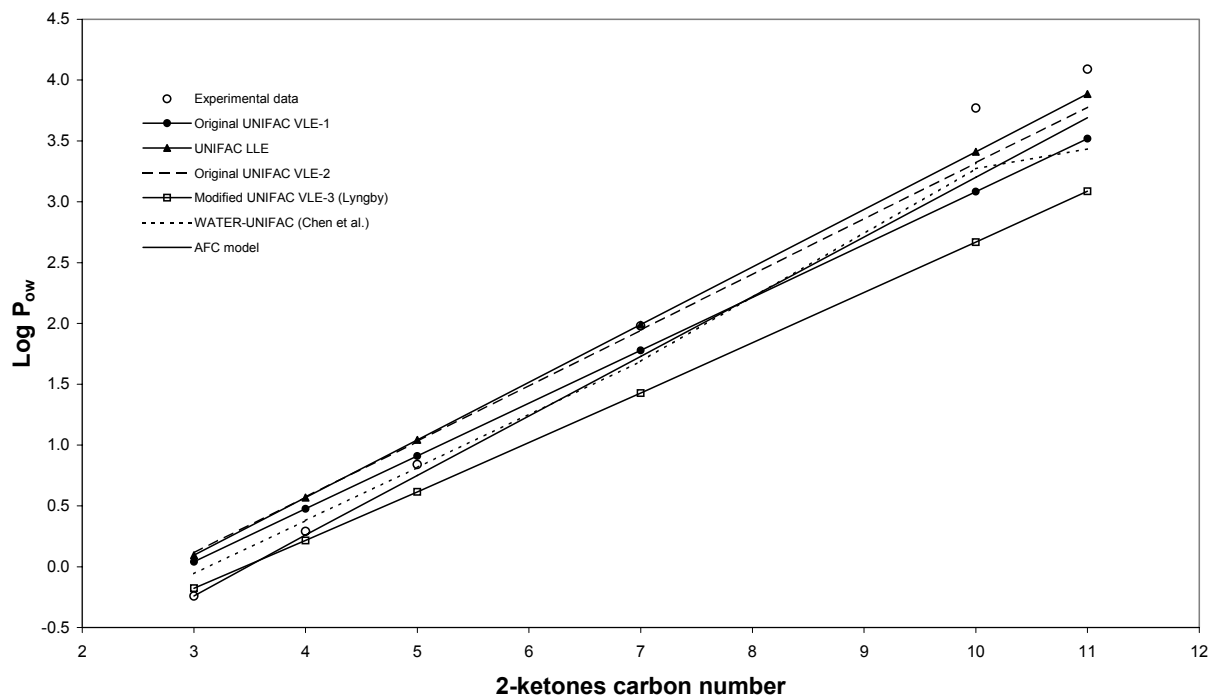


Figure 2.6 Octanol – water partition coefficient for *2-ketones* predicted from group-contribution models and compared with experimental data at 298.15 K. Experimental data from Sangster (1989).

Finally, in Figure 2.7 (next page), the residual ($\log P_{ow}^{\text{exp}} - \log P_{ow}^{\text{cal}}$) is plotted against the $\log P_{ow}^{\text{exp}}$ to check for possible systematic errors in the models.

The models are evaluated based on the average absolute deviation (AAD) defined as follows:

$$AAD = \frac{1}{NP} \sum_{i=1}^{NP} \left(\left| \log P_{ow}^{\text{exp},i} - \log P_{ow}^{\text{cal},i} \right| \right)$$

NP is the total number of data points.

In Tables 2.2 and 2.3, the AAD for all the GC models investigated are tabulated for the considered mono-functional and the poly-functional chemicals.

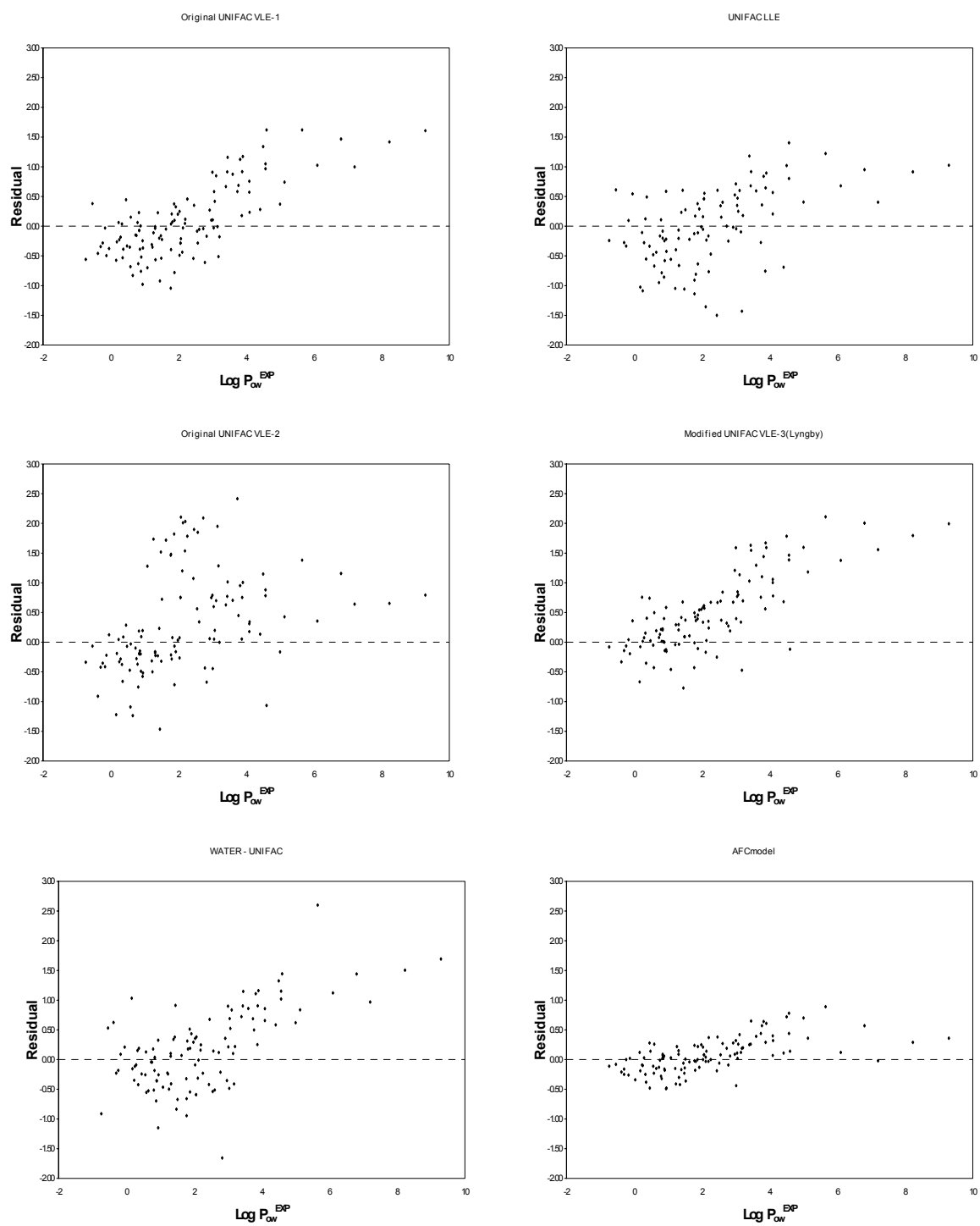


Figure 2.7 Plots of the Residual (experimental – predicted $\log P_{ow}$) vs. the predicted $\log P_{ow}$ for mono-functional compounds by the UNIFAC models and the AFC correlation model.

Table 2.2 Comparison of $\log P_{ow}$ calculated from the UNIFAC models and the AFC correlation model

solute	data points	AAD					AFC model
		original UNIFAC VLE-1	UNIFAC LLE	original UNIFAC VLE-2	modified UNIFAC VLE-3	WATER UNIFAC	
alkanols	13	0.39	0.31	0.38	0.43	0.40	0.25
phenols	8	0.22	0.42	0.72	0.70	0.53	0.09
carboxylic acids	15	0.50	0.42	0.54	0.74	0.62	0.20
aldehydes	7	0.24	0.78	0.79	0.41	0.59	0.16
amines	15	0.58	na ^c	0.62	0.40	na ^c	0.19
ethers	13	0.50	0.36	0.66	0.38	0.35	0.26
hydrocarbons	17	0.88	0.73	1.09	1.32	0.95	0.41
ketones	13	0.27	0.26	0.49	0.38	0.26	0.19
esters	14	0.27	0.89	0.77	0.37	0.32	0.17
aromatics ^a	30	0.32	0.53	1.30	0.46	0.42	0.17
total data points	115	0.46	0.52	0.68	0.60	0.51	0.23
		0.36 ^b	0.48 ^b	0.60 ^b	0.48 ^b	0.43 ^b	0.20 ^b

^a Aromatics for all functional groups

^b Amines and hydrocarbons are excluded

^c na: not available group parameters

Table 2.3 Calculation of $\log P_{ow}$ for poly - functional molecules from the UNIFAC models and the AFC correlation model

solute	$\log P_{ow}^{\text{exp}}$	AAD					WATER UNIFAC	AFC model
		original UNIFAC VLE-1	UNIFAC LLE	original UNIFAC VLE-2	modified UNIFAC VLE-3			
triethylene glycol	-2.08	0.43	-1.11	-0.18	-0.64	-0.63	-1.75	
diethanolamine	-1.43	-0.40	na ^a	-0.37	-1.00	-1.68	-1.71	
ethylene glycol	-1.36	-0.72	-3.14	0.53	-1.04	-1.14	-1.20	
ethanolamine	-1.31	-0.57	na ^a	-0.85	-0.82	na ^a	-1.61	
1,3-propanediol	-1.04	-1.15	-1.11	-1.18	-1.22	-0.70	-0.71	
triethanolamine	-1.00	-0.28	na ^a	-0.86	-1.18	-1.90	-2.48	
propylene glycol	-0.92	-0.46	-0.68	-0.36	-0.64	-0.70	-0.78	
2,3-butanediol	-0.92	-1.05	-1.01	-1.09	-1.11	-0.26	-0.36	
1,4-butanediol	-0.83	-1.05	-1.01	-1.09	-1.11	na ^a	-0.22	
2-methoxyethanol	-0.77	0.35	-0.47	0.41	-0.38	-0.26	-0.91	
<i>2-(2-hydroxy-propoxy)-1-propanol</i>	-0.67	-0.72	-0.97	-0.94	-0.99	0.29	-0.64	
ethylcarbitol	-0.54	-0.12	-1.34	-0.79	-0.96	0.43	-0.69	
dimethylcarbitol	-0.36	0.24	-2.10	-0.86	-1.19	0.58	-0.48	
2-ethoxyethanol	-0.28	0.79	0.00	0.87	0.02	0.18	-0.42	
isopropylcellosolve	0.05	-0.47	-0.98	-0.79	-0.86	0.62	0.00	
butylcarbitol	0.56	-0.06	-1.19	-0.72	-0.89	1.31	0.29	
isobutylcellosolve	0.75	-0.45	-0.94	-0.77	-0.83	1.05	0.49	
1,3-benzenediol	0.80	2.26	0.18	-0.61	-1.36	2.22	1.03	
2-butoxyethanol	0.83	1.66	0.95	1.78	0.83	1.05	0.57	
diethoxymethane	0.84	-0.20	-1.39	-0.82	-1.02	1.06	0.79	
1,2-benzenediol	0.88	2.26	0.18	-0.61	-1.36	2.22	1.03	
hexylcarbitol	1.70	-0.03	-1.09	-0.68	-0.86	2.18	1.27	
total data points	22	0.85	0.93	0.98	0.86	0.66	0.29	

^a na: not available group parameters

To facilitate the understanding on the performance of the models, we first discuss the various families separately in sections 2.4.2 – 2.4.4 and then summarise our conclusions in section 2.4.5.

2.4.2 The Partitioning of Hydrocarbons

As shown in Figure 2.2, all the GC models underestimate significantly the experimental data for n-alkanes. This result is not entirely surprising, since aliphatic hydrocarbons in aqueous solutions represent highly non-ideal solutions, which are known to be difficult to model. The AFC model yields by far the best results for n-alkanes. In Table 2.2, the AAD for the hydrocarbons (aliphatic, aromatic, and cyclo-compounds) are tabulated. The *UNIFAC VLE-1* and *WATER UNIFAC* have practically the same accuracy due to the fact that the interaction parameters between water and the alkane group in *WATER UNIFAC* have not been re-estimated, unlike other functional groups. Zhang et al.¹⁷ have shown, in their work on activity coefficients at infinite dilution in aqueous systems, that most UNIFAC models, except the modified UNIFAC by Hooper et al.³⁰, are inadequate and highly underestimate the experimental data. However, the Hooper method has been specifically developed for correlation of LLE for water/hydrocarbon mixtures. Moreover, the aromatic hydrocarbons due to their delocalised electrons are less non-ideal in aqueous solutions than the aliphatic hydrocarbons. For such systems, it was shown that all the UNIFAC models, except *UNIFAC VLE-2*, are suitable for P_{ow} calculations.

2.4.3 The Partitioning of Oxygenated Compounds

Figure 2.3 shows graphically the octanol-water partition coefficient vs. the carbon number for 1-alkanols. Most of the GC models provide acceptable results for lower compounds (carbon number < 4), especially *UNIFAC LLE*, whereas for higher compounds, most of the models, except *UNIFAC LLE*, underestimate highly the experimental data. Generally, *UNIFAC LLE* and AFC provide acceptable results for both low and high molecular weight alkanols. The relatively lower AAD for *UNIFAC LLE* and AFC (Table 2.2) than for the other UNIFAC models for alkanols verifies this point. Similarly, *UNIFAC LLE* and the AFC model are the best models for phenols as well. Despite the fact that *UNIFAC VLE-1* provides the lowest AAD, this model is not

recommended due to the rather suspicious activity coefficient values e.g. 0.06 of phenol in the octanol phase.

In Figure 2.4, the octanol-water partition coefficient vs. the carbon number for aliphatic carboxylic acids is graphically shown. All the UNIFAC models provide satisfactory results for lower compounds (carbon number < 4), whereas they, progressively for higher carbon numbers, tend to underestimate the experimental data. Nevertheless, the *UNIFAC VLE-2* perform relatively better than the other UNIFAC models over the entire range of hydrophobicity i.e. for both lower and higher carbon numbers. Moreover, the AFC correlation model is excellent for carboxylic acids.

In Figure 2.5, the octanol-water partition coefficient vs. the carbon number for aliphatic aldehydes is graphically shown. The experimental data point for acetaldehyde is rather suspicious, since it deviates from the linear trend, indicated by the other experimental data points. Considering this, the original *UNIFAC VLE-1* and AFC are the most accurate models for predicting the octanol-water partition coefficient. *UNIFAC LLE* overestimates significantly the experimental data points for both low and high molecular weight aldehydes.

The plot of octanol-water partition coefficients for 2-ketones vs. the carbon number is shown in Figure 2.6. The *modified UNIFAC VLE-3* performs well for lower compounds (carbon number < 4), but highly underestimate the experimental data for heavier 2-ketones. The AFC and the *WATER UNIFAC* models provide the best overall performance.

In the case of ethers and esters, *WATER UNIFAC* and the AFC model are recommended for P_{ow} predictions (Table 2.2).

2.4.4 The Partitioning of Amines, Aromatics, and Complex Compounds

In the case of amines, the *UNIFAC LLE* and the *WATER UNIFAC* models cannot be applied due to lack of the interaction parameters. As shown in Table 2.2, all UNIFAC models provide very poor results for the amines considered. However, the AFC model is the best among all the GC models.

The GC models have also been applied to P_{ow} calculations for aromatic chemicals for all the different functional groups. It was shown that *UNIFAC VLE-2* failed to predict P_{ow} accurately for the aromatics investigated (Table 2.2). However, the other models

provided satisfactory predictions, especially the AFC model, *UNIFAC VLE-1*, and *WATER UNIFAC*.

The performance of the GC models for polyfunctional molecules e.g. glycols and alkanolamines has also been considered. The predicted results for the octanol – water partition coefficient are summarised in Table 2.3. The AFC correlation model is superior to the UNIFAC models in accordance to the results obtained for mono-functional molecules. However, the *WATER UNIFAC* and the *UNIFAC LLE* models provide acceptable and less scattered results, especially the *WATER UNIFAC*, compared to the other UNIFAC models. Kuramochi et al.¹⁸ showed that *UNIFAC VLE-1* and the *modified UNIFAC VLE-3*, which are applied for biochemicals such as amino acids, their derivatives and sugars, provide very scattered and typically overestimated P_{ow} results.

2.4.5 Summary

As indicated from the summarised plots of Figure 2.1, the AFC correlation model is superior to all UNIFAC models. Moreover, all UNIFAC models tend to underestimate the octanol-water partition coefficient for highly hydrophobic compounds. *UNIFAC VLE-2*, unlike the other UNIFAC models, yields very scattered results, especially for aromatic and poly-functional compounds. Thus, this UNIFAC model cannot be recommended despite that it contains one of the most recent revisions of UNIFAC table. This conclusion may indicate the need for the revision of Hansen et al., 1992²⁸ parameter table. It can be observed from the residual plots that all UNIFAC models, except the *modified UNIFAC VLE-3*, do not show any obvious pattern i.e. the negative and positive errors are approximately equally distributed. The *modified UNIFAC VLE-3* has mainly positive residuals, as shown in Figure 2.7, which implies that the model has an overestimating tendency. Based on these conclusions and their performance for poly-functional molecules as well we recommend the *UNIFAC LLE* and the *WATER UNIFAC* model for the estimation of the octanol-water partition coefficients. Further work is required to include the amine group in these models so that complex compounds of practical importance such as amino-alcohols can be modelled, as well as to carefully reestimate a few group parameters e.g. aldehydes for which these two models have an inferior behaviour.

2.5 Conclusions

The partition coefficients of 115 mono-functional chemicals between an octanol and water phase have been critically evaluated by use of five UNIFAC models (*UNIFAC VLE-1 & VLE-2*, *UNIFAC LLE*, *modified UNIFAC VLE-3*, and *WATER UNIFAC*) and the empirical AFC correlation model. This correlation model was shown to be superior to all UNIFAC models in all cases. However, the AFC correlation is limited to the octanol-water partition coefficient and cannot be employed to other partition coefficients e.g. oil/water of these chemicals. Among the various more general GC UNIFAC models, the *UNIFAC LLE* and the *WATER UNIFAC* are recommended to predict the partitioning of molecules between the water and octanol phase. This conclusion is also valid for the 22 poly-functional compounds (production chemicals) that we have investigated. Still problems are encountered for specific chemicals which only partly could be attributed to the experimental data. Thus, we believe that the group-contribution concept has possibly exhausted its applicability to account for highly asymmetric systems, especially aqueous solutions with complex poly-functional chemicals. New thermodynamic concepts and models are thus necessary for obtaining quantitatively correct predictions. The novel association theories e.g. CPA⁵, SAFT³¹ may provide such a successful yet general alternative to the classical UNIFAC approach. Our future work will follow this direction.

References

- (1) Sangster, J. Octanol-water partition coefficients of simple organic compounds. *J. Phys. Chem. Ref. Data.* **1989**, 18 (3), 1111-1229.
- (2) Chen, F.; Holten-Andersen, J.; Tyle, H. New developments of the UNIFAC model for environmental application. *Chemosphere.* **1993**, 26 (7), 1325-1354.
- (3) Apelblat, A. Correlation between Activity and solubility of water in some aliphatic alcohols. *Ber. Bunsenges. Phy. Chem.* **1983**, 87, 2-5.
- (4) Kontogeorgis, G.M.; Voutsas, E.C.; Yakoumis, I.V.; Tassios, D.P. An equation of state for associating fluids. *Ind. Eng. Chem. Res.* **1996**, 35, 4310-4318.
- (5) Kontogeorgis, G.M.; Yakoumis, I.V.; Meijer, H.; Hendriks, E.; Moorwood, T. Multicomponent phase equilibrium calculations for water-methanol-alkane mixtures. *Fluid Phase equilibria.* **1999**, 158-160, 201-209.
- (6) Economou, I.G.; Tsonopoulos, C. Associating models and mixing rules in equations of state for water hydrocarbon/hydrocarbon mixtures. *Chem. Eng. Sci.* **1997**, 52, 511.
- (7) Wu, J.; Prausnitz, J.M. Phase equilibria for systems containing hydrocarbons, water, and salt: An extended Peng-Robinson equation of state. *Ind. Eng. Chem. Res.* **1998**, 37, 1634-1643.
- (8) Fredenslund, Aa.; Jones, R.L.; Prausnitz, J.M. Group-contribution estimation of activity coefficients in nonideal liquid mixtures. *AIChE J.* **1975**, 21, 1086.
- (9) Magnussen, T.; Rasmussen, P.; Fredenslund, Aa. UNIFAC parameters table for prediction of liquid-liquid equilibria. *Ind. Eng. Chem. Process Des. Dev.* **1981**, 20, 133.
- (10) Derr, E.L.; Deal, C.H. Analytical solutions of groups: Correlation of activity coefficients through structural group parameters. *Inst. Chem. Eng. Symp. Ser.* **1969**, 3 (32), 40.
- (11) Arbuckle, W.B. Estimating activity coefficients for use in calculating environmental parameters. *Environ. Sci. Technol.* **1983**, 17(9), 537-542.
- (12) Campbell, J.R.; Luthy, R.G. Prediction of aromatic solute partition coefficients using the UNIFAC group contribution model. *Environ. Sci. Technol.* **1985**, 19, 980-985.

- (13) Banerjee, S.; Howard, P.H. Improved estimation of solubility and partitioning through correction of UNIFAC-derived activity coefficients. *Environ. Sci. Technol.* **1988**, 22, 839-841.
- (14) Bastos, J.C.; Soares, M.E.; Medina, A.G. Infinite dilution activity coefficients by UNIFAC group contribution. *Ind. Eng. Chem. Res.* **1988**, 27, 1269.
- (15) Wienke, G.; Gmehling, J. Prediction of octanol-water partition coefficients, Henry coefficients and water solubilities using UNIFAC. *Toxicological and Environmental Chemistry.* **1998**, 65, 57-86.
- (16) Voutsas, E.C.; Tassios, D.P. Prediction of infinite-dilution activity coefficients in binary mixtures with UNIFAC. A critical evaluation. *Ind. Eng. Chem. Res.* **1996**, 35, 1438-1445.
- (17) Zhang, S.; Hiaki, T.; Hongo, M.; Kojima, K. Prediction of infinite dilution activity coefficients in aqueous solutions by group contribution models. A critical evaluation. *Fluid Phase Equilibria.* **1998**, 144, 97-112.
- (18) Kuramochi, H.; Noritomi, H.; Hoshino, D.; Kato, S.; Nagahama, K. Application of UNIFAC models to partition coefficients of biochemicals between water and n-octanol or n-butanol. *Fluid Phase Equilibria.* **1998**, 144, 87-95.
- (19) Hansch, C.; Leo, A. *Substituent constants for correlation analysis in chemistry and biology*; Wiley: New York, 1979.
- (20) Rekker, R.F.; Mannhold, R. *Calculation of drug lipophilicity*; VCH Verlagsgesellschaft: Weinheim, 1992.
- (21) Meylan, W.M.; Howard, P.H. Atom/fragment contribution method for estimating octanol – water partition coefficients. *J. Pharm. Sci.* **1995**, 84, 83-92.
- (22) Suzuki, T.; Kudo, Y. *J. Computer – Aided Mol. Des.* **1990**, 4, 155-98.
- (23) Thomas, E.R.; Eckert, C.A. Prediction of limiting activity coefficients by a modified separation energy density model and UNIFAC. *Ind. Eng. Chem. Process Des. Dev.* **1984**, 23, 194-209.
- (24) Howell, W.J.; Karachewski, A.M.; Stephenson, K.M.; Eckert, C.A.; Park, J.G.; Carr, P.W.; Rutan, S.C. An improved MOSCED Equation for the prediction and application of infinite dilution activity coefficients. *Fluid Phase Equilibria.* **1989**, 52, 151-160.

- (25) Eckert, C.A.; Sherman, S.R. Measurement and prediction of limiting activity coefficients. *Fluid Phase Equilibria*. **1996**, 116, 333-342.
- (26) Sherman, S.R.; Trampe, D.B.; Bush, D.M.; Schiller, M.; Eckert, C.A.; Dallas, A.J.; Li, J.; Carr, P.W. Compilation and correlation of limiting activity coefficients of nonelectrolytes in water. *Ind. Eng. Chem. Res.* **1996**, 35, 1044-1058.
- (27) Hansen, H.K.; Rasmussen, P.; Fredenslund, Aa.; Schiller, M.; Gmeling, J. Vapor-liquid equilibria by UNIFAC group contribution. 5. Revision and Extension. *Ind. Eng. Chem. Res.* **1991**, 30, 2352.
- (28) Hansen, H.K.; Coto, B.; Kuhlmann, B. UNIFAC with linearly temperature-dependent group-interaction parameters. SEP 9212 (Internal Report). Department of Chemical Engineering, DTU, Lyngby, 1992.
- (29) Larsen, B.L.; Rasmussen, P.; Fredenslund, Aa. A modified UNIFAC group-contribution model for prediction of phase equilibria and heats of mixing. *Ind. Eng. Chem. Res.* **1987**, 26, 2274.
- (30) Hooper, H.H.; Michel, S.; Prausnitz, J.M. Correlation of liquid-liquid equilibria for some water-organic liquid systems in the region 20-250 °C. *Ind. Eng. Chem. Res.* **1988**, 27, 2182-2187.
- (31) Huang, S.H.; Radosz, M. Equation of state for small, large, polydisperse and associating molecules. *Ind. Eng. Chem. Res.* **1990**, 29, 2284.

Chapter 3

Liquid-Liquid Equilibria for Glycols + Hydrocarbons: Data and Correlation

Liquid-liquid equilibrium data for 7 binary glycol-hydrocarbon systems have been measured in the temperature range 32 °C to 80 °C and pressure equal to 1 bar. The measured systems are monoethylene glycol (MEG) + heptane, methylcyclohexane (MCH), hexane, propylene glycol (PG) + heptane, diethylene glycol (DEG) + heptane, triethylene glycol (TEG) + heptane, and tetraethylene glycol (TETRA) + heptane. The data obtained were correlated with the NRTL model and two different versions of the UNIQUAC equation. The NRTL model and one of the UNIQUAC equations (UQ 4) have a linear temperature-dependent interaction parameter term, while the other UNIQUAC equation (UQ 2) has an interaction parameter that is independent of the temperature. There was a fairly good agreement between the experimental data and the models with an average deviation in the composition for both phases of 3 % for both NRTL and UQ 4 and 15 % for UQ 2. These results indicate the necessity of using the linearly dependent interaction parameters.

3.1 Introduction

In the oil industry, various chemicals are added to both production streams and processing streams in order to maintain flow assurance e.g. to inhibit gas hydrate formation. These chemicals may have a negative effect on the marine environment and might be found in the refined products going to the consumer, which is evidently not desired. In the recent years, there has been an increasing demand from environmental agencies and the petrochemical industry to assess the risk of these hazardous chemicals on the marine environment and their potential threat to humans. Thus, it is important to know the partitioning of such chemicals between the gas, crude oil, and water phase either by experimental measurements or from thermodynamic models. Experimental measurements can be rather expensive and time consuming.

The production chemicals considered in this work are the glycols such as monoethylene glycol and triethylene glycol. Monoethylene glycol has been used extensively in the petrochemical industry to prevent gas hydrate formation in transportation lines for gas and crude oil, and triethylene glycol is used in gas dehydration units.

Development of thermodynamic models requires experimental data to assess their validity and confirm their range of applicability. A few ternary LLE data are available in the literature for glycols, hydrocarbons, and water, while binary data between glycols and hydrocarbons are very scarce. Binary liquid-liquid equilibrium data for glycols and hydrocarbons are often reported only for the composition of the hydrocarbon phase.

In this work, the solubility of each component in both phases is measured by gas chromatography. Earlier measurements of glycols and hydrocarbons have been carried out by the synthetic method for heptane and monoethylene glycol¹, triethylene glycol², tetraethylene glycol², diethylene glycol³. In the synthetic method, also known as the cloud point method, the solubility is measured for a mixture of known composition by determining the temperature where phase separation occurs.

The measured experimental data are correlated to local composition based activity coefficient models such as NRTL and UNIQUAC.

3.2 Experimental Section

3.2.1 Chemicals

The alkanes and the glycols were obtained from MERCK Eurolab AS (0945 Oslo). Table 3.1 summarises both the specifications of the used chemicals obtained by MERCK and the measured water content. The water content was measured at 1 bar by a Karl-Fischer apparatus of type Mitsubishi Moisture Meter Model CA-06. The coulometric titration method was applied since the water content in all the samples was below 1 mass %. The chemicals were used without any further purification.

Table 3.1 Specification of the applied chemicals

chemical	specified purity as mass %	specified water content as mass %	measured water content as mass %
ethylene glycol	> 99.5	max. 0.1	0.027
diethylene glycol	> 99.0	< 0.3	0.066
triethylene glycol	> 99.0	< 0.3	0.072
tetraethylene glycol	> 97.0	not specified	0.116
1,2-propylene glycol	≥ 99.0	≤ 0.2	0.031
acetone	> 99.8	max. 0.05	0.032
methylcyclo- hexane	> 98.0	not specified	not measured
n-heptane	> 99.0	max. 0.01	not measured
n-hexane	> 99.0	max. 0.01	not measured

3.2.2 Experimental Procedure

The liquid-liquid equilibrium measurements of glycols and hydrocarbons were carried out at 1 bar in two identical 550 cm³ glass equilibrium cells. Sampling through a needle from each of the two phases was feasible since the cells were equipped with several vertical orifices sealed with Teflon-coated septa. The sampling was carried out twice for each phase in order to check the reproducibility of the measurements. An illustration of the experimental set-up, which consists of the sampling part and the analysis part, is shown in Figure 3.1.

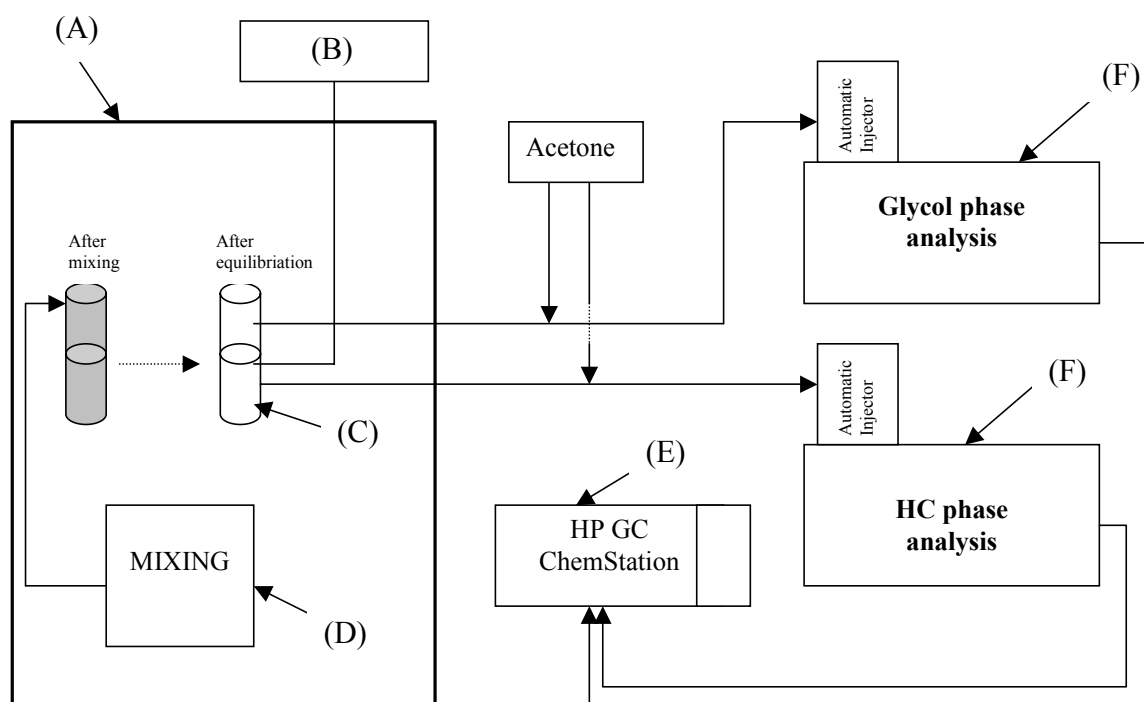


Figure 3.1 Sketch of the experimental apparatus: (A) air heated oven, (B) thermometer, (C) equilibrium cell, (D) Shaker, (E) computer for data analysis, (F) gas chromatograph.

The binary glycol-hydrocarbon mixture was shaken for approximately 18 h, which was sufficient to achieve equilibrium. The mixture was then transferred to the glass equilibrium cells for a 6 h separation process. Both the mixing and separation were performed at the desired temperature in an air-heated oven, which can operate from -35 °C to 100 °C. When the mixture was transferred to the glass equilibrium cells for separation, both phases were cloudy and became transparent after ~ 2 h, which indicated that the mixture reached the equilibrium state.

A FLUKE 52 K-type thermometer (precision ± 0.1 °C) was used for the temperature measurements. The thermometer was calibrated with a PT-100 element (precision ± 0.03 °C) from 0 °C to 100 °C.

3.2.3 Sampling and Analysis

Samples from the two phases were withdrawn and analysed by gas-liquid chromatography (glc). The hydrocarbon phase was analysed for trace amount of glycols using the column and conditions for glc A, and the glycol phase was analysed for trace

amount of hydrocarbons using glc B. Characteristics and the temperature programs of glc A and B are found in Table 3.2.

Table 3.2 Characteristics and temperature programs of the two HP 5890, SERIES II Gas Chromatographs with a HP 6890 Injector

	glc A	glc B
column type	HP-PONA un-polar capillary column	CP-Wax 52 CB polar capillary column
column length	50 m	28 m
column inside diameter	0.2 mm	0.53 mm
column film thickness	0.5 μm	1 μm
detector type	FID	FID
detector temperature	300 $^{\circ}\text{C}$	275 $^{\circ}\text{C}$
carrier gas	helium	Helium
flow pressure	44.0 psi	3.3 psi
syringe size	10 μL	10 μL
injection volume	0.2 μL	1.0 μL
plunger speed	fast	fast
splitless injection	no	no
inlet oven temperature	300 $^{\circ}\text{C}$	275 $^{\circ}\text{C}$
<u>Temperature Program</u>		
initial temperature	60 $^{\circ}\text{C}$	80 $^{\circ}\text{C}$
initial time	2.00 min	2.00 min
rate	10 $^{\circ}\text{C}/\text{min}$	10 $^{\circ}\text{C}/\text{min}$
final temperature	200 $^{\circ}\text{C}$	200 $^{\circ}\text{C}$
final time	5.00 min	5.00 min

The gas chromatographs are equipped with an enhanced integrator tool set for identification and quantification purposes.

The samples were withdrawn manually after equilibration with a preheated needle in order to avoid phase separation during sampling. Prior to analysis, acetone was added to the sample of both phases to ensure a homogeneous phase before injection into the glc

(Figure 3.1). For the glycol phase the mass of acetone added was equal to the mass of sample, and acetone equal to 1/3 mass of sample was added to the hydrocarbon sample. In principle, there should be no uncertainty connected with the concentration determination as a result of adding acetone since the calculations were normalized not to include acetone. Nevertheless, to eliminate that uncertainty, the mass of acetone added to the standard samples (for constructing the calibration curve) was the same amount as that added to the withdrawn samples. Improved analysis results were obtained when the standard samples were analyzed at the same time as the actual samples. The standard samples were prepared by dissolving the analyte in acetone after which the second component was added. All three chemicals that constitute the standard mixture were weighted and the uncertainty of the weight was 3 % for the utmost diluted standard sample.

The reproducibility of the gas chromatographs ranged to 5 % for the worst case and 1 to 2 % in most cases. The enhanced integrator was used to optimize the area calculation and the samples were injected into the gas chromatograph automatically. As a result, an internal standard was unnecessary.

The calibration curves for all the considered components were linear. As an example, figures 3.2a and 3.2b show the calibration curve for ethylene glycol and heptane with their respective R^2 correlation values.

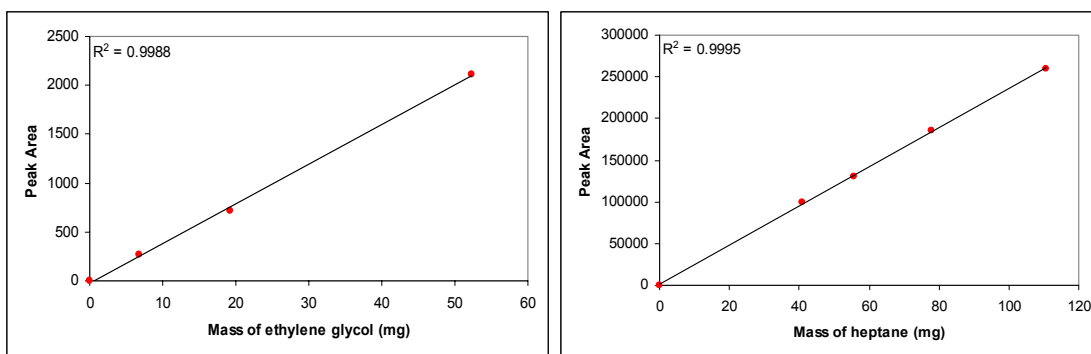


Figure 3.2a Calibration curve for ethylene glycol. **Figure 3.2b** Calibration curve for heptane with glc B. with glc A.

The composition in each phase was calculated according to the normalization method, where acetone was excluded from the calculation. The composition of the glycols and the hydrocarbons as function of temperature was determined within an uncertainty of 2% and 5%, respectively.

Figure 3.3 shows a representative gas chromatogram (obtained from glc A) for the heptane-acetone-ethylene glycol (MEG) mixture and the quantification report of heptane in ethylene glycol.

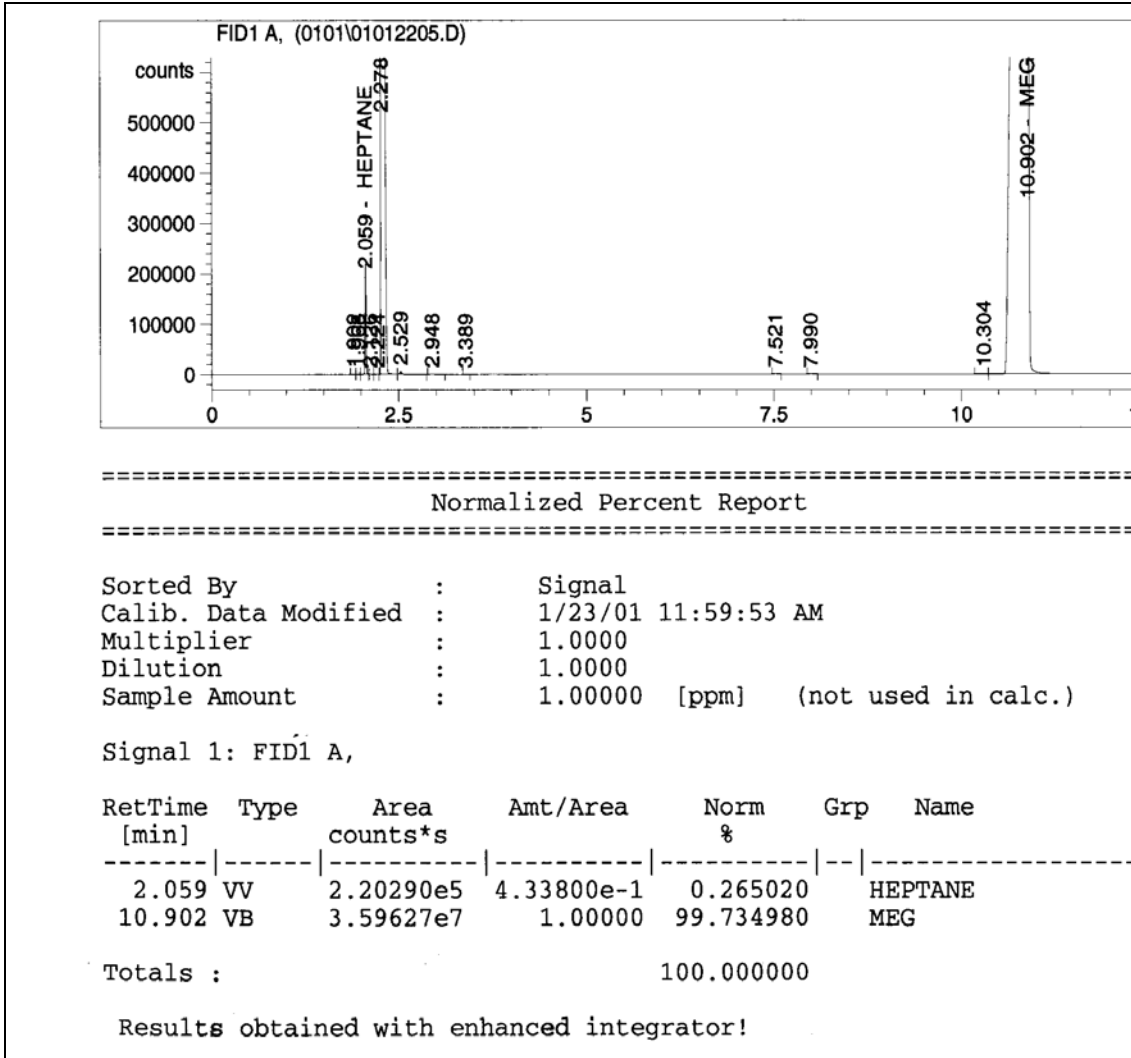


Figure 3.3 Gas chromatogram (for glc A) with the quantification report of heptane in ethylene glycol.

The equation used to calculate the mass fraction w of an analyte i is:

$$w_i = \frac{A_i \cdot RF_i}{\sum_{i=1}^2 (A_i \cdot RF_i)} \quad (3.1)$$

where A_i (denoted Area in figure 3.3) is the peak area of component i , and RF_i (denoted Amt/Area in figure 3.3) is the response factor of component i .

3.3 Results and Data Correlation

3.3.1 Experimental Results

The mutual solubility data for monoethylene glycol and different hydrocarbons (heptane, methylcyclohexane, and hexane) as function of temperature are given in Table 3.3.

Table 3.3 Mutual solubility data of the monoethylene glycol (1) + hydrocarbon (2) systems expressed in mass fraction (w) as function of temperature. I = glycol-rich phase and II = hydrocarbon-rich phase

	t (°C)	$100w_1^{II}$	$100w_2^I$
heptane	42.8	0.0198	0.1478
	49.6	0.0287	0.1532
	56.6	0.0399	0.1760
	63.4	0.0553	0.1903
	68.0	0.0677	0.2024
	73.8	0.0867	0.2119
	78.7	0.1066	0.2238
methylcyclohexane	39.5	0.0176	0.3591
	45.3	0.0238	0.3741
	51.3	0.0313	0.4085
	59.2	0.0446	0.4556
	68.9	0.0677	0.4937
	78.7	0.0971	0.5931
hexane	34.8	0.0153	0.1889
	39.6	0.0202	0.2085
	44.5	0.0250	0.2137
	49.3	0.0327	0.2239
	57.2	0.0472	0.2343

The mutual solubility data for different glycols (propylene glycol, diethylene glycol, triethylene glycol, and tetraethylene glycol) and n-heptane as function of temperature are given in Table 3.4.

Table 3.4 Mutual solubility data of the glycol (1) + heptane (2) systems expressed in mass fraction (w) as function of temperature. I = glycol-rich phase and II = hydrocarbon-rich phase

	t (°C)	$100w_1^{II}$	$100w_2^I$
propylene glycol	34.9	0.0634	1.0948
	39.7	0.0806	1.2506
	44.5	0.1110	1.4807
	49.4	0.1247	1.5465
	59.2	0.1970	1.8377
	68.9	0.2849	2.0197
	78.7	0.4218	2.0662
diethylene glycol	39.6	0.0523	0.6699
	49.9	0.0785	0.7751
	59.9	0.1223	0.8356
	69.9	0.1779	0.8730
	79.9	0.2526	1.0227
triethylene glycol	36.2	0.0914	0.7478
	42.6	0.1150	0.8484
	48.9	0.1456	0.9460
	57.9	0.2073	1.0639
	68.0	0.2864	1.2095
	77.8	0.3928	1.3107
tetraethylene glycol	32.5	0.3043	1.0268
	38.0	0.3557	1.0783
	43.8	0.4217	1.1836
	48.8	0.4628	1.2123
	56.9	0.5599	1.3643
	65.4	0.6404	1.5079
	74.8	0.7699	1.6864
	80.4	0.8702	1.8350

Figure 3.4 shows a comparison of the solubility of monoethylene glycol in n-heptane. It can be seen that the experimental results obtained in this work are in excellent agreement with the data from the literature.

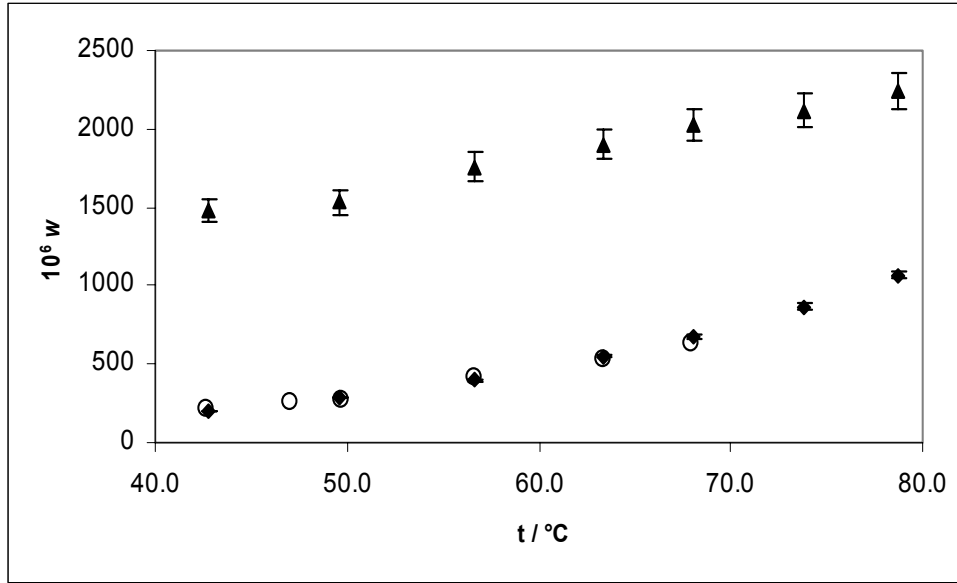


Figure 3.4 Mutual solubility of the monoethylene glycol (1) + heptane (2) system: \blacklozenge , w_1^{II} , this work; \blacktriangle , w_2^I , this work; \circ , w_1^{II} , Staveley and Milward¹. I = glycol-rich phase and II = hydrocarbon-rich phase.

3.3.2 Data Correlation

The experimental data were correlated using the NRTL⁴ and the UNIQUAC⁵ model. Several versions of these models are found in the literature with different expression for describing the temperature dependency of the binary interaction parameters. The ones used here are outlined below. The excess Gibbs energy for the NRTL model is given by

$$\frac{g_{NRTL}^E}{RT} = \sum_{i=1}^m x_i \frac{\sum_{j=1}^m \tau_{ji} G_{ji} x_j}{\sum_{l=1}^m G_{li} x_l} \quad (3.2)$$

$$G_{ij} = \exp(-\alpha_{ij} \tau_{ij}), \quad (\alpha_{ij} = \alpha_{ji}) \quad (3.3)$$

$$\tau_{ij} = a_{ij} + \frac{b_{ij}}{T} \quad (3.4)$$

where x_i is the mole fraction of component i , α_{ij} is the non-randomness parameter, and τ_{ij} is the interaction parameter. For a binary mixture, the NRTL model contains five parameters, two binary interaction parameters for each component and the non-randomness parameter for the binary mixture. The non-randomness parameter is

between 0 and 1, and a recommended value by Renon and Prausnitz⁴ is 0.2 for LLE. However, in this work this parameter is optimised along with the other binary interaction parameters.

The excess Gibbs energy for the UNIQUAC model is given by

$$\frac{g_{UNIQUAC}^E}{RT} = \frac{g^E(c)}{RT} + \frac{g^E(r)}{RT} \quad (3.5)$$

$$\frac{g^E(c)}{RT} = \sum_{i=1}^m x_i \ln \frac{\Phi_i}{x_i} + \frac{Z}{2} \sum_{i=1}^m q_i x_i \ln \frac{\theta_i}{\Phi_i} \quad (3.6)$$

$$\frac{g^E(r)}{RT} = - \sum_{i=1}^m q_i x_i \ln \left(\sum_{j=1}^m \theta_j \tau_{ji} \right) \quad (3.7)$$

where $g^E(c)$ and $g^E(r)$ are the combinatorial and the residual contributions. The segment fraction Φ and the area fraction θ are given by

$$\Phi_i = \frac{r_i x_i}{\sum_{j=1}^m r_j x_j}, \quad \theta_i = \frac{q_i x_i}{\sum_{j=1}^m q_j x_j} \quad (3.8)$$

$$\tau_{ij} = \exp \left[- \frac{U_{ij}}{T} \right] \quad (3.9)$$

$$U_{ij} = a_{ij} \quad (UQ 2) \quad (3.10)$$

$$U_{ij} = a_{ij} + b_{ij} T \quad (UQ 4) \quad (3.11)$$

where r_i and q_i are pure-component relative volume and surface area parameters, respectively, and τ_{ij} is the interaction parameter. The coordination number Z was set to 10. Two parameters, U_{ij} and U_{ji} , are required for each binary mixture. These parameters are temperature dependent as described above.

The parameters in both models were found by minimising the objective function

$$F = \sum_{i=1}^{NP} \sum_{j=1}^{NOC} \left(1 - \frac{K_{D_{ij}^{calc}}}{K_{D_{ij}^{exp}}} \right)^2 \quad (3.12)$$

where NP is the number of experimental data points, NOC is number of components, and K_D is the distribution coefficient defined as the ratio between mole fraction i in phase I and mole fraction i in phase II .

Minimisation of the objective function was implemented with the commercial software PRO/II⁶ of SimSci. The optimisation of the 5-parameter NRTL equation and the 4-parameter UNIQUAC model (UQ 4) has led to multiple sets of parameters when different initial estimates of the parameters are used. The parameters, which were selected, were those which yielded the best fit and the lowest relative deviation. Nevertheless, the parameters obtained from the 2-parameter UNIQUAC model (UQ 2) were unique even with different initial estimates. In Tables 3.5 and 3.6, the optimised values of the interaction parameters for the UNIQUAC and NRTL models are given.

Table 3.5 Interaction parameters for the temperature-independent UNIQUAC model (UQ 2) and the temperature-dependent (UQ 4) for the glycol (i) + hydrocarbon (j) systems

system	model type	binary interaction parameters			
		a_{ij} / K	a_{ji} / K	b_{ij}	b_{ji}
monoethylene glycol (i) + heptane (j)	UQ 2	226.63	909.07		
	UQ 4	162.12	2116.6	0.19139	-3.557
monoethylene glycol (i) + methylcyclohexane(j)	UQ 2	215.42	916.96		
	UQ 4	171.9	2090.7	0.12097	-3.4972
monoethylene glycol (i) + hexane (j)	UQ 2	248.19	916.77		
	UQ 4	139.50	2232.0	0.34445	-3.9751
propylene glycol (i) + heptane (j)	UQ 2	63.55	667.37		
	UQ 4	186.51	1309.9	-0.38902	-1.9005
diethylene glycol (i) + heptane (j)	UQ 2	97.42	543.25		
	UQ 4	33.014	1150.1	0.18988	-1.7972
triethylene glycol (i) + heptane (j)	UQ 2	102.09	359.05		
	UQ 4	56.79	725.57	0.13587	-1.1052
tetraethylene glycol (i) + heptane (j)	UQ 2	132.22	208.10		
	UQ 4	74.2	348.57	0.1765	-0.42884

Table 3.6 Interaction parameters for the temperature dependent NRTL model for the glycol (*i*) + hydrocarbon (*j*) systems. α_{ij} is the nonrandomness parameter.

system	binary interaction parameters				α_{ij}
	a_{ij}	a_{ji}	b_{ij} / K	b_{ji} / K	
monoethylene glycol (<i>i</i>) + heptane (<i>j</i>)	0.76226	-7.9586	1924.3	4938.4	0.39867
monoethylene glycol (<i>i</i>) + methylcyclohexane (<i>j</i>)	0.040125	-8.1325	1281.9	4487.9	0.18264
monoethylene glycol (<i>i</i>) + hexane (<i>j</i>)	0.84609	-7.7434	1716.7	4823.1	0.38069
propylene glycol (<i>i</i>) + heptane (<i>j</i>)	-1.9112	-6.4613	2055.9	3954.8	0.40
diethylene glycol (<i>i</i>) + heptane (<i>j</i>)	-1.6333	-7.6360	1790.7	4378.1	0.27906
triethylene glycol (<i>i</i>) + heptane (<i>j</i>)	-2.4885	-5.441	1853.7	3557.9	0.2691
tetraethylene glycol (<i>i</i>) + heptane (<i>j</i>)	-1.3819	-2.0214	1310.9	2201.6	0.2677

Table 3.7 gives the percentage average absolute deviation, AAD (%), of the composition in both phases over the considered temperature range with the three models.

Table 3.7 AAD (%) for the seven binary systems considered with the three activity coefficient models.

I = glycol-rich phase and *II* = hydrocarbon-rich phase

system	UQ 2		UQ 4		NRTL	
	<i>I</i>	<i>II</i>	<i>I</i>	<i>II</i>	<i>I</i>	<i>II</i>
monoethylene glycol (<i>i</i>) + heptane (<i>j</i>)	1.2	31.5	1.6	1.5	1.6	1.0
monoethylene glycol (<i>i</i>) + methylcyclohexane (<i>j</i>)	3.4	32.7	2.8	2.2	1.6	1.1
monoethylene glycol (<i>i</i>) + hexane (<i>j</i>)	2.0	19.0	2.0	1.5	2.4	2.3
propylene glycol (<i>i</i>) + heptane (<i>j</i>)	12.0	40.3	6.1	6.0	4.8	7.6
diethylene glycol (<i>i</i>) + heptane (<i>j</i>)	2.7	28.0	2.4	1.5	4.3	2.0
triethylene glycol (<i>i</i>) + heptane (<i>j</i>)	4.8	21.6	2.5	1.3	2.3	1.0
tetraethylene glycol (<i>i</i>) + heptane (<i>j</i>)	1.7	5.4	1.3	3.7	1.1	3.2

Both the NRTL model and the UQ 4 model predict the experimental data for both phases with an AAD of 3 %, while the deviation is 15 % for the UQ 2 model. However, the deviation is only 4 % for the glycol-rich phase for the UQ 2 model. In Figure 3.5,

the NRTL model is compared to the experimental data for the monoethylene glycol + heptane system.

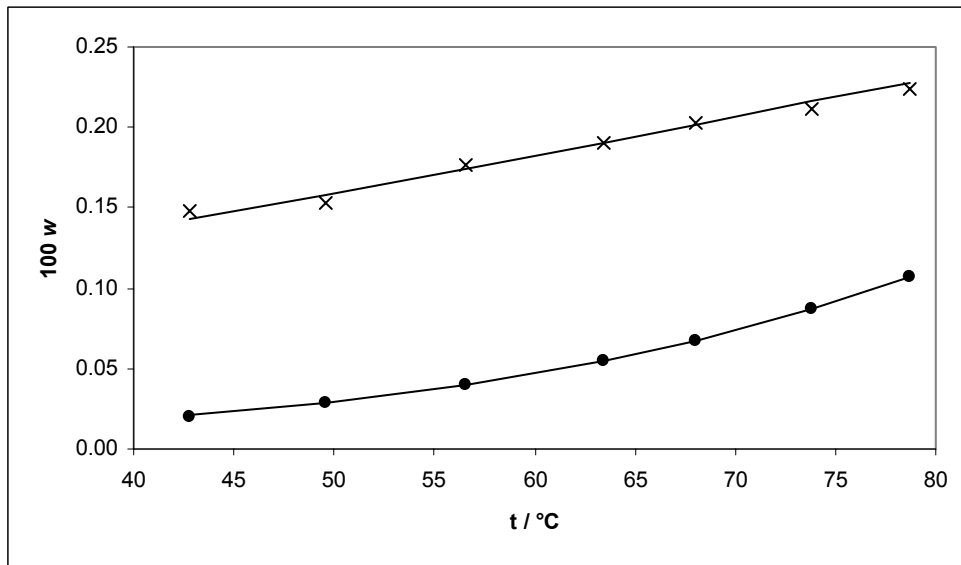


Figure 3.5 Modelling of the LLE split for the monoethylene glycol (1) + heptane (2) system.

●, w_1^{II} , experimental; ×, w_2^I , experimental; solid lines, NRTL model. *I* = glycol-rich phase and *II* = hydrocarbon-rich phase.

The two UNIQUAC models are compared with the experimental data for the same system in Figure 3.6.

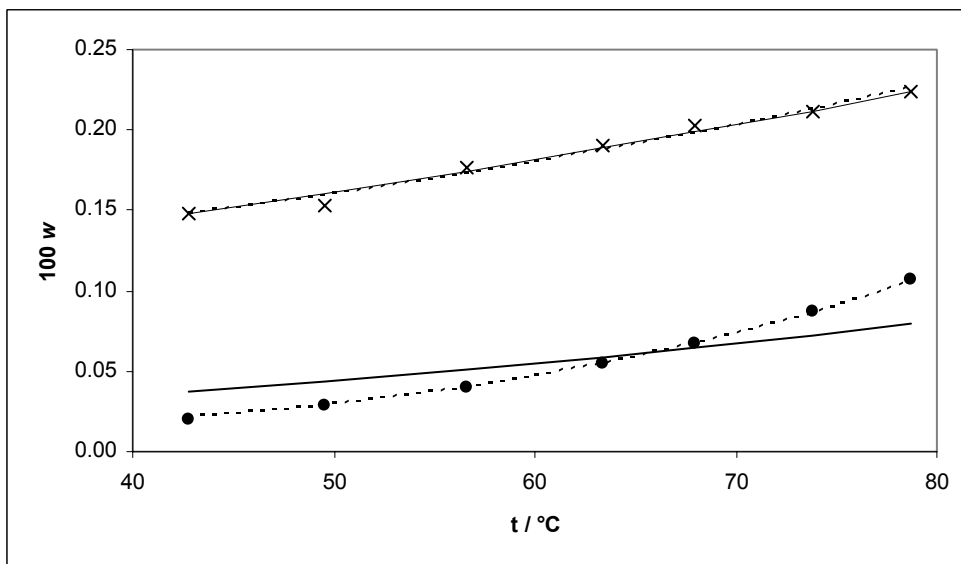


Figure 3.6 Modelling of the LLE split for the monoethylene glycol (1) + heptane system (2).

●, w_1^{II} , experimental; ×, w_2^I , experimental; solid lines, UNIQUAC 2 model; dashed lines, UNIQUAC 4 model. *I* = glycol-rich phase and *II* = hydrocarbon-rich phase.

Both the NRTL and the UNIQUAC 4 models give an excellent correlation of the experimental solubility data for both the liquid phases. UNIQUAC 2, however, has some difficulty in predicting correctly the solubility of monoethylene glycol in n-heptane.

3.4 Conclusions

Liquid-liquid equilibrium data for seven binary glycol + hydrocarbon systems were measured in the temperature range 32 °C to 80 °C using glc for the analysis. The measured data was successfully correlated with the temperature-dependent UNIQUAC and NRTL models. The temperature-independent UNIQUAC model was not as successful.

References

- (1) Staveley, L. A. K.; Milward, G. L. Some thermodynamic properties of glycols in benzene, heptane, and cyclohexane. *J. Chem. Soc.* **1957**, 4369.
- (2) Rawat, B. S.; Prasad, G. Liquid-liquid equilibria for benzene-n-heptane systems with triethylene glycol, tetraethylene glycol, and sulfolane containing water at elevated temperatures. *J. Chem. Eng. Data.* **1980**, *25*, 227-230.
- (3) Johnson, G. C.; Francis, A. W. Ternary liquid system, benzene-heptane-diethylene glycol. *Ind. Eng. Chem.* **1954**, *46*, 1662-1668.
- (4) Renon, H.; Prausnitz, J. M. Local compositions in thermodynamic excess functions for liquid mixtures. *AIChE J.* **1968**, *14*, 135-144.
- (5) Abrams, D. S.; Prausnitz, J. M. Statistical thermodynamic of liquid mixtures: a new expression for the excess Gibbs energy of partly or completely miscible systems. *AIChE J.* **1975**, *21*, 116-128.
- (6) Simulation software *PRO/II* of SimSci (version 5.11). Simulations sciences Inc., 601 S. Valencia Avenue, Brea, CA 92621, USA.

Chapter 4

Application of the CPA Equation of State to Glycol-Hydrocarbons Liquid-Liquid Equilibria

The CPA equation of state is a thermodynamic model, which combines the well-known cubic SRK equation of state and the association term proposed by Wertheim, typically employed in models like SAFT. CPA has been shown in the past to be a successful model for phase equilibria calculations for systems containing water, hydrocarbons and alcohols. In this work, CPA is applied for the first time to liquid-liquid equilibria for systems containing glycols and hydrocarbons. It is shown that excellent correlation is achieved with solely a single interaction parameter per binary system. The correlation procedure as well as the nature of the experimental data play a crucial role in the parameter estimation and they are thus extensively discussed.

4.1 Introduction

Equations of state have traditionally been applied to modelling systems with non-polar and slightly polar compounds. For associating compounds, however, a new concept has evolved in recent years with the development of equations of state combining the physical effects from the classical models and a chemical contribution¹. An example of this new concept is an equation of state abbreviated CPA – Cubic Plus Association. CPA has been applied extensively to the modelling of vapour–liquid equilibria (VLE) for alcohol–hydrocarbon systems², in correlating liquid–liquid equilibria (LLE) for alcohol–hydrocarbon mixtures³, as well as for binary aqueous systems containing hydrocarbons⁴.

The CPA model has also been applied to the multicomponent systems, namely prediction of VLE and LLE for ternary mixtures consisting of water–alcohol–hydrocarbons, including the prediction of the partitioning of methanol between water and hydrocarbons^{5,6}.

The applicability of the CPA model has been so far limited to associating systems containing water, methanol and other alcohols. For the first time here, phase equilibria calculations with CPA are carried out for systems containing glycols and glycol-ethers. Glycols are used in the oil and the gas industry for several operational purposes. Ethylene glycol (MEG) is used to prevent gas hydrate formation. MEG has also been added to water for the purpose of depressing the freezing point of water. Diethylene glycol and triethylene glycol have been long used for the dehydration of natural gas. If the water is not removed from natural gas this could cause hydrate formation at high pressure and low temperature and corrossions in the transportation lines.

The purpose of this work is to extend the ability of CPA to calculating liquid – liquid phase equilibria for glycol-hydrocarbon systems. The development of the CPA model implies parameterisation of the model based on pure-compound liquid densities and vapour pressures. Such parameterisation is essential for future extension of the model to multicomponent systems involving glycols, water and hydrocarbons, which can be considered as the ultimate goal of this project.

4.2 The CPA Equation of State - Model Description

The Cubic-Plus-Association (CPA) model is an equation of state that combines the simplicity of a cubic equation of state (the Soave-Redlich-Kwong) and an association (chemical) term. While the SRK model accounts for the physical interaction contribution between the species, the association term in CPA takes into account the specific site-site interaction due to hydrogen bonding between like molecules (self-association) and unlike molecules (cross-association or solvation).

The association term employed in CPA is identical with the one used in SAFT, and has been derived from statistical mechanics by Wertheim (1987)⁷ based on the first order perturbation theory. Chapman et al. (1989, 1990)^{8,9} simplified Wertheim's theory using

the first-order thermodynamic perturbation theory (TPT-1), which allows chainlike and treelike clusters but not closed loops. In addition, the activity of each bonding site in a molecule is independent of the other bonding sites of the same molecule. Thus, steric self-hindrances are neglected.

The CPA equation of state can be expressed in terms of the compressibility factor Z as

$$Z = Z^{SRK} + Z^{assoc}$$

The compressibility factor contribution from the SRK equation of state is

$$Z^{SRK} = \frac{V_m}{V_m - b} - \frac{a(T)}{RT(V_m + b)} \quad (4.1)$$

and the contribution from the association term is given by

$$Z^{assoc} = \sum_i x_i \sum_i \rho_i \sum_{A_i} \left[\left(\frac{1}{X_{A_i}} - \frac{1}{2} \right) \frac{\partial X_{A_i}}{\partial \rho_i} \right] \quad (4.2)$$

where V_m is the molar volume, X_{A_i} is the mole fraction of the molecule i not bonded at site A , i.e. the monomer fraction, and x_i is the superficial (apparent) mole fraction of component i . The small letters i and j are used to index the molecules, and capital letters A and B are used to index the bonding sites on a given molecule.

X_{A_i} , which is the key parameter in the association term, is calculated by solving the following set of equations

$$X_{A_i} = \frac{1}{1 + \rho \sum_j x_j \sum_{B_j} X_{B_j} \Delta^{A_i B_j}} \quad (4.3)$$

where B_j indicates summation over **all** sites.

$\Delta^{A_i B_j}$, the association (binding) strength between site A on molecule i and site B on molecule j is given by

$$\Delta^{A_i B_j} = g(\rho)^{ref} \left[\exp\left(\frac{\varepsilon^{A_i B_j}}{RT}\right) - 1 \right] b_{ij} \beta^{A_i B_j} \quad (4.4)$$

$\varepsilon^{A_i B_j}$ and $\beta^{A_i B_j}$ are the association energy and volume of interaction between site A of molecule i and site B of molecule j , respectively, and $g(\rho)^{ref}$ is the radial distribution function for the reference fluid.

CPA uses the hard-sphere radial distribution function that is given by

$$g(\rho) = \frac{2-\eta}{2(1-\eta)^3} \quad \eta = \frac{1}{4}b\rho \quad (4.5)$$

where η is the reduced fluid density.

The employment of the hard-sphere radial distribution function is an approximation since CPA employs the van der Waals repulsive term of SRK and not the more rigorous Carnahan-Starling term for the hard-sphere fluid.

Kontogeorgis et al.⁶ proposed a simplified version of the radial distribution function, which provides similar values but offers some computational advantages:

$$g(\rho) = \frac{1}{1-1.9\eta} \quad \eta = \frac{1}{4}b\rho \quad (4.6)$$

All phase equilibria calculations performed in this thesis are based on the simplified CPA model (referred to as sCPA) employing the simplified radial distribution function, Eq. (4.6).

In the calculation of the fugacity coefficient in phase equilibria calculations, the Newton-Raphson iteration method is applied to calculate the volume from the CPA equation of state. This method needs the first and second derivatives of X_{A_i} with respect to the density, and as seen in Eq. (4.2) this calculation is not quite straightforward, especially for the second derivative. Yakoumis et al.⁴ and Michelsen and Hendriks (2001)¹⁰ proposed a much simpler general expression for the association term

$$Z^{assoc} = -\frac{1}{2} \left(1 + \rho \frac{\partial \ln g}{\partial \rho} \right) \sum_i x_i \sum_{A_i} (1 - X_{A_i}) \quad (4.7)$$

The derivation of the pressure and chemical potential for the association term using Michelsen and Hendriks' simpler approach is shown in Appendix A.

It is evident from Eq. (4.7) that for non-associating compounds the association term is zero, and the SRK model is retained.

The energy parameter $a(T)$ in the SRK part is given by a Soave-type temperature dependency as follows

$$a = a_0(1 + c_1(1 - \sqrt{T_r}))^2 \quad (4.8)$$

while b is temperature independent.

The CPA model has five pure-compound parameters; three for non-associating compounds (a_0 , b , c_1) and two additional parameters for associating compounds (ε^{A,B_j} , β^{A,B_j}). The five pure-compound parameters are usually obtained by fitting experimental vapor pressure and saturated liquid density data. For non-associating compounds, the parameters can either be found from vapor pressures and liquid densities or from critical data and the acentric factor.

As seen by Eq. (4.7), the contribution of the association compressibility factor in CPA depends on the choice of association scheme i.e. number and type of association sites for the associating compound.

Huang and Radosz¹¹ have classified eight different association schemes, and in this work we have employed the so-called 2B and the 4C association schemes, which are hereafter explained

The 2B association scheme:

$$\begin{aligned} \Delta^{AA} &= \Delta^{BB} = 0 \\ \Delta^{AB} &\neq 0 \\ X_A &= X_B = \frac{-1 + \sqrt{1 + 4\rho\Delta^{AB}}}{2\rho\Delta^{AB}} \end{aligned} \quad (4.9)$$

The 4C association scheme:

$$\begin{aligned} \Delta^{AA} &= \Delta^{AB} = \Delta^{BB} = \Delta^{CC} = \Delta^{CD} = \Delta^{DD} = 0 \\ \Delta^{AC} &= \Delta^{AD} = \Delta^{BC} = \Delta^{BD} \neq 0 \\ X_A &= X_B = X_C = X_D = \frac{-1 + \sqrt{1 + 8\rho\Delta^{AC}}}{4\rho\Delta^{AC}} \end{aligned} \quad (4.10)$$

The capital letters A, B, C, and D are used to index the sites on a given molecule. The 2B scheme has been assigned to alcohols, and the 4C scheme for water and glycols. These schemes are in agreement with the accepted physical picture that alcohols form linear oligomers and water three-dimensional structures. As expected, the association

strength between two similar sites is zero since two lone pairs electrons or protons cannot attract each other. The attraction can only occur between a lone pair electron and a proton.

The extension of the CPA EoS to mixtures requires mixing rules only for the parameters of the SRK-part, while the extension of the association term to mixtures is straightforward. The mixing and combining rules for a and b are the classical van der Waals one-fluid ones

$$a = \sum_i \sum_j x_i x_j a_{ij} \quad (4.11)$$

$$b = \sum_i \sum_j x_i x_j b_{ij} \quad (4.12)$$

where the combining rules are given as

$$a_{ij} = \sqrt{a_i a_j} (1 - k_{ij}) \quad (4.13)$$

$$b_{ij} = \frac{b_i + b_j}{2} (1 - l_{ij}) \quad (4.14)$$

The binary interaction parameter for the co-volume l_{ij} is set to zero in this work resulting in a linear mixing rule for the b-parameter

$$b = \sum_i x_i b_i \quad (4.15)$$

4.3 Database Used in the Parameter Estimation

The five parameters of the CPA equation of state were determined by simultaneous regression of vapour pressures and saturated liquid densities. It was, thus, very important to verify the reliability of those pure-compound data. The DIPPR¹² database is typically employed as a source of “experimental” vapour pressure and liquid density data, often without appropriate critical evaluation. It has been established for instance, that the DIPPR expression for the liquid density for water could not, with a single set of parameters, accurately describe the physical behaviour of water’s density from the triple to the critical point. Three sets of parameters had to be employed at different temperature ranges to get an adequate description of the liquid density for water¹³.

Glycols are known to be very non-volatile compounds. Thus experimental measurements of their vapour pressures at low temperatures are quite uncertain,

especially in the vicinity of the triple point. At high temperatures, on the other hand, glycols tend to chemically decompose which again makes the measurement of their vapour pressure unreliable.

Two different DIPPR correlations from 1989 and 2001 were investigated and compared to the raw experimental data. In Figures 4.1 and 4.2 are shown the two DIPPR correlations together with the raw experimental data for ethylene glycol and tetraethylene glycol.

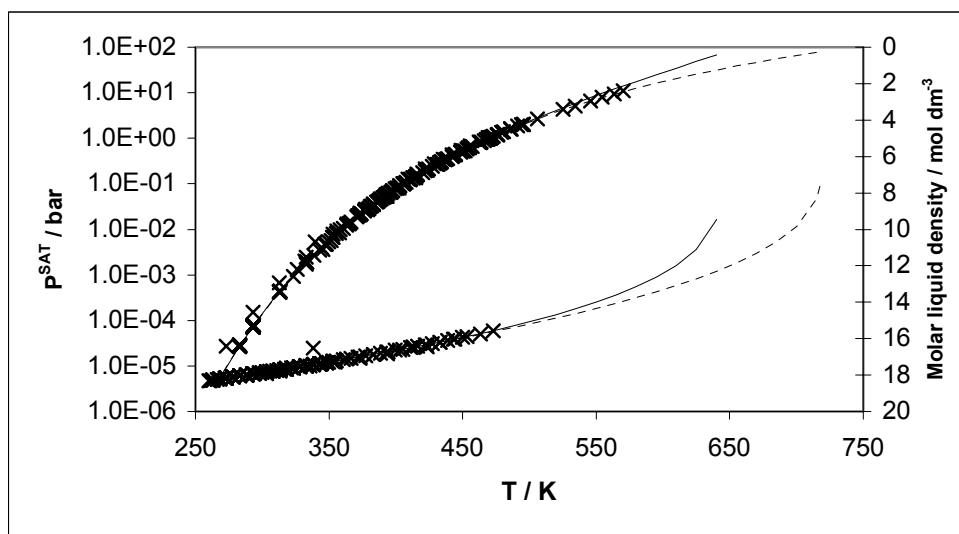


Figure 4.1 The difference between the DIPPR correlations for vapor pressure and liquid density for ethylene glycol: solid lines, DIPPR 1989; dashed lines, DIPPR 2001; x, experimental raw data.

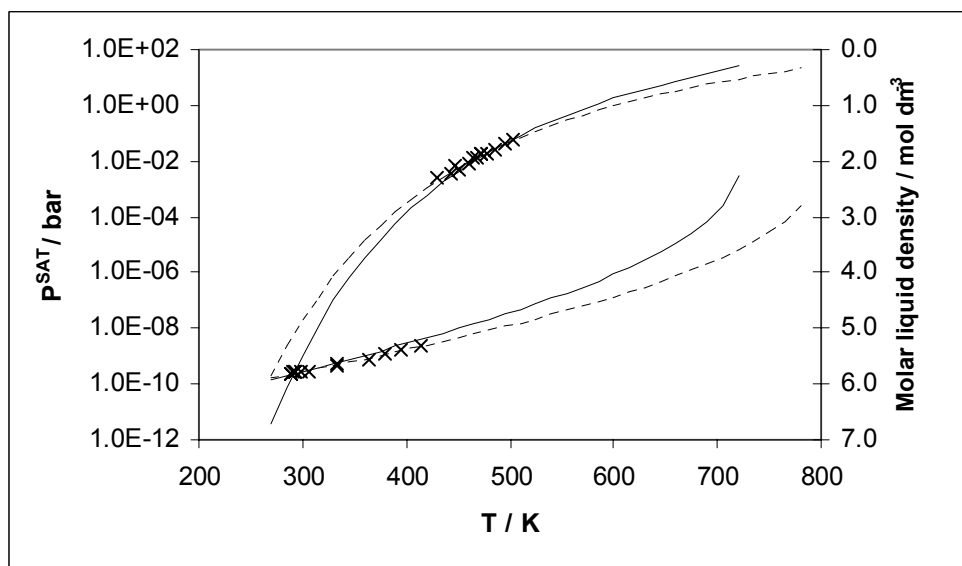


Figure 4.2 The difference between the DIPPR correlations for vapor pressure and liquid density for tetraethylene glycol: solid lines, DIPPR 1989; dashed lines, DIPPR 2001; x, experimental raw data.

These figures provide useful information that need to be carefully considered. It is observed that the DIPPR correlations extend much further than the actually measured data for the two considered physical properties, especially for tetraethylene glycol. The DIPPR equations provide both a correlation of the measured data and an extrapolation from the triple to the critical point at the same time. It can also be seen, that the two different DIPPR correlations only coincide at the temperature range where the measured data exist. The dissimilarity of the two DIPPR correlations is possibly due to the different critical points employed in the extrapolation. It is seen from Table 4.1 that the critical data, especially the critical temperatures, used in the most recent DIPPR correlation of 2001 are much closer to the experimental data obtained by Nikitin et al.¹⁴ compared to the DIPPR–1989 correlation.

Table 4.1 Critical pressures and temperatures from two DIPPR databases and the experimental data from Nikitin et al.¹⁴ for glycols. P X: P indicates predicted value obtained by the method of Lydersen and X indicates the reliability code given as: 1 < 0.2% error; 2 < 1%; 3 < 3%; 4 < 5%; 5 < 10%; 6 < 25%

compound	DIPPR database, 1989		DIPPR database, 2001		Nikitin et al., 1995	
	P _c (bar)	T _c (K)	P _c (bar)	T _c (K)	P _c (bar)	T _c (K)
ethylene glycol	75.3 (P 5)	645 (P 4)	82.0	720	82.0 ± 3	720 ± 11
1,2-propylene glycol	61.0 (P 5)	626 (P 4)	61.0 (P 5)	626 (P 4)	na ^a	na ^a
diethylene glycol	46.0 (P 5)	680 (P 3)	46.0 (P 5)	744.6	47.7 ± 2	753 ± 11
triethylene glycol	33.2 (P 6)	700 (P 5)	33.2 (P 6)	769.5	33.0 ± 1	797 ± 12
tetraethylene glycol	25.9 (P 5)	722 (P 4)	25.9 (P 5)	795 (P 4)	32.0 ± 1	800 ± 12

Thus, the determination of the CPA parameters has been based on the DIPPR–2001 version for all glycols. The constants for the DIPPR correlations and their uncertainties are tabulated in Table 4.2 on next page.

^a na: critical properties not available

Table 4.2 DIPPR–2001 correlation constants for the vapour pressure, P^S , and liquid density, ρ^L of glycols

	ethylene glycol		1,2-propylene glycol		diethylene glycol		triethylene glycol		tetraethylene glycol	
	P^S	ρ^L	P^S	ρ^L	P^S	ρ^L	P^S	ρ^L	P^S	ρ^L
A	84.09	1.315	212.8	1.0923	142.45	0.83692	152.48	0.59672	132.72	0.46246
B	-10411	0.25125	-15420	0.26106	-15050	0.26112	-16449	0.26217	-16634	0.26085
C	-8.1976	720	-28.109	626	-16.318	744.6	-17.67	769.5	-14.643	795
D	1.6536E-18	0.21868	2.1564E-5	0.20459	5.9506E-18	0.2422	6.4481E-18	0.24631	3.0521E-18	0.27179
E	6.0		2.0		6.0		6.0		6.0	
T_{\min} / K	260.2		213.2		262.7		266.0		268.2	
T_{\max} / K	720.0		626.0		744.6		769.5		795.0	
error	< 3%	< 1%	< 5%	< 3%	< 10%	< 3%	< 10%	< 3%	< 25%	< 5%

$$P^S = \exp\left(A + \frac{B}{T} + C \cdot \ln(T) + D \cdot T^E\right) \quad (\text{Pa})$$

$$\rho^L = \frac{A}{B \left(1 + \left(\frac{T}{C}\right)^D\right)} \quad (\text{mol dm}^{-3})$$

Nikitin et al.¹⁴ evaluated the error in the experimental determination of the critical pressure of glycols to be equal to $0.04 P_c$ (bar), and of the critical temperature equal to $0.015 T_c$ (K). These errors are listed in Table 4.1. It should be noted that the DIPPR correlations incorporate both the experimental uncertainty and the error of the DIPPR's equations. Thus, care should be exercised on the optimisation of the five CPA parameters based on DIPPR correlations so as to obtain physically meaningful parameters. How this is performed is discussed in a forthcoming section of the manuscript. When CPA parameters are optimised based on pure-compound vapour pressures and saturated liquid densities at different temperature ranges, it results in multiple sets of CPA parameters providing equally satisfactory correlation. The choice of the most successful parameter set needs, thus, to be based on other information e.g. liquid–liquid equilibrium data for glycol + hydrocarbon systems. Measurements of LLE for seven binary glycol + hydrocarbon systems have recently been published¹⁵.

An alternative way of selecting the appropriate set of CPA parameters is by testing their suitability for other – than phase equilibria – properties. Enthalpy, heat capacity and the second virial coefficient are some of the physical properties, which can be estimated by an equation of state. In this work, we considered the second virial coefficients, which can be obtained by DIPPR–2001. However, the correlations for the second virial coefficients provided for glycols were based on a group contribution (GC) method, developed by McCann et al.¹⁶, and not on measured data. McCann et al.¹⁶ report the accuracy of the GC method for glycols to be below 25%. Moreover, the group contribution approach is not based on glycol data at all, but only on seven datasets for alcohols¹⁷. To our knowledge, no experimental data for the second virial coefficient for glycols have been reported in the literature. Thus, the use of second virial coefficient data for selecting the appropriate glycol parameters does not seem to be a useful alternative to using mixture data.

4.4 Correlation of LLE - Choice of the Association Scheme for Glycols

The first step towards finding the five parameters of the CPA model is to assign the association scheme i.e. number of association sites and type of association for the considered compounds, namely the glycols in this study. In this work, both the two-site (2B) (Eq. 4.9) and the four-site (4C) (Eq. 4.10) association schemes were investigated. From a molecular structure point of view, it could be stated that since alcohols with one hydroxyl group (–OH) are being modelled with a 2B association scheme, then glycols with double hydroxyl groups and ether groups might be assigned a four-site association scheme. This is the case if steric hindrance and other effects are not considered. However, the actual association picture should be derived based on calculations for each glycol individually. Ethylene glycol is, from a molecular weight point of view, the smallest glycol containing two hydroxyl groups. The other glycols considered in this work are larger than ethylene glycol and they contain ether groups in addition to the two hydroxyl groups.

Thus, since ethylene glycol is the strongest association molecule of the series, the choice of the association scheme for all glycols was based on ethylene glycol.

Ethylene glycol was also selected for determining the nature of the association of glycols due to the abundance of experimental vapour pressure and liquid density data compared to other glycols. Furthermore, the experimental critical temperature and pressure for ethylene glycol have been used in the DIPPR correlation, whereas predicted values have been employed for the other glycols (Table 4.1).

An optimisation procedure was developed in this work, according to which the five CPA parameters were regressed based on reliable vapour pressure and liquid density data for the pure compounds. The objective function used is:

$$OF = \sum_{i=1}^{NP} \left(\frac{P_i^{Dippr} - P_i^{cal}}{P_i^{Dippr}} \right)^2 + \sum_{i=1}^{Ndat} \left(\frac{\rho_i^{Dippr} - \rho_i^{cal}}{\rho_i^{Dippr}} \right)^2 \quad (4.16)$$

where NP is the number of data points used in the regression. A step of $\Delta T_r = 0.01$ in the reduced temperature was used in the calculations corresponding to 7.2 °C for ethylene glycol. The reduced triple point temperature for ethylene glycol is 0.36.

The parameter estimation results for ethylene glycol obtained from the 2B and the 4C association schemes are tabulated in Tables 4.3 and 4.4, respectively.

Table 4.3 Optimized CPA parameters for ethylene glycol with the **2B** association scheme at four different temperature ranges based on pure-compound vapor pressure and saturated liquid density data

	Set 1	Set 2	Set 3	Set 4
a_0	13.6984	14.0009	13.5279	13.9928
b	0.0514	0.0508	0.0510	0.0517
c_1	0.8735	0.4941	0.6048	0.8882
ε	229.203	318.676	298.863	221.663
β	0.01396	0.0029	0.0048	0.0141
T_r range	0.40 – 0.90	0.36 – 0.90	0.36 – 0.99	0.45 – 0.99
ΔP (%) ^a	0.24	1.69	1.67	0.46
$\Delta \rho$ (%) ^b	0.66	1.23	1.14	0.67

Table 4.4 Optimized CPA parameters for ethylene glycol with the **4C** association scheme at four different temperature ranges based on pure-compound vapor pressure and saturated liquid density data

	Set 1	Set 2	Set 3	Set 4
a_0	7.1420	8.8661	8.2899	14.6970
b	0.0510	0.0500	0.0505	0.0525
c_1	1.7333	0.3362	0.6226	1.1099
ε	138.246	238.342	220.464	101.031
β	0.0839	0.0105	0.0159	0.0184
T_r range	0.40 – 0.90	0.36 – 0.90	0.36 – 0.99	0.45 – 0.99
ΔP (%) ^a	1.07	1.94	2.56	1.16
$\Delta \rho$ (%) ^b	0.51	1.90	1.90	0.72

^a Average absolute deviation in the vapor pressures

^b Average absolute deviation in the saturated liquid densities

The CPA parameters in Tables 4.3 and 4.4 are sets of the many equally satisfactorily parameters obtained from the optimization. All parameters were obtained solely from pure-compound vapor pressure and liquid density data as obtained from the DIPPR–2001 correlation. The raw data were not used. Figure 4.1 shows that the experimental measurements of the vapor pressure and saturated liquid density for ethylene glycol are only available up to 0.80 and 0.66 in reduced temperature. Tables 4.3 and 4.4 demonstrate that the optimized parameters are strongly affected by the chosen temperature interval. The co-volume parameter, however, is independent of the initial estimate and temperature range, in agreement to previous CPA investigations¹⁻³.

The selection of the “physically correct” parameters to be used for mixture calculations is not a simple task due the aforementioned uncertainties associated with the DIPPR correlations. The uncertainties of these correlations are estimated up to 3% for the vapor pressure and 1% for the saturated liquid density (Table 4.2). However, even such estimates of uncertainties are unclear due to lack of experimental data over extensive temperature ranges.

Consequently, due to these uncertainties, the selection of the truthful parameters of the CPA model cannot be solely based on vapor pressures and liquid densities. It is observed, for instance, from Table 4.2 that the uncertainty in the vapor pressure of diethylene glycol is less than 10% and for tetraethylene glycol is less than 25%. It is rather meaningless to estimate the model’s parameters from DIPPR correlations alone when so high uncertainties are associated with the so-called “experimental data”. Even if the uncertainty could be considered quite reasonable for parameter estimation, multiple sets of CPA parameters are obtained which correlate equally well the pure-compound experimental data. The CPA parameters in Tables 4.3 and 4.4 have been employed in the correlation of LLE for the ethylene glycol + n-heptane system. The results are shown graphically in Figures 4.3 – 4.10. The employed parameters for alkanes were obtained from Yakoumis et al.²

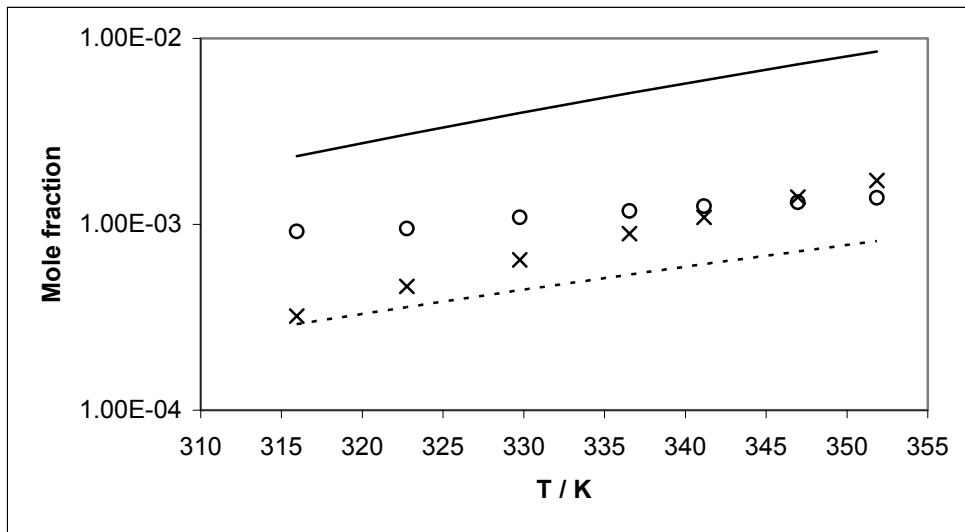


Figure 4.3 LLE for ethylene glycol (1) + n-heptane (2) system with CPA using the set 1 parameters for MEG from Table 4.3 with a $k_{ij} = 0.042$: \times , x_1^{II} , experimental; \circ , x_2^I , experimental; solid line, x_1^{II} , CPA; dashed line, x_2^I , CPA. I = Glycol-rich phase and II = Hydrocarbon-rich phase.

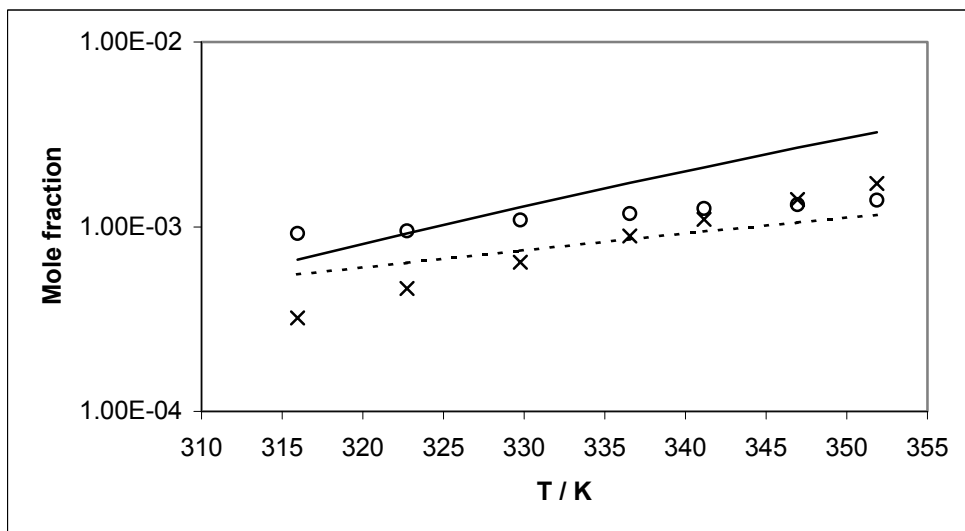


Figure 4.4 LLE for ethylene glycol (1) + n-heptane (2) system with CPA using the set 2 parameters for MEG from Table 4.3 with a $k_{ij} = 0.083$: \times , x_1^{II} , experimental; \circ , x_2^I , experimental; solid line, x_1^{II} , CPA; dashed line, x_2^I , CPA. I = Glycol-rich phase and II = Hydrocarbon-rich phase.

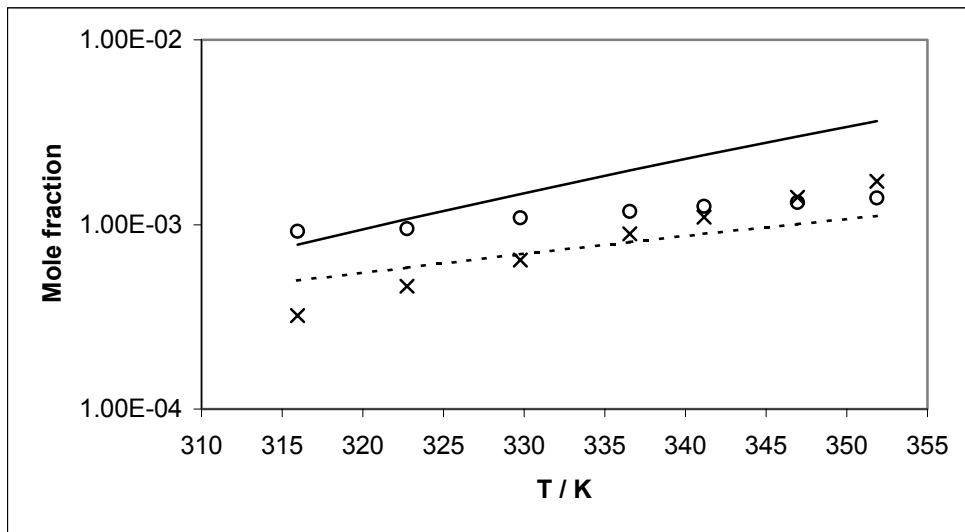


Figure 4.5 LLE for ethylene glycol (1) + n-heptane (2) system with CPA using the set 3 parameters for MEG from Table 4.3 with a $k_{ij} = 0.079$: \times , x_1^{II} , experimental; \circ , x_2^I , experimental; solid line, x_1^{II} , CPA; dashed line, x_2^I , CPA. I = Glycol-rich phase and II = Hydrocarbon-rich phase.

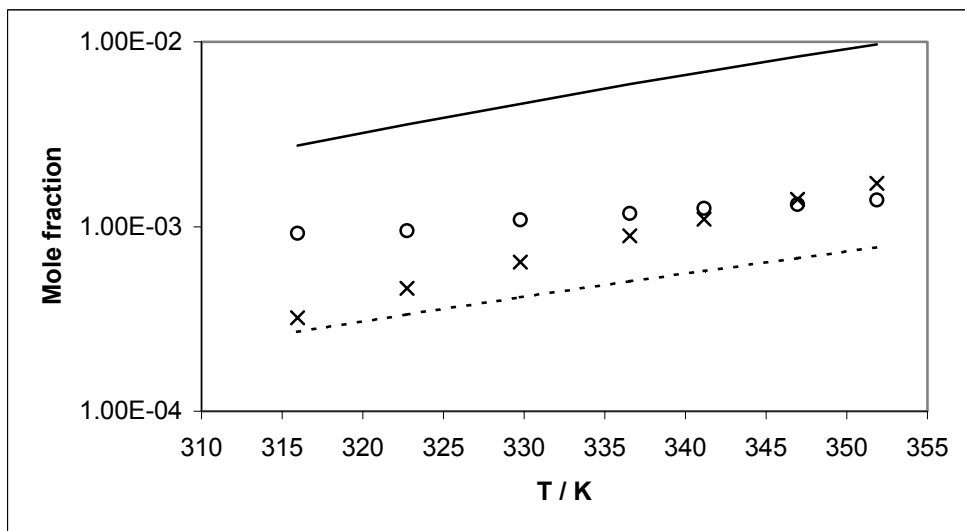


Figure 4.6 LLE for ethylene glycol (1) + n-heptane (2) system with CPA using the set 4 parameters for MEG from Table 4.3 with a $k_{ij} = 0.038$: \times , x_1^{II} , experimental; \circ , x_2^I , experimental; solid line, x_1^{II} , CPA; dashed line, x_2^I , CPA. I = Glycol-rich phase and II = Hydrocarbon-rich phase.

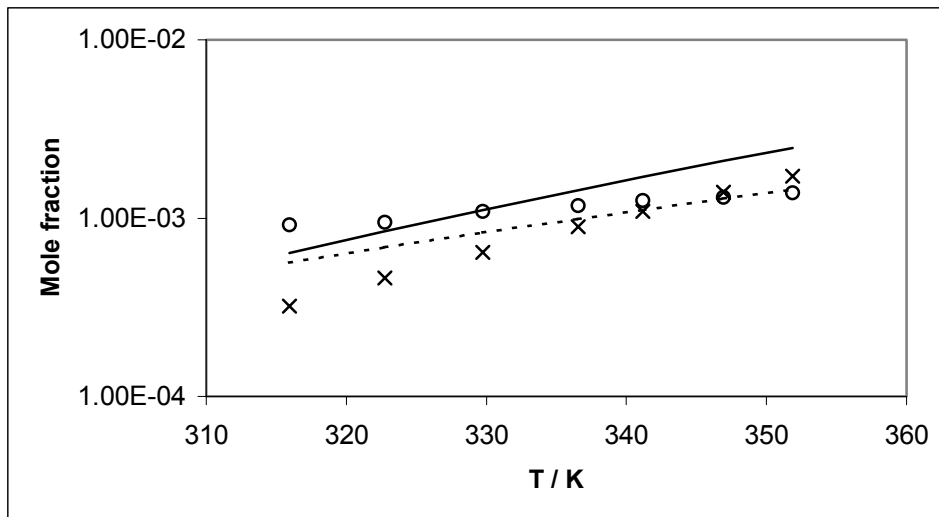


Figure 4.7 LLE for ethylene glycol (1) + n-heptane (2) system with CPA using the set 1 parameters for MEG from Table 4.4 with a $k_{ij} = 0.031$: \times , x_1^{II} , experimental; o , x_2^I , experimental; solid line, x_1^{II} , CPA; dashed line, x_2^I , CPA. I = Glycol-rich phase and II = Hydrocarbon-rich phase.

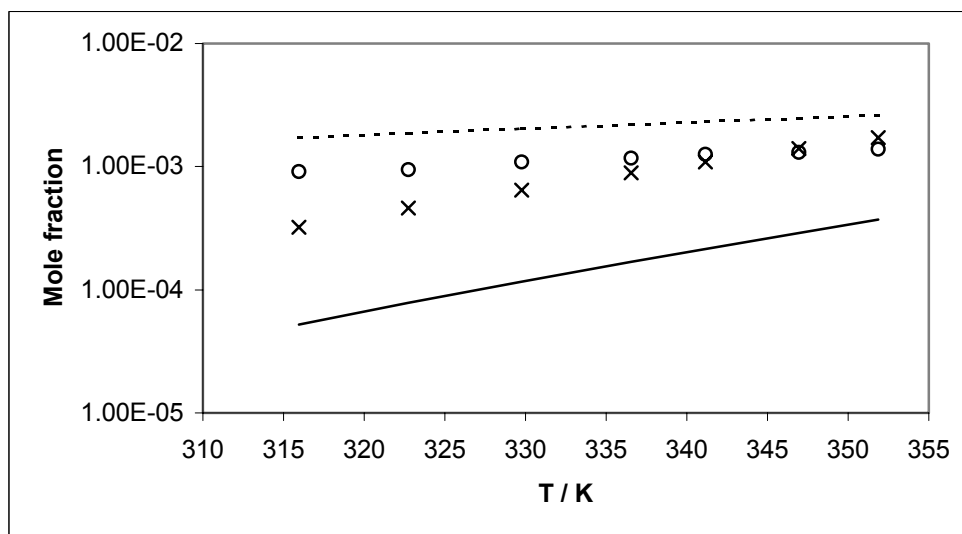


Figure 4.8 LLE for ethylene glycol (1) + n-heptane (2) system with CPA using the set 2 parameters for MEG from Table 4.4 with a $k_{ij} = 0.082$: \times , x_1^{II} , experimental; o , x_2^I , experimental; solid line, x_1^{II} , CPA; dashed line, x_2^I , CPA. I = Glycol-rich phase and II = Hydrocarbon-rich phase.

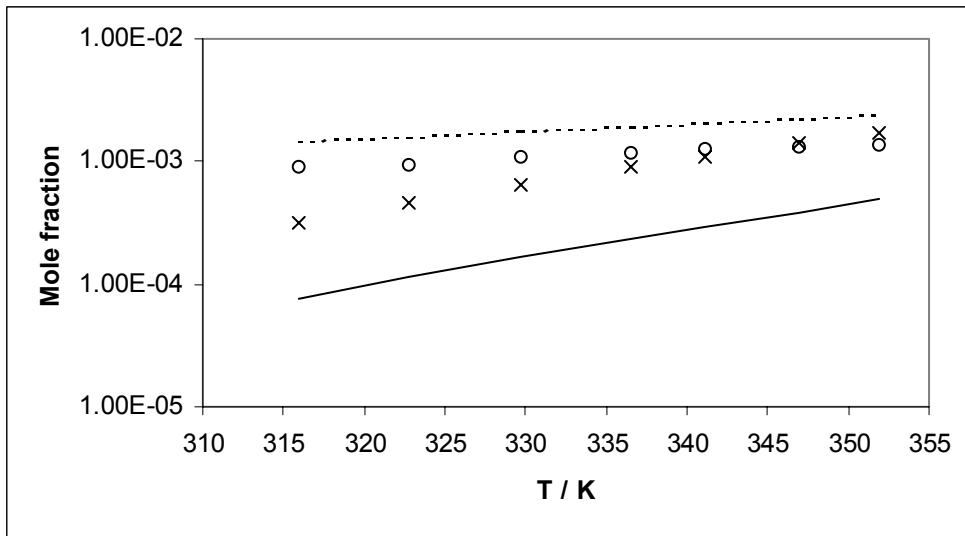


Figure 4.9 LLE for ethylene glycol (1) + n-heptane (2) system with CPA using the set 3 parameters for MEG from Table 4.4 with a $k_{ij} = 0.077$: \times , x_1^{II} , experimental; o , x_2^I , experimental; solid line, x_1^{II} , CPA; dashed line, x_2^I , CPA. I = Glycol-rich phase and II = Hydrocarbon-rich phase.

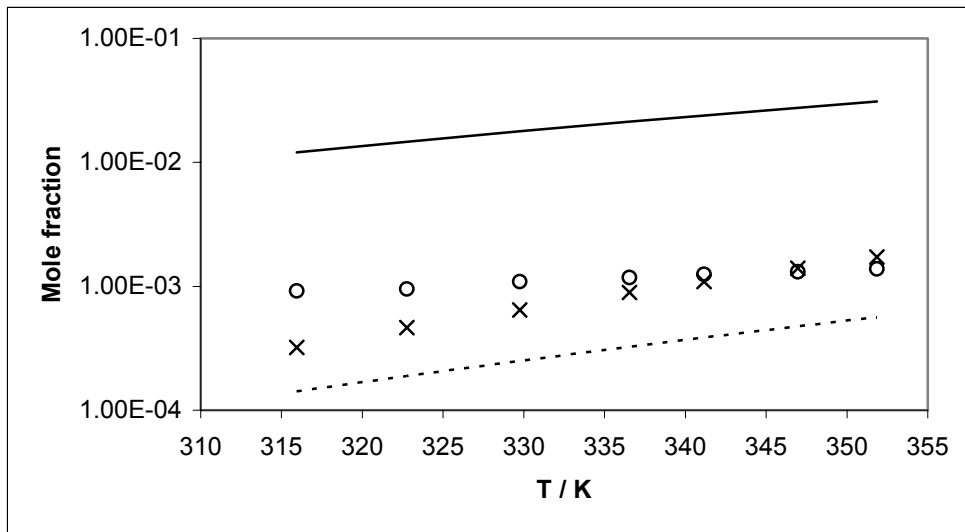


Figure 4.10 LLE for ethylene glycol (1) + n-heptane (2) system with CPA using the set 4 parameters for MEG from Table 4.4 with a $k_{ij} = -0.018$: \times , x_1^{II} , experimental; o , x_2^I , experimental; solid line, x_1^{II} , CPA; dashed line, x_2^I , CPA. I = Glycol-rich phase and II = Hydrocarbon-rich phase.

4.5 Correlation of LLE for Glycol - Hydrocarbon Systems

It has been pointed out previously that it is not sufficient to estimate the CPA parameters based solely on pure-compound vapour pressure and liquid density data due to the large uncertainty of the DIPPR correlations. This approach results in multiple sets of CPA parameters which provide excellent correlation of the DIPPR-generated data. Further restrictions need, thus, to be imposed on the parameter optimisation procedure by including binary LLE data in the optimisation between the considered glycol and an inert hydrocarbon (alkane). In this context, the binary LLE data have only been used to facilitate the selection of the physically correct parameter set among the multiple sets obtained, as well as to the selection of the suitable association scheme.

To illustrate that, the CPA parameters for ethylene glycol (MEG) were determined from pure-compound data and binary mutual solubility data for ethylene glycol and n-heptane and subsequently used to correlate LLE for MEG with two different hydrocarbons, n-hexane and methylcyclohexane. The CPA parameters for ethylene glycol and the temperature-independent binary interaction parameter for the ethylene glycol + n-heptane system are listed in Table 4.5.

Table 4.5 Optimised CPA parameters for glycols with the 4C association scheme based on pure-compound vapour pressure, saturated liquid density, and LLE data in addition to the binary interaction parameters between the glycols and n-heptane

	MEG	PG	DEG	TEG	Tetra-EG
a_0	10.819	13.836	26.408	39.126	46.654
B	0.0514	0.0675	0.0921	0.1321	0.1777
c_1	0.6744	0.9372	0.7991	1.1692	2.0242
ε	197.52	174.42	196.84	143.37	4.79
β	0.0141	0.0190	0.0064	0.0188	3.79
T_r range	0.40 – 0.90	0.44 – 0.77	0.49 – 0.86	0.49 – 0.82	0.54 – 0.90
ΔP (%)	0.90	4.78	1.77	3.04	0.49
$\Delta \rho$ (%)	1.58	1.50	1.58	1.61	2.26
k_{ij}	0.047	0.032	0.065	0.094	0.097
T_c (K)	720.0	626.0 (P 4)	744.6	769.5	795.0 (P 4)
P_c (bar)	82.0	61.0 (P 5)	46.0 (P 5)	33.2 (P 6)	25.9 (P 5)

The LLE correlation for all three systems is graphically shown in Figures 4.11 – 4.13. The CPA equation performs very satisfactory for all three binary systems with small and sound values of the binary interaction parameter.

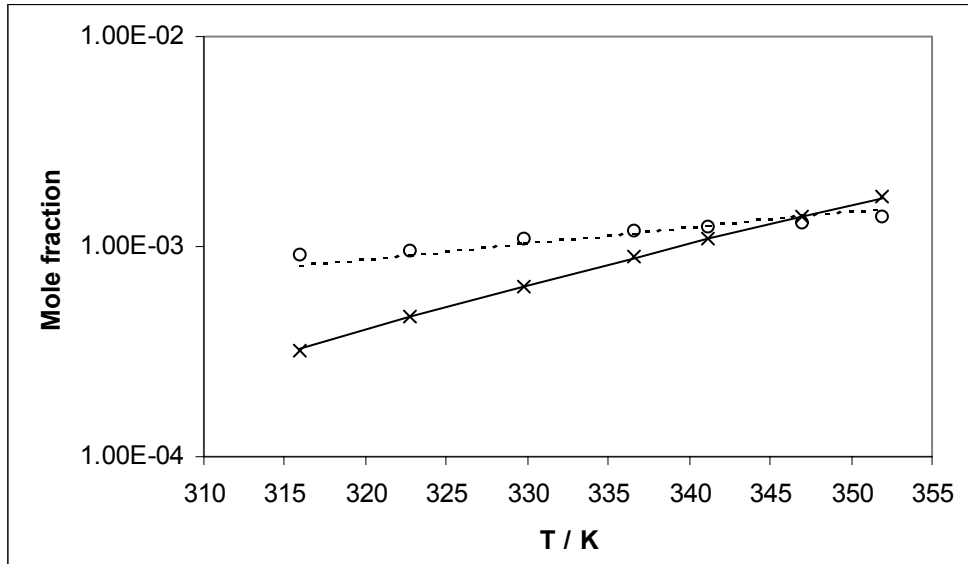


Figure 4.11 LLE for ethylene glycol (1) + n-heptane (2) system with CPA using parameters for MEG from Table 4.5 with a $k_{ij} = 0.047$: \times , x_1^{II} , experimental; o , x_2^I , experimental; solid line, x_1^{II} , CPA; dashed line, x_2^I , CPA. I = Glycol-rich phase and II = Hydrocarbon-rich phase.

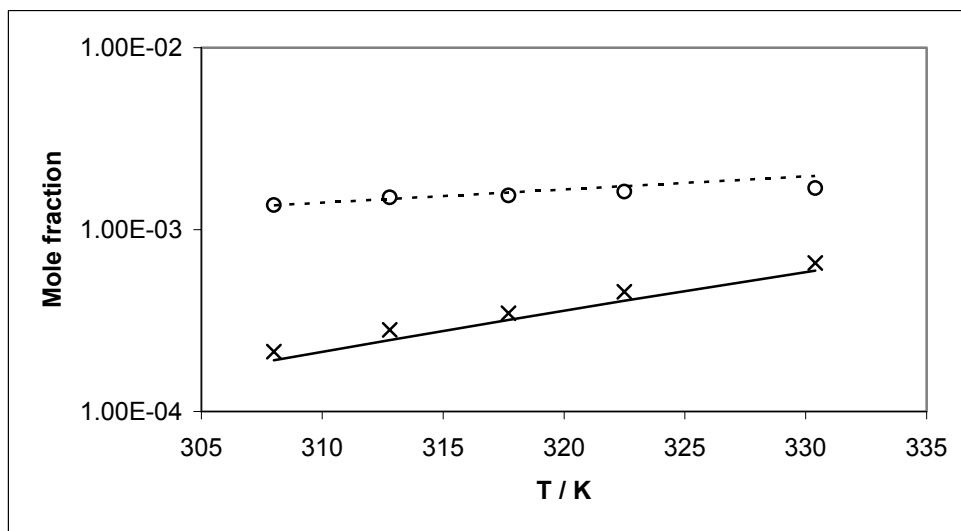


Figure 4.12 LLE for ethylene glycol (1) + n-hexane (2) system with CPA using parameters for MEG from Table 4.5 with a $k_{ij} = 0.059$: \times , x_1^{II} , experimental; o , x_2^I , experimental; solid line, x_1^{II} , CPA; dashed line, x_2^I , CPA. I = Glycol-rich phase and II = Hydrocarbon-rich phase.

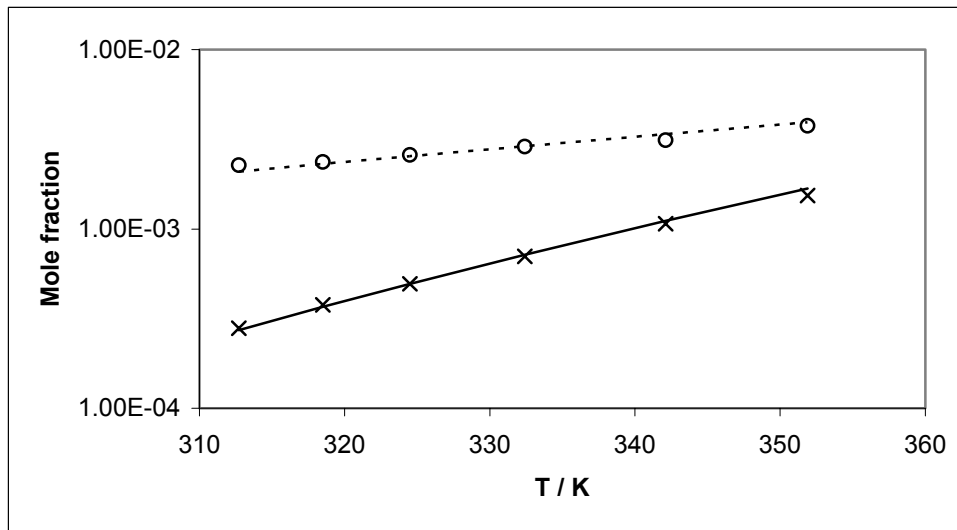


Figure 4.13 LLE for ethylene glycol (1) + methylcyclohexane (2) system with CPA using parameters for MEG from Table 4.5 with a $k_{ij} = 0.061$: \times , x_1^I , experimental; \circ , x_2^I , experimental; solid line, x_1^I , CPA; dashed line, x_2^I , CPA. I = Glycol-rich phase and II = Hydrocarbon-rich phase.

The same optimisation approach has been also employed for 1,2-propylene glycol, diethylene glycol, triethylene glycol, and tetraethylene glycol. The CPA parameters for these glycols are also listed in Table 4.5 in addition to the temperature range, correlation errors, binary interaction parameters, and the critical temperature and pressure applied. Excellent LLE correlations are obtained for all the systems, and are shown in Figure 4.14 – 4.16.

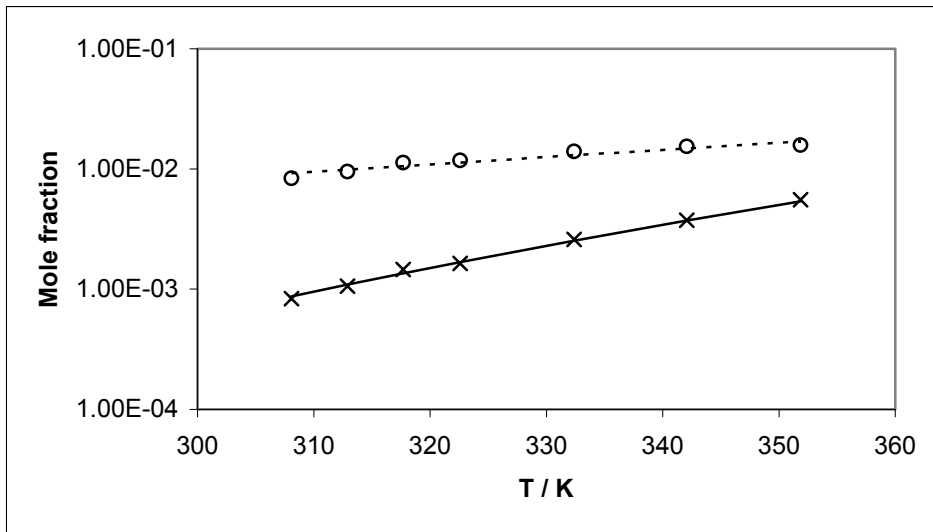


Figure 4.14 LLE for 1,2-propylene glycol (1) + n-heptane (2) system with CPA using parameters for PG from Table 4.5 with a $k_{ij} = 0.032$: \times , x_1^{II} , experimental; o , x_2^I , experimental; solid line, x_1^{II} , CPA; dashed line, x_2^I , CPA. I = Glycol-rich phase and II = Hydrocarbon-rich phase.

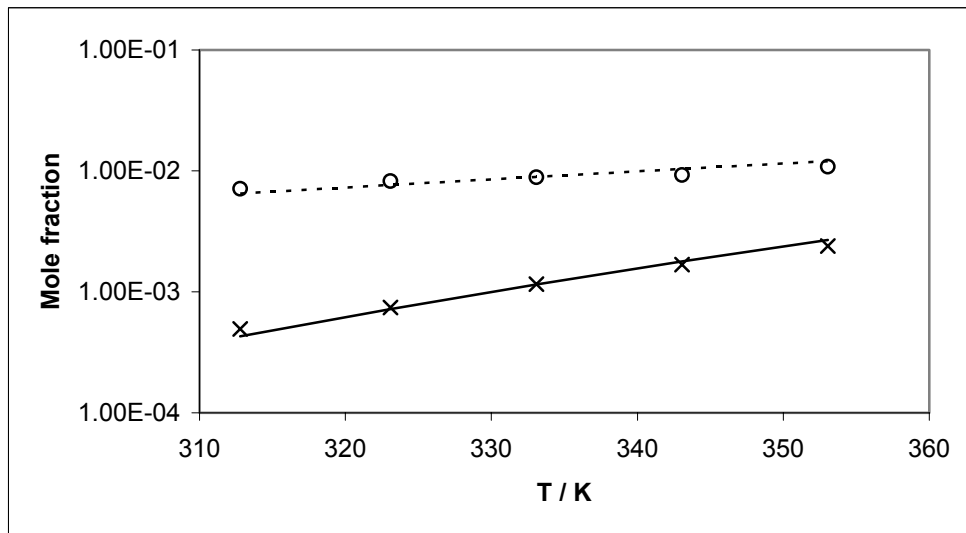


Figure 4.15 LLE for diethylene glycol (1) + n-heptane (2) system with CPA using parameters for DEG from Table 4.5 with a $k_{ij} = 0.065$: \times , x_1^{II} , experimental; o , x_2^I , experimental; solid line, x_1^{II} , CPA; dashed line, x_2^I , CPA. I = Glycol-rich phase and II = Hydrocarbon-rich phase.

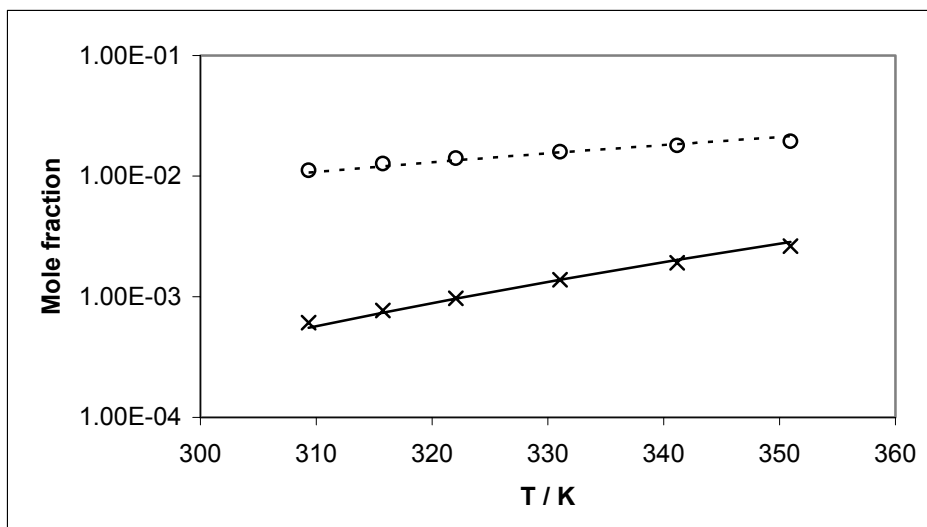


Figure 4.16 LLE for triethylene glycol (1) + n-heptane (2) system with CPA using parameters for TEG from Table 4.5 with a $k_{ij} = 0.094$: \times , x_1^{II} , experimental; o , x_2^I , experimental; solid line, x_1^{II} , CPA; dashed line, x_2^I , CPA. I = Glycol-rich phase and II = Hydrocarbon-rich phase.

The results for tetraethylene glycol however are treated separately later due to the rather peculiar behaviour of this glycol compared to the others. The temperature ranges have been chosen on the basis of the availability and the reliability of the raw experimental pure-compound data and the critical pressure and temperature.

Since an l_{ij} -parameter in the co-volume b is not introduced, the temperature-independent binary interaction parameter k_{ij} may reflect the size difference between the glycols and n-heptane. It is seen from Table 4.5 that the k_{ij} for all the considered glycols except 1,2-propylene glycol increases with the molecule size of the glycols. The critical temperature for 1,2-propylene glycol, unlike the other glycols, has not been measured experimentally but estimated by the method of Lydersen¹⁸, which is not very reliable for these types of compounds. This is further verified by Table 4.1, where the estimated critical temperature for 1,2-propylene glycol is 626 K, T_c for a smaller molecule such ethylene glycol is much higher (720 K). Thus T_c of 1,2-propylene glycol is rather questionable. The optimised parameters for 1,2-propylene glycol must be used thus with some caution, since the pure-compound vapour pressure data from DIPPR have

been based on this poorly estimated critical temperature. This may also explain why the k_{ij} does not follow the general trend mentioned above.

4.5.1 The Case of Tetraethylene Glycol (Tetra-EG)

In this section we elaborate and further analyse the optimisation results obtained for Tetra-EG, due to its rather peculiar behaviour compared to the other considered glycols. The CPA parameters were initially estimated for Tetra-EG based on pure-compound vapour pressure and liquid density at different temperature ranges without the employment of the binary LLE data. Characteristic optimisation results are shown in Table 4.6.

Table 4.6 Optimized CPA parameters for Tetra-EG for the 2B and the 4C association schemes at three different temperature ranges based on pure-compound vapor pressure and saturated liquid density data

	Set 1 (2B)	Set 2 (4C)	Set 3 (4C)
a_0	62.913	62.920	61.972
b	0.1747	0.1747	0.1731
c_1	1.5274	1.5273	1.5394
ε	1.6E-4	4.0E-5	133.24
β	5.4E-2	1.2E-2	2.5E-4
T_r range	0.54 – 0.90	0.54 – 0.90	0.35 – 0.99
ΔP (%)	0.64	0.64	1.44
$\Delta \rho$ (%)	1.09	1.09	2.35

The experimental uncertainty reported by DIPPR–2001 for the vapour pressure is 25% and 5% for the liquid density. Thus, it is practically impossible to determine parameters based solely on pure-compound data. The obtained results are, however, very interesting, especially the association parameters. The physical parameters obtained, a_0 , b , and c_1 seem to be unique at all temperature ranges. It is also seen that the association energy parameters (ε) are extremely small, close to zero, for two out of the three sets of Table 4.6 (except set 3). In those cases, the association strength is almost zero. An exception is the third set. It is observed that the association volume parameter (β) for set 3 is two orders of magnitude smaller than for the other two sets, which may indicate that this combination of the associating parameters also result in a negligible association

strength. We also determined the CPA parameters for the inert n-heptane assuming a four-site (4C) association scheme. The resulting parameters are shown in Table 4.7.

Table 4.7 Optimised parameters for n-heptane with the 4C association scheme based on pure-compound vapour pressure and saturated liquid density data

T_r range	a_0	b	c_1	ε	β	ΔP (%)	$\Delta \rho$ (%)
0.40 – 0.90	28.944	0.1249	0.9146	82.73	4.0E-4	0.14	0.77

It is seen from Table 4.7 that the given combination of the associating parameters also results in an association strength equal to zero, which should be expected since n-heptane is a non-associating compound.

It is the same case as in set 3. Since the 2B and the 4C association schemes give similar results, this indicates that the association contribution is not significant for Tetra-EG. The physical parameters obtained for n-heptane in Table 4.7 are identical to those parameters calculated without taken into account the association contribution.

Parameter sets 2 and 3 (Table 4.6) were employed in the correlation of LLE for the Tetra-EG + n-heptane system, which is shown in Figure 4.17.

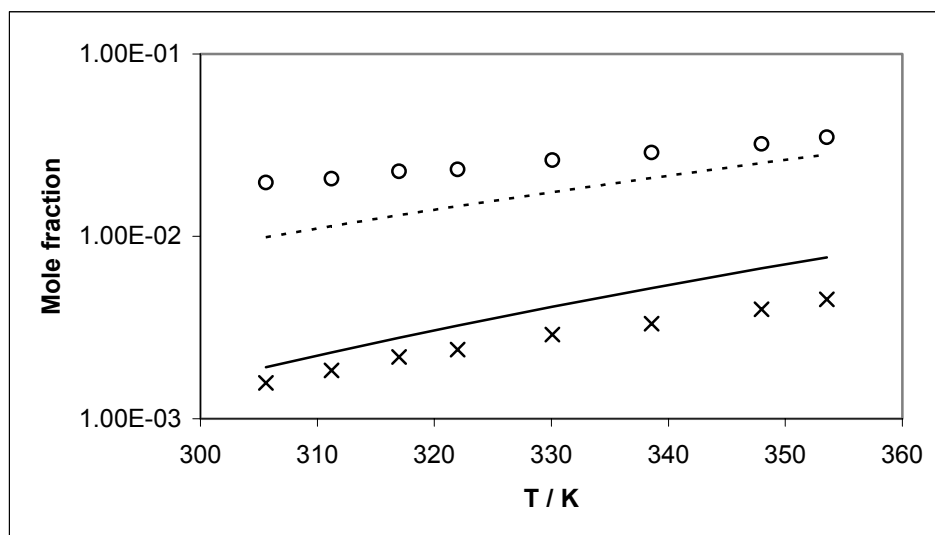


Figure 4.17 LLE for tetraethylene glycol (1) + n-heptane (2) system with CPA using set 2 and set 3 parameters for Tetra-EG from Table 4.6 with a $k_{ij} = 0.128$ and $k_{ij} = 0.119$, respectively: \times , x_1^{II} , experimental; o , x_2^I , experimental; solid line, x_1^{II} , CPA; dashed line, x_2^I , CPA. I = Glycol-rich phase and II = Hydrocarbon-rich phase.

The temperature-independent binary interaction parameter has been regressed from the LLE experimental data. The LLE correlation, which is identical with both parameter sets, provides a reasonable correlation of the experimental mutual solubility data.

The results obtained for Tetra-EG have so far been based, as mentioned, on pure-compound data, which contain large experimental uncertainty and indicate that Tetra-EG does not self-associate. This finding is supported by the fact that the measured critical temperature for Tetra-EG is only 3 degrees lower than the critical temperature for TEG with a much lower molecular weight (Table 4.1). An investigation was performed of the trend between the critical temperature and the molecular weight for MEG, TEG, DEG, Tetra-EG, and PEG (300). It can be observed from Figure 4.18 that tetraethylene glycol does not comply with the general trend of increasing critical temperature as a function of increasing molecular weight for various glycols.

A possible explanation for that particular behavior could be that Tetra-EG fold within itself (similar to carbohydrate) due to its long carbon chain, and thus give rise to decreased ability to associate (fewer sites would then be available).

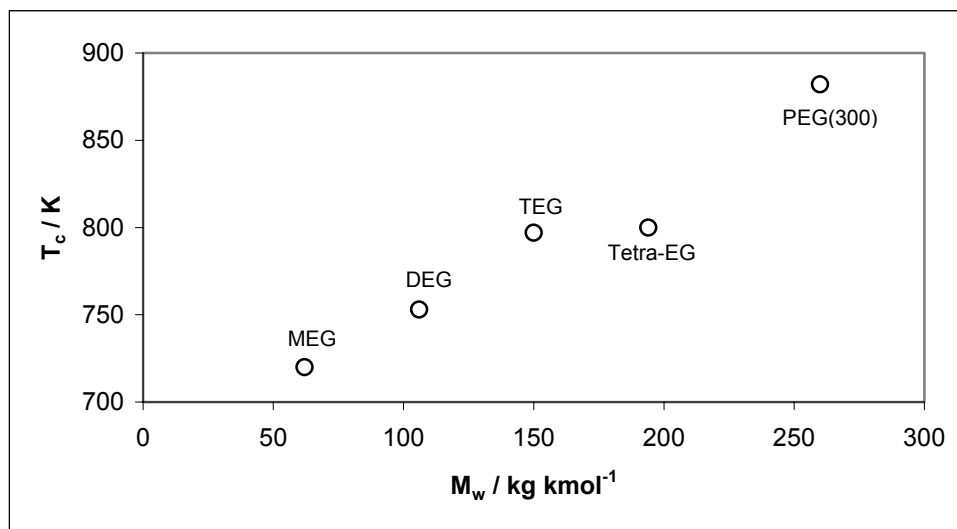


Figure 4.18 The trend of the critical temperature as a function of the molecular weight of glycols.

Consequently, the classical SRK equation has been applied to model the same binary system as before. The LLE correlation is shown graphically in Figure 4.19, where it is

seen that SRK successfully correlates the binary system with a slightly larger interaction parameter ($k_{ij} = 0.152$) compared to CPA ($k_{ij} = 0.128$ (set 2) and 0.119 (set 3)).

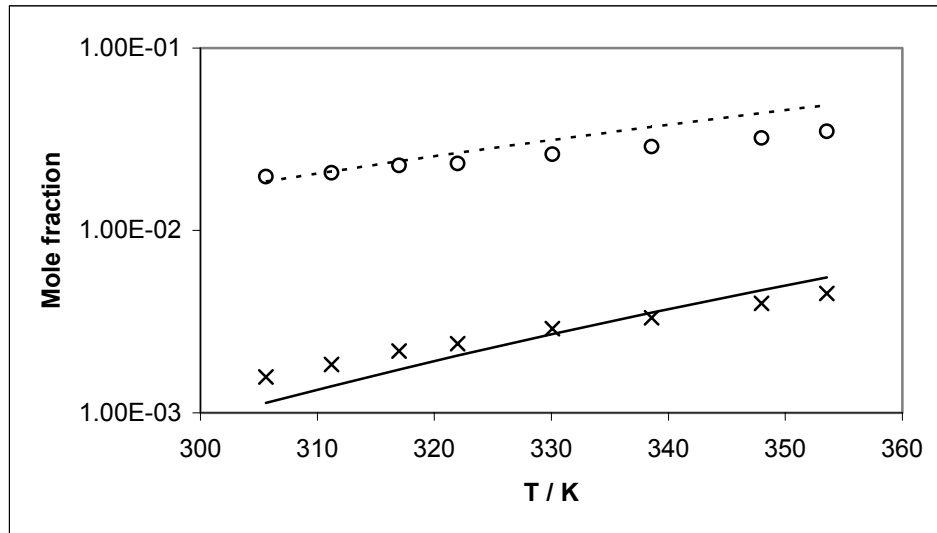


Figure 4.19 LLE for tetraethylene glycol (1) + n-heptane (2) system with the SRK equation using $T_c = 795$ K, $P_c = 25.9$ bar, and the acentric factor for Tetra-EG with a $k_{ij} = 0.152$: \times , x_1^{II} , experimental; o , x_2^I , experimental; solid line, x_1^{II} , SRK; dashed line, x_2^I , SRK. *I* = Glycol-rich phase and *II* = Hydrocarbon-rich phase.

This indicates that the association contribution for Tetra-EG is negligible, unlike for the MEG + n-heptane system, where the SRK-type equation of state gave a poor LLE correlation (as seen later in Figure 4.21).

It is known that Tetra-EG and water are completely miscible and the binary system of those compounds exhibit negative deviations from Raoult's law, which may indicate strong attraction forces, hydrogen bonding, between Tetra-EG and water. The last calculations that have been carried out in this section were to employ LLE binary data in the CPA parameter optimisation in addition to pure-compound data. In Table 4.5, the CPA parameter set is listed with its correlation error. It is noted that the association energy has a much lower value than for other glycols. The obtained parameters provide an excellent LLE correlation that is shown in Figure 4.20 with a relative lower interaction parameter value.

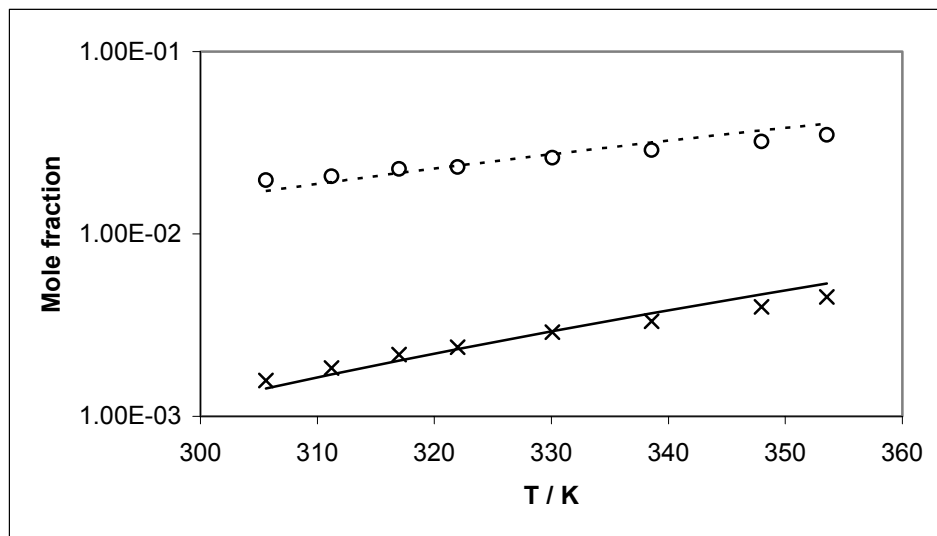


Figure 4.20 LLE for tetraethylene glycol (1) + n-heptane (2) system with CPA using parameters for Tetra-EG from Table 4.5 with a $k_{ij} = 0.101$: \times , x_1^I , experimental; \circ , x_2^I , experimental; solid line, x_1^II , CPA; dashed line, x_2^II , CPA. I = Glycol-rich phase and II = Hydrocarbon-rich phase.

In Table 4.8, the difference in normal boiling points between the glycols and aliphatic hydrocarbons, with similar molecular weight, has been calculated.

Table 4.8 Difference in normal boiling points between glycols and aliphatic hydrocarbons

glycols	M_w	T_b (K)	hydrocarbons	M_w	T_b (K)	ΔT_b
MEG	60.1	470.45	C_4H_{10}	58.1	272.65	198
DEG	106.1	518.15	C_7H_{16}	100.2	371.58	147
TEG	150.2	561.5	$C_{11}H_{24}$	156.3	469.08	92
Tetra-EG	194.2	602.7	$C_{14}H_{30}$	198.4	526.73	76

This difference provides an indication of the association strength attributed to the glycols. It is seen in Table 4.8 that the difference is decreasing with increasing molecular weight indicating that association becomes less pronounced at higher molecular weight. However, the difference does not vanish totally for Tetra-EG as would be expected for a completely non-associating compound. Moreover, the difference in the normal point temperature for TEG and Tetra-EG is less pronounced as what we would have expected.

It is seen in the Table 4.9 that the infinite dilution activity coefficient¹⁹ decreases with increasing size of the glycol. Based on that assumption, Tetra-EG self-associates to a certain extent but in any case much less than the other glycols of lower molecular weight.

Table 4.9 Infinite dilution activity coefficients between n-heptane and glycols

binary system	t (°C)	γ_1^∞
n-heptane (1) + monoethylene glycol (2)	60	610
n-heptane (1) + diethylene glycol (2)	60	118.1
n-heptane (1) + triethylene glycol (2)	60	49.8
n-heptane (1) + tetraethylene glycol (2)	60	35.6

4.6 Comparison of the SRK and CPA Equations of State

The performance of the SRK and CPA equations of state is presented in this section. Two versions of the RK equation, which have been proposed by Soave²⁰ and Mathias and Copeman²¹, have been employed.

Soave²⁰ proposed the following modification of the Redlich–Kwong (RK) EOS which considerably improves the vapor pressure for non-polar compounds:

$$Z^{SRK} = \frac{V_m}{V_m - b} - \frac{a_c \cdot \alpha(T_r)}{RT(V_m + b)} \quad (4.1)$$

$$\alpha(T_r, \omega) = [1 + m_{SRK} (1 - \sqrt{T_r})]^2 \quad (4.17)$$

$$m_{SRK} = 0.480 + 1.574\omega - 0.176\omega^2 \quad (4.18)$$

Mathias and Copeman²¹ suggested that a three-parameter alpha function is more suitable for representing the vapor pressure of polar compounds:

$$\alpha(T_r) = [1 + C_1(1 - \sqrt{T_r}) + C_2(1 - \sqrt{T_r})^2 + C_3(1 - \sqrt{T_r})^3]^2 \quad (4.19)$$

The parameters C_1 , C_2 , and C_3 are regressed to experimental vapor pressure data over extensive temperature ranges.

The a_c and the b (co-volume) parameters in Eq. (4.1) are obtained by imposing the critical point conditions, that is:

$$\left(\frac{\partial P}{\partial V}\right)_{P_c, T_c} = \left(\frac{\partial^2 P}{\partial^2 V}\right)_{P_c, T_c} = 0 \quad (4.20)$$

which results in $a_c = 0.42748 \frac{(RT_c)^2}{P_c}$ and $b = 0.08664 \frac{RT_c}{P_c}$.

The models have been compared for both the representation of the pure-compound vapor pressure and saturated liquid density for MEG as well as for correlating LLE for the ethylene glycol + n-heptane system.

4.6.1 Results

The Mathias-Copeman parameters (C_1, C_2, C_3) for ethylene glycol ($T_c = 720$ K) were regressed based on vapor pressure data in the reduced temperature range 0.4–0.9. The results of the optimization and the obtained errors are shown in Table 4.10.

Table 4.10 Mathias-Copeman's parameters for MEG based on pure-compound vapor pressure data

T_r range	C_1	C_2	C_3	ΔP (%)	$\Delta \rho$ (%)
0.40 – 0.90	1.1121	0.9679	-1.4200	0.23	20

The obtained parameters were then used to correlate LLE for the ethylene glycol + n - heptane system, which is shown graphically in Figure 4.21 (next page)

The performance of Soave's RK in correlating LLE for the ethylene glycol + n-heptane system is similar to that of Mathias–Copeman. This indicates that the alpha function with three parameters (C_1, C_2, C_3) instead of one ($m_{SRK}(\omega)$) in SRK does not improve the performance in LLE correlation. In both RK versions (Soave and Mathias–Copeman) the percentage error in the density is approximately the same and equal to 20%. Even though the calculated vapor pressure is much improved when the Mathias–Copeman expression is used (0.23%) compared to SRK with Soave's expression (21%), the LLE performance is identical.

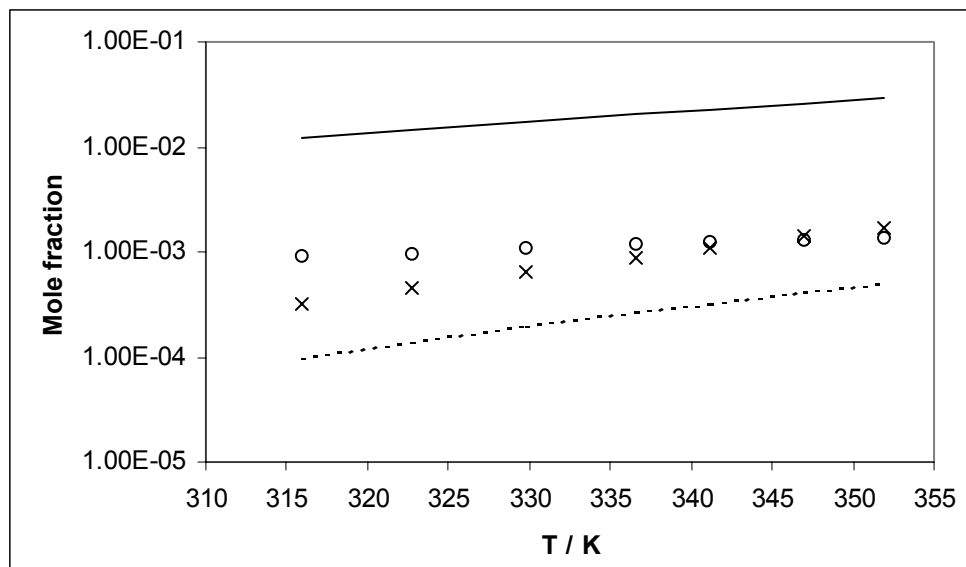


Figure 4.21 LLE for ethylene glycol (1) + n-heptane (2) system with MC-SRK using parameters for MEG from Table 4.10 with a $k_{ij} = 0.094$: \times , x_1^{II} , experimental; \circ , x_2^I , experimental; solid line, x_1^{II} , MC-SRK; dashed line, x_2^I , MC-SRK. I = Glycol-rich phase and II = Hydrocarbon-rich phase.

Thus liquid-liquid phase equilibria is unaffected by the good prediction ability of the pure-compound vapor pressure. We investigated whether LLE correlation could be improved if the liquid density for the pure-compounds could be well predicted/correlated.

4.6.2 An “Alternative” Approach

As seen earlier, the CPA model was able to correlate very satisfactorily LLE for the system ethylene glycol + n-heptane. In addition, the rather small value of the binary interaction parameter indicates that the strong attraction forces i.e. association/polar forces are taken explicitly into account by the association contribution of the equation. In order to verify that the success of the CPA equation is due to the association term and not the additional parameters, the following computational experiment was conducted: SRK parameters (a_0 , b , and the three Mathias-Copeman constants) were regressed by minimizing vapor pressure and liquid density data simultaneously, as was done in the CPA optimization approach.

The results are shown in Table 4.11. At the same time, the importance of adding liquid density information into the optimization is studied.

Table 4.11 Parameters obtained by the Mathias-Copeman modified RK equation for MEG based on pure-compound vapor pressure and liquid density data

T_r range	a_0	b	C_1	C_2	C_3	ΔP (%)	$\Delta \rho$ (%)
0.40 – 0.90	16.254	0.0514	0.9839	0.9564	-1.2608	0.24	0.94

Similar overall performance as before has been obtained with this revision of SRK as well; i.e. no difference between Soave's RK and this five-parameter-optimized RK is observed in the quality of the LLE correlation. As expected, the errors in the vapor pressure and the liquid density for the pure-compounds are improved. Figure 4.11 shows the LLE correlation by CPA. The large improvement achieved should thus be attributed to the association contribution.

4.7 Temperature Extrapolation Capabilities of CPA

We have shown that the CPA model, based on parameters obtained by pure-compound data and binary LLE data over a limited temperature range, could provide an excellent correlation of LLE over that particular temperature range. The binary LLE data were merely used to select the right CPA parameters among multiple parameter sets. The CPA parameters for MEG selected from the MEG + n-heptane system are successfully used for the other binary MEG + hydrocarbon systems. In this section the ability of the CPA model to extrapolate with respect to temperature is investigated. Such investigation is feasible since for three binary glycol systems, the solubility of one or both phases was measured at higher temperatures than for those binaries used in the selection of the CPA parameters. These test binaries are: diethylene glycol + n-heptane²², triethylene glycol + n-heptane²³, and tetraethylene glycol + n-heptane²³.

In Figures 4.22 – 4.24, the predictions of the mutual solubility data are graphically shown.

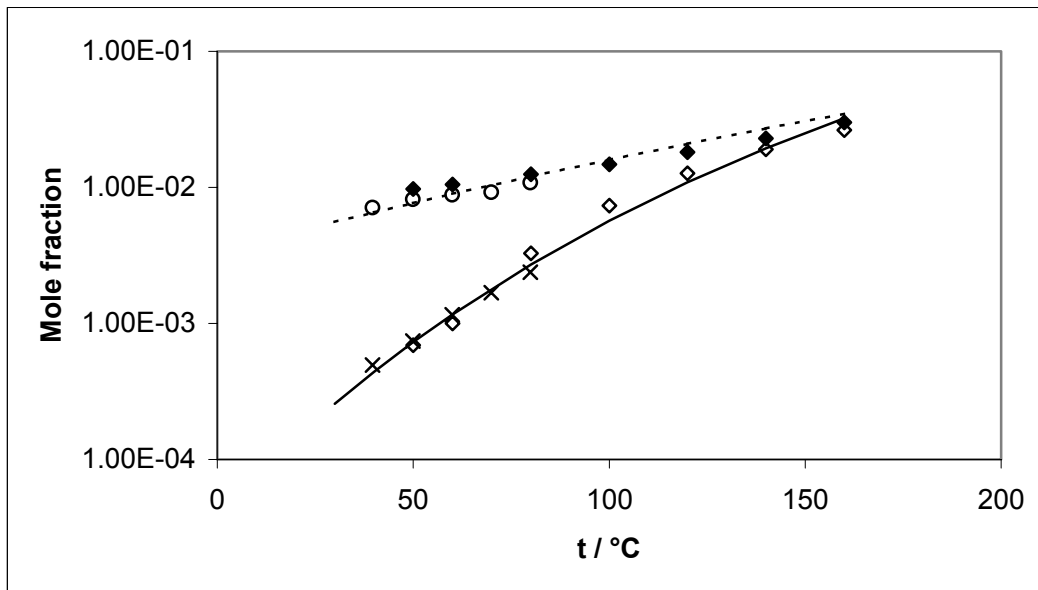


Figure 4.22 LLE for diethylene glycol (1) + n-heptane (2) system with CPA using parameters for DEG from Table 4.5 with a $k_{ij} = 0.065$: \times , x_1^{II} , Derawi et al.; \diamond , x_1^{II} , Johnson et al.; \circ , x_2^I , Derawi et al.; \blacklozenge , x_2^I , Johnson et al.; solid line, x_1^{II} , CPA; dashed line, x_2^I , CPA. I = Glycol-rich phase and II = Hydrocarbon-rich phase.

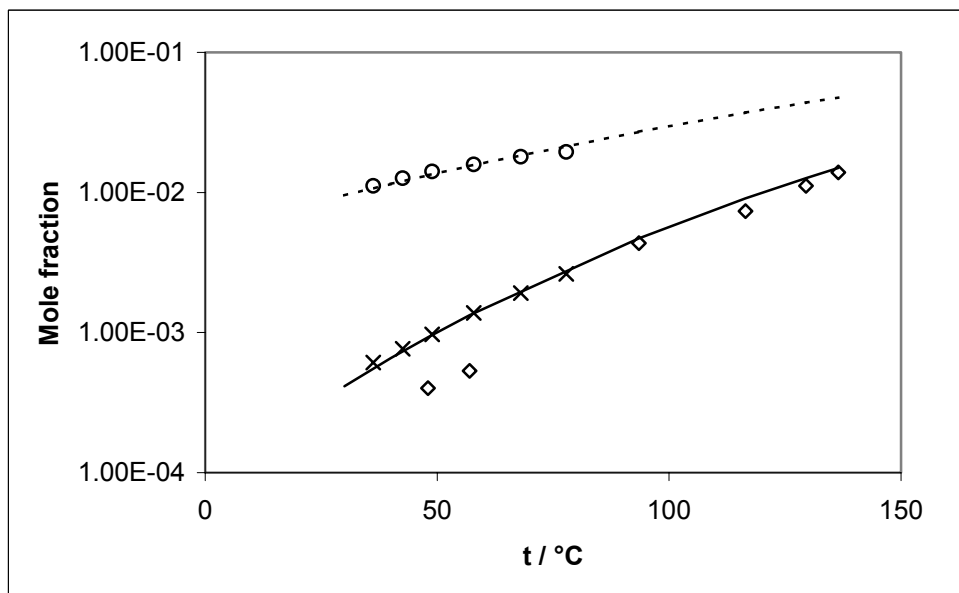


Figure 4.23 LLE for triethylene glycol (1) + n-heptane (2) system with CPA using parameters for TEG from Table 4.5 with a $k_{ij} = 0.094$: \times , x_1^{II} , Derawi et al.; \diamond , x_1^{II} , Rawat et al.; \circ , x_2^I , Derawi et al.; solid line, x_1^{II} , CPA; dashed line, x_2^I , CPA. I = Glycol-rich phase and II = Hydrocarbon-rich phase.

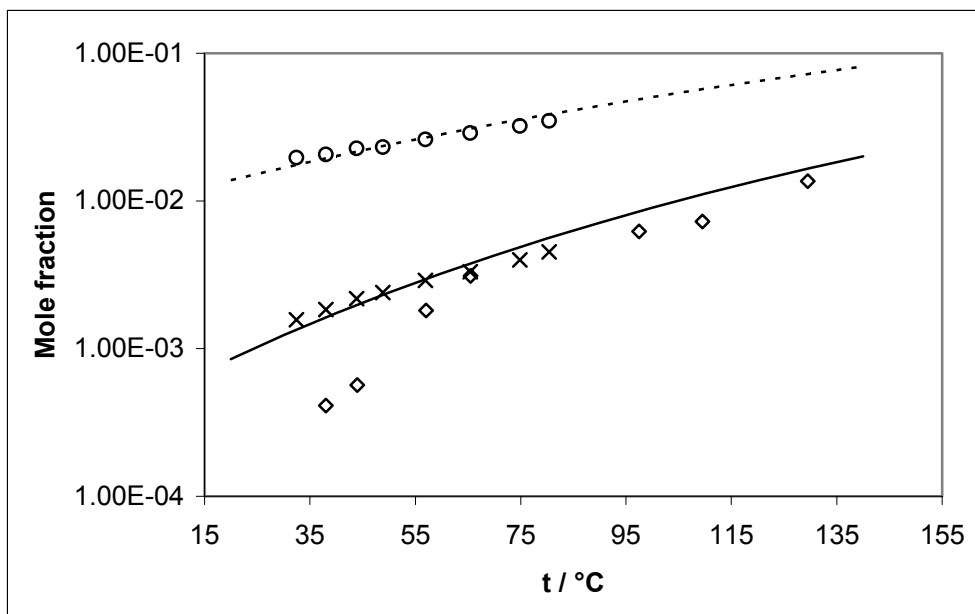


Figure 4.24 LLE for tetraethylene glycol (1) + n-heptane (2) system with CPA using parameters for Tetra-EG from Table 4.5 with a $k_{ij} = 0.101$: \times , x_1^{II} , Derawi et al.; \diamond , x_1^{II} , Rawat et al.; o, x_2^I , Derawi et al.; solid line, x_1^{II} , CPA; dashed line, x_2^I , CPA. I = Glycol-rich phase and II = Hydrocarbon-rich phase.

The experimental data by Rawat et al.²³ at low temperatures are not particularly reliable as discussed by Derawi et al.¹⁵ It can be seen that the prediction of the solubility data is excellent for all systems over the whole temperature range, especially for diethylene glycol + n-heptane system where the solubility for both phases have been measured. These results further support the investigations presented in previous sections on the success of CPA for LLE of glycol/alkanes.

It can also be noted that the binary interaction parameters employed in the prediction of the mutual solubility over the rather extended temperature range of 100 K are temperature independent. This is an interesting result that supports the use of the association term of Wertheim.

4.8 Conclusions

The CPA equation of state was successfully applied to the correlation of liquid–liquid equilibria for glycols + alkane systems with the four–site (4C) association model for the pure glycols. A single, temperature–independent binary interaction parameter was sufficient to provide a very satisfactorily LLE correlation. Moreover, an excellent capability of CPA in the extrapolation of temperature has been shown based on this single binary interaction parameter.

It was necessary to incorporate LLE data in the optimization procedure in order to select the proper parameter set due to large uncertainty in the experimental pure–compound vapor pressure and liquid density data for glycols.

The comparison of CPA with the SRK model had shown that CPA performs much better than SRK in correlating LLE. This is attributed to the association term in CPA, which is based on Wertheim’s theory.

References

- (1) Kontogeorgis, G. M.; Voutsas, E. C.; Yakoumis, I. V.; Tassios, D. P. An equation of state for associating fluids. *Ind. Eng. Chem. Res.* **1996**, *35*, 4310–4318.
- (2) Yakoumis, I. V.; Kontogeorgis, G. M.; Voutsas, E. C.; Tassios, D. P. Vapor–liquid equilibria for alcohol/hydrocarbon systems using the CPA equation of state. *Fluid Phase Equilibria.* **1997**, *130*, 31–47.
- (3) Voutsas, E. C.; Kontogeorgis, G. M.; Yakoumis, I. V.; Tassios, D. P. Correlation of liquid–liquid equilibria for alcohol/hydrocarbon mixtures using the CPA equation of state. *Fluid Phase Equilibria.* **1997**, *132*, 61–75.
- (4) Yakoumis, I. V.; Kontogeorgis, G. M.; Voutsas, E. C.; Hendriks, E. M.; Tassios, D. P. Prediction of phase equilibria in binary aqueous systems containing alkanes, cycloalkanes, and alkenes with the cubic-plus-association equation of state. *Ind. Eng. Chem. Res.* **1998**, *37*, 4175–4182.
- (5) Voutsas, E. C.; Yakoumis, I. V.; Tassios, D. P. Prediction of phase equilibria in water/alcohol/alkane systems. *Fluid Phase Equilibria.* **1999**, *158–160* , 151–163.
- (6) Kontogeorgis, G. M.; Yakoumis, I. V.; Meijer H.; Hendriks, E. M.; Moorwood, T. Multicomponent phase equilibrium calculations for water–methanol–alkane mixtures. *Fluid Phase Equilibria.* **1999**, *158–160* , 201–209.
- (7) Wertheim, M. S. Thermodynamic perturbation theory of polymerization. *J. Chem. Phys.* **1987**, *87*, 7323
- (8) Chapman, W. G.; Gubbins, K. E.; Jackson, G.; Radosz, M. SAFT: Equation-of-state solution model for associating fluids. *Fluid Phase Equilibria.* **1989**, *52*, 31–38.
- (9) Chapman, W. G.; Gubbins, K. E.; Jackson, G.; Radosz, M. New reference equation of state for associating liquids. *Ind. Eng. Chem. Res.* **1990**, *29*, 1709–1721.
- (10) Michelsen, M. L.; Hendriks, E. M. Physical properties from association models. *Fluid Phase Equilibria.* **2001**, *180*, 165–174.

- (11) Huang, S. H.; Radosz, M. Equation of state for small, large, polydisperse, and associating molecules. *Ind. Eng. Chem. Res.* **1990**, *29*, 2284-2294.
- (12) Daubert, T. E.; Danner, R. P. *Physical and thermodynamic properties of pure compounds: data compilation*; Hemisphere: New York, 1989 & 2001.
- (13) Perry, R. H.; Green, D. W. *Perry's chemical engineers' handbook*; McGraw-Hill: New York, 1997.
- (14) Nikitin, E. D.; Pavlov, P. A.; Popov, A. P. (Gas + liquid) critical temperatures and pressures of polyethene glycols from HOCH₂CH₂OH to H(OCH₂CH₂)_v ≈ 13.2 OH. *J. Chem. Thermodynamics.* **1995**, *27*, 43-51.
- (15) Derawi, S. O.; Kontogeorgis, G. M.; Stenby, E. H.; Haugum, T.; Fredheim, A. O. Liquid-liquid equilibria for glycols + hydrocarbons: Data and correlation. *J. Chem. Eng. Data.* **2002**, *47*, 169-173.
- (16) McCann, D. W.; Danner, R. P. Prediction of second virial coefficients of organic compounds by a group contribution method. *Ind. Eng. Chem. Process Des. Dev.* **1984**, *23*, 529-533.
- (17) Dymond, J. H.; Smith, E. B. *The virial coefficients of gases: a critical compilation*; Oxford: London, 1969.
- (18) Reid, R. C.; Prausnitz, J. M.; Poling, B. E. *The properties of gases and liquids*; McGraw-Hill: United States of America, 1987.
- (19) Gmehling, J.; Menke, J.; Schiller, M. Activity coefficients at infinite dilution C₁ – C₉. *DECHEMA Chemistry Data Series*, **1994**, Vol. 9, Part 3. Frankfurt am Main.
- (20) Soave, G. Equilibrium constants from a modified Redlich-Kwong equation of state. *Chemical Engineering Science.* **1972**, *27(6)*, 1197-1203.
- (21) Mathias, P. M.; Copeman, T. W. Extension of the Peng-Robinson equation of state to complex mixtures: evaluation of the various forms of the local composition concept. *Fluid Phase Equilibria.* **1983**, *13*, 91-108.
- (22) Johnson, G. C.; Francis, A. W. Ternary liquid system, benzene-heptane-diethylene glycol. *Ind. Eng. Chem.* **1954**, *46*, 1662-1668.
- (23) Rawat, B. S.; Prasad, G. Liquid-liquid equilibria for benzene-n-heptane systems with triethylene glycol, tetraethylene glycol, and sulfolane containing water at elevated temperatures. *J. Chem. Eng. Data.* **1980**, *25*, 227-230.

Chapter 5

Extension of the CPA Equation of State to Glycol-Water Cross-Associating Systems

The application of the CPA equation of state has been extended to mixtures containing cross-associating compounds such as glycols and water. In this case, combining rules are required in the association term of CPA for the cross-association energy and volume parameters. Different types of such combining rules have been suggested over the past years for association models such as SAFT. These are tested in this work for CPA in terms of their correlation and prediction capabilities for vapor-liquid equilibria of glycol-water systems. Comparisons with SRK are also provided. It has been found, that the arithmetic mean combining rule for the cross-association energy parameter and the geometric mean for the cross-association volume parameter provide overall the best results for cross-associating systems containing glycols and water. Moreover, preliminary results show that the CPA model can be used to predict multi-component, multiphase equilibria for glycol/water/hydrocarbons based solely on binary interaction parameters.

5.1 Introduction

The CPA equation of state is a thermodynamic model that explicitly accounts for strong directional attractive forces such as molecular association. Such strong attractive forces have a pronounced effect on fluid properties and hence phase behavior, e.g. vapor-liquid equilibria (VLE) and liquid-liquid equilibria (LLE). CPA combines the well-known SRK cubic equation of state and the thermodynamic perturbation theory (TPT) developed by Wertheim (discussed in section 4.2). In the previous chapter, CPA has been successfully applied in correlating LLE for glycol/alkane systems. For such systems, no cross-association parameters were needed between the associating compound (glycol) and the inert compound (alkane).

In this chapter we focus on mixtures containing more than one associating compound such as methanol, water, and glycols, which can cross-associate with each other. The association types and schemes for these components have been established in previous works by Derawi et al.¹ and Kontogeorgis et al.², and will subsequently be applied. Both water and glycols are assumed to have 4 association sites (4C model by Huang and Radosz³). The application of the CPA equation of state to multicomponent mixtures does not require mixing rules for the association term. However, combining rules for the association energy parameter and the association volume are required. Successful phase behavior modeling can, to a great extent, be dependent on the accurate description of the cross-association. Only few publications deal in the literature with this issue using association theories such as CPA and SAFT⁴⁻⁷. These are mostly limited to alcohol-water and acid-water systems.

Suresh and Beckman⁴ in their SAFT study of cross-associating systems containing water, alcohols, and carboxylic acids related both the cross-association energy and volume to the self-association parameters of the two components by the geometric mean values as follows:

$$\varepsilon^{A_i B_j} = \sqrt{\varepsilon^{A_i B_i} \varepsilon^{A_j B_j}} \quad (5.1)$$

$$\beta^{A_i B_j} = \sqrt{\beta^{A_i B_i} \beta^{A_j B_j}} \alpha_{ij} \quad (5.2)$$

where α_{ij} is a correction parameter to the geometric mean combining rule for $\beta^{A_i B_j}$ that adjusts the extent of cross-association volume between the two species.

Fu and Sandler⁵, in their simplified SAFT theory, suggested using the geometric mean rule for the cross-association energy (Eq. 5.1) and the arithmetic mean rule for the cross-association volume:

$$\beta^{A_i B_j} = \frac{\beta^{A_i B_i} + \beta^{A_j B_j}}{2} \quad (5.3)$$

No adjustable parameters were used.

Three different sets of combining rules for CPA using a combination of both the geometric and the arithmetic mean rules have been tested by Voutsas et al.⁶ for alcohol-water systems. They concluded that the best choice is the arithmetic rule for the cross-association energy and the geometric rule for the cross-association volume. Another approach, which also has been tested by Voutsas et al.⁶ is the so-called Elliott rule proposed by Suresh and Elliott⁷. Elliott's rule provides good correlation results for VLE, but rather poor for describing LLE in water/heavy alcohols mixtures. Elliott's rule performs satisfactorily for water-methanol systems (and other lower alcohols up to propanol). For example, Kontogeorgis et al.² applied with success Elliott's rule in CPA for the prediction of multicomponent LLE of methanol, water and alkanes.

In this work, the CPA equation of state (in its simplified form, Eq. 4.6) is extended for glycol-water systems. Different sets of combining rules for the cross-association parameters (energy and volume) are tested in correlating and predicting VLE for glycol-water systems. In the next section, the extension of CPA to cross-associating systems is provided. The results and discussion follow in section 5.3 while section 5.4 presents the application to one multicomponent cross-associating system. We end with our conclusions.

5.2 Extension of CPA to Cross-Associating Systems

The CPA equation of state for mixtures can be expressed in terms of the compressibility factor Z as follows:

$$Z = \frac{V_m}{V_m - b} - \frac{a(T)}{RT(V_m + b)} - \frac{1}{2} \left(1 + \rho \frac{\partial \ln g}{\partial \rho} \right) \sum_i x_i \sum_{A_i} (1 - X_{A_i}) \quad (5.4)$$

X_{A_i} is the mole fraction of the molecule i not bonded at site A , i.e. the monomer mole fraction and x_i is the superficial (apparent) mole fraction of component i .

X_{A_i} is calculated by solving the following set of equations:

$$X_{A_i} = \frac{1}{1 + \rho \sum_j x_j \sum_{B_j} X_{B_j} \Delta^{A_i B_j}} \quad (5.5)$$

$\Delta^{A_i B_j}$, the association strength between site A on molecule i and site B on molecule j , is given by:

$$\Delta^{A_i B_j} = g(\rho) \left[\exp\left(\frac{\varepsilon^{A_i B_j}}{RT}\right) - 1 \right] b_{ij} \beta^{A_i B_j} ; \quad g(\rho) = \frac{1}{1 - 1.9\eta} \quad \eta = \frac{1}{4} b \rho \quad (5.6)$$

$\varepsilon^{A_i B_j}$ and $\beta^{A_i B_j}$ are the association energy and volume between site A of molecule i and site B of molecule j , respectively. Combining rules for the association energy and volume parameters are needed between different molecules, i.e. $i \neq j$. Alternatively, a combining rule for the association strength $\Delta^{A_i B_j}$ would be sufficient, such as the Elliott rule ($\Delta^{A_i B_j} = \sqrt{\Delta^{A_i B_i} \Delta^{A_j B_j}}$).

The extension of the CPA EoS to mixtures requires mixing rules only for the parameters of the physical (SRK)-part, while the extension of the association term to mixtures is straightforward (Eq. 5.4). The mixing and combining rules for a and b are the classical van der Waals one-fluid ones (Equations 4.11 - 4.15).

The binary interaction parameter in the energy term k_{ij} , which is the only adjustable parameter needed in the CPA equation of state, is estimated from experimental binary phase equilibrium data. When CPA is extended to cross-associating mixtures e.g. alcohols-water or glycols-water, combining rules are needed for the cross-association energy and volume parameters ($\varepsilon^{A_i B_j}$, $\beta^{A_i B_j}$) or for the association strength $\Delta^{A_i B_j}$. In this work, both the geometric and the arithmetic mean are investigated as combining rules for the cross-association energy and volume parameters resulting in four different cases. The combining rules tested here are summarized in Table 5.1.

Table 5.1 Proposed combining rules for the cross-association energy and volume in the association term of CPA

	cross-association energy ($\varepsilon^{A_1 B_2}$)	cross-association volume ($\beta^{A_1 B_2}$)	adjustable parameter
combining rule 1 (CR-1)	$\varepsilon^{A_1 B_2} = \frac{\varepsilon^{A_1 B_1} + \varepsilon^{A_2 B_2}}{2}$	$\beta^{A_1 B_2} = \sqrt{\beta^{A_1 B_1} \beta^{A_2 B_2}}$	k_{12}
combining rule 2 (CR-2)	$\varepsilon^{A_1 B_2} = \frac{\varepsilon^{A_1 B_1} + \varepsilon^{A_2 B_2}}{2}$	$\beta^{A_1 B_2} = \frac{\beta^{A_1 B_1} + \beta^{A_2 B_2}}{2}$	k_{12}
combining rule 3 (CR-3)	$\varepsilon^{A_1 B_2} = \sqrt{\varepsilon^{A_1 B_1} \varepsilon^{A_2 B_2}}$	$\beta^{A_1 B_2} = \sqrt{\beta^{A_1 B_1} \beta^{A_2 B_2}}$	k_{12}
combining rule 4 (CR-4)	$\varepsilon^{A_1 B_2} = \sqrt{\varepsilon^{A_1 B_1} \varepsilon^{A_2 B_2}}$	$\beta^{A_1 B_2} = \frac{\beta^{A_1 B_1} + \beta^{A_2 B_2}}{2}$	k_{12}
	cross-association strength ($\Delta^{A_1 B_2}$)		adjustable parameter(s)
the Elliott rule (ER)	$\Delta^{A_1 B_2} = \sqrt{\Delta^{A_1 B_1} \Delta^{A_2 B_2}}$		k_{12}
modified Elliott rule (MER)	$\Delta^{A_1 B_2} = \sqrt{\Delta^{A_1 B_1} \Delta^{A_2 B_2}} (1 - e_{12})$		k_{12} and e_{12}

Suresh and Elliot⁷ proposed a combining rule for the association strength $\Delta^{A_i B_j}$, which had been referred previously as the Elliott rule. This rule is also investigated in this work together with a modified version, where an additional binary interaction parameter e_{12} is used. These combining rules denoted as (ER and MER, respectively) are also shown in Table 5.1.

Voutsas et al.⁶ have shown that Elliott's rule fails to correlate satisfactorily LLE for heavy alcohol-water systems with a single binary interaction parameter. However, Elliott's rule provides good results for the VLE correlation in alcohol-water systems.

The glycols considered in this work, except MEG, are heavier than n-butanol. However, they are completely miscible with water and thus only VLE data are available. As indicated theoretically in Appendix B and by the results of Voutsas et al.⁶, the CR-1 combining rule of Table 5.1 may be more suitable than Elliott's rule for these heavy glycol-water systems which in terms of size difference are closer to the butanol-water than to the methanol-water system.

In this study, the different sets of combining rules are compared with respect to their prediction and correlation performance of isothermal VLE data in methanol-water and glycol-water systems. The binary cross-associating mixtures considered here are methanol-water^{8,9}, ethylene glycol-water¹⁰, diethylene glycol-water¹¹, and triethylene glycol-water¹². The CPA pure-compound parameters have been obtained by Kontogeorgis et al.² and Derawi et al.¹ (work presented in chapter 4), and are listed in Table 5.2.

Table 5.2 CPA pure-compound parameters for water, methanol, ethylene glycol (MEG), diethylene glycol (DEG) and triethylene glycol (TEG)

compound	ref.	b (dm ³ mol ⁻¹)	a_0 (bar dm ⁶ mol ⁻²)	c_1	ε (bar dm ³ mol ⁻¹)	β
water	[2]	0.014515	1.2277	0.67359	166.55	0.0692
methanol	[2]	0.030978	4.0531	0.43102	245.91	0.0161
MEG	[1]	0.0514	10.819	0.6744	197.52	0.0141
DEG	[1]	0.0921	26.408	0.7991	196.84	0.0064
TEG	[1]	0.1321	39.126	1.1692	143.37	0.0188

All the binary systems have been checked for thermodynamic consistency with the exception of the triethylene glycol-water system. For this particular system, the total pressure and the liquid mole fraction were calculated from the measured water activity in solutions of triethylene glycol and water using an isopiestic method with LiCl as reference electrolyte. Since the vapor mole fraction was lacking, a consistency test could not be performed. However, Parrish et al.¹³ have verified the reliability of the indirectly measured P-x experimental data for this particular system.

5.3 Results and Discussion

In Tables 5.3 and 5.4 (pages 85 and 86), the performance of the CPA model with the different sets of combining rules (listed in Table 5.1) and of the Mathias-Copeman SRK model are presented. The Mathias-Copeman constants are given in Table 5.5.

Table 5.5 The Mathias-Copeman constants (C_1 , C_2 , C_3) for the SRK equation of state and its correlation error for the vapor pressure

compound	ref.	C_1	C_2	C_3	$\Delta P(\%)$
ethylene glycol	this work	1.1121	0.9679	-1.4200	0.23
diethylene glycol	this work	1.5556	-1.6873	4.5357	1.16
triethylene glycol	this work	1.9673	-3.5617	7.3424	1.27
cyclohexane	this work	0.8453	-0.4302	1.0133	0.03
methylcyclohexane	this work	0.8989	-0.5453	1.2130	0.36
methanol	[14]	1.4450	-0.8150	0.2486	0.87
water	[14]	1.0873	-0.6377	0.6345	0.54

Vapor-liquid phase equilibria calculations have been performed with the two models using both an optimised k_{ij} (correlation of the experimental data) and with a binary interaction parameter with the value zero (prediction). The k_{ij} has been obtained by minimising the following objective function:

$$OF = \sum_{n=1}^{NP} \left(\frac{P_{bub}^{exp} - P_{bub}^{cal}}{P_{bub}^{exp}} \right)^2 + (y^{cal} - y^{exp})^2 \quad (5.7)$$

P_{bub} is the bubble point pressure and y is the composition in the gas phase. For the TEG-water system, the second term in the objective function was omitted since only P-x data were available.

The following summarize our observations:

1. For the methanol-water system: the CR-1 and CR-3 combining rules (as well as the Elliott one) are the best choices for correlating the experimental data. However, their prediction ability ($k_{ij}=0$) is less satisfactory compared to CR-2 and CR-4. In Figures 5.1 and 5.2 the VLE plots for the CR-1 and CR-2 rules are shown.

Table 5.3 VLE correlation and prediction results with CPA and combining rules CR-1, CR-2, CR-3, and CR-4 (Table 5.1)

system	ref.	NP	T (K)	CR-1			CR-2			CR-3			CR-4		
				k_{ij}	$\Delta P(\%)^a$	$\Delta y100^b$									
methanol	[8]	10	298.15	-0.094	1.80	0.60	-0.024	5.86	1.85	-0.138	1.57	1.06	-0.068	3.25	0.99
+				0.0	22.31	8.69	0.0	7.86	3.16	0.0	38.63	12.88	0.0	14.46	6.45
water	[9]	18	333.15	-0.055	0.57	0.78	0.065	5.24	2.94	-0.119	1.90	0.66	-0.004	2.52	1.63
				0.0	7.66	2.09	0.0	10.83	3.72	0.0	19.69	3.93	0.0	2.51	1.64
MEG	[10]	19	343.15	-0.028	1.81	0.11	0.113	9.51	0.27	-0.039	1.32	0.10	0.101	8.82	0.25
+				0.0	5.96	0.06	0.0	16.12	0.72	0.0	8.00	0.07	0.0	13.97	0.61
water	[10]	23	363.15	-0.012	2.29	0.45	0.155	10.68	0.72	-0.025	1.76	0.45	0.142	9.96	0.69
				0.0	3.19	0.36	0.0	21.59	2.29	0.0	5.49	0.27	0.0	20.23	2.10
DEG	[11]	13	393.15	-0.115	1.65	0.15	0.272	28.04	1.48	-0.128	1.56	0.18	0.262	27.04	1.36
+				0.0	26.12	1.07	0.0	37.75	5.54	0.0	29.31	1.18	0.0	36.84	5.20
water															
TEG	[12]	24	297.60	-0.211	5.62	-- ^c	-0.162	12.10	-- ^c	-0.215	5.28	-- ^c	-0.166	11.52	-- ^c
+				0.0	70.25	-- ^c	0.0	46.89	-- ^c	0.0	72.66	-- ^c	0.0	48.68	-- ^c
water	[12]	16	332.60	-0.201	3.77	-- ^c	-0.157	8.20	-- ^c	-0.205	3.60	-- ^c	-0.161	7.78	-- ^c
				0.0	53.56	-- ^c	0.0	38.59	-- ^c	0.0	54.87	-- ^c	0.0	39.68	-- ^c

^a Average absolute percentage error in the bubble point pressure

^b Average absolute deviation in the vapor phase mole fraction

^c Lack of experimental vapor mole fraction

Table 5.4 VLE correlation and prediction results with CPA using the Elliott and MER rules and the Mathias-Copeman SRK equation of state

system	ref.	NP	T (K)	the Elliott rule (ER)			The modified Elliott rule (MER)				Mathias-Copeman SRK		
				k_{ij}	$\Delta P(\%)^a$	$\Delta y100^b$	k_{ij}	e_{ij}	$\Delta P(\%)^a$	$\Delta y100^b$	k_{ij}	$\Delta P(\%)^a$	$\Delta y100^b$
methanol +	[8]	10	298.15	-0.114	1.06	0.69	-0.116	0.0081	1.11	0.73	-0.098	3.42	1.16
				0.0	29.29	10.56							
water	[9]	18	333.15	-0.088	0.72	0.33	-0.068	-0.043	0.24	0.57	-0.080	1.51	1.04
				0.0	13.65	3.01							
MEG +	[10]	19	343.15	-0.115	2.68	0.11	-0.063	-0.121	0.67	0.10	-0.058	0.46	0.08
				0.0	24.03	0.30							
water	[10]	23	363.15	-0.115	2.67	0.43	-0.059	-0.109	0.84	0.43	-0.054	0.67	0.37
				0.0	25.56	0.49							
DEG +	[11]	13	393.15	-0.361	13.78	0.63	-0.120	-0.449	1.59	0.16	-0.170	5.65	0.38
				0.0	112.13	2.48							
water													
TEG +	[12]	24	297.60	-0.372	13.64	-- ^c	-0.258	-0.420	4.15	-- ^c	-0.236	2.36	-- ^c
				0.0	170.03	-- ^c							
water	[12]	16	332.60	-0.337	10.35	-- ^c	-0.238	-0.443	3.15	-- ^c	-0.231	2.77	-- ^c
				0.0	106.39	-- ^c							

^a Average absolute percentage error in the bubble point pressure

^b Average absolute deviation in the vapor phase mole fraction

^c Lack of experimental vapor mole fraction

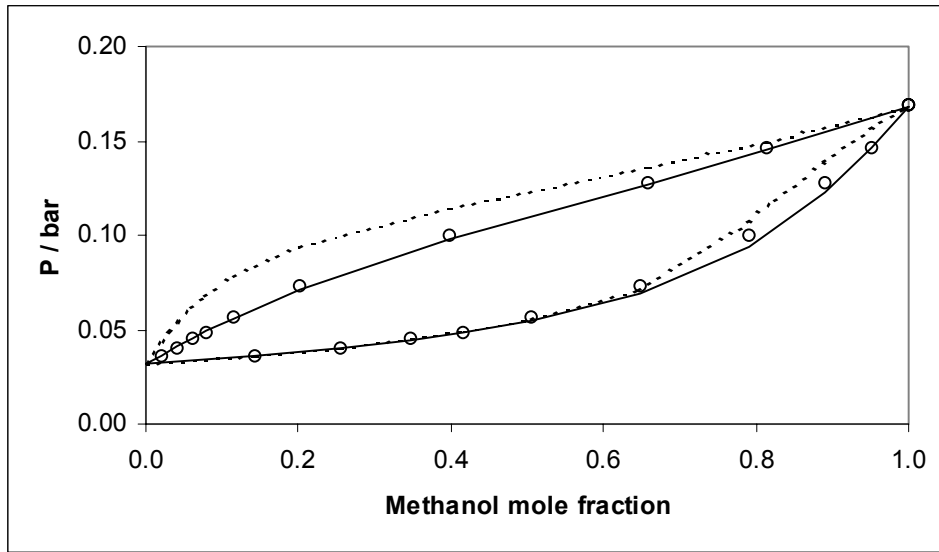


Figure 5.1 CPA-correlation and prediction of the methanol-water VLE at $T = 298.15$ K employing the CR-1 combining rule with a $k_{ij} = -0.094$ (solid line) and $k_{ij} = 0$ (dashed line). The circles are the experimental points.

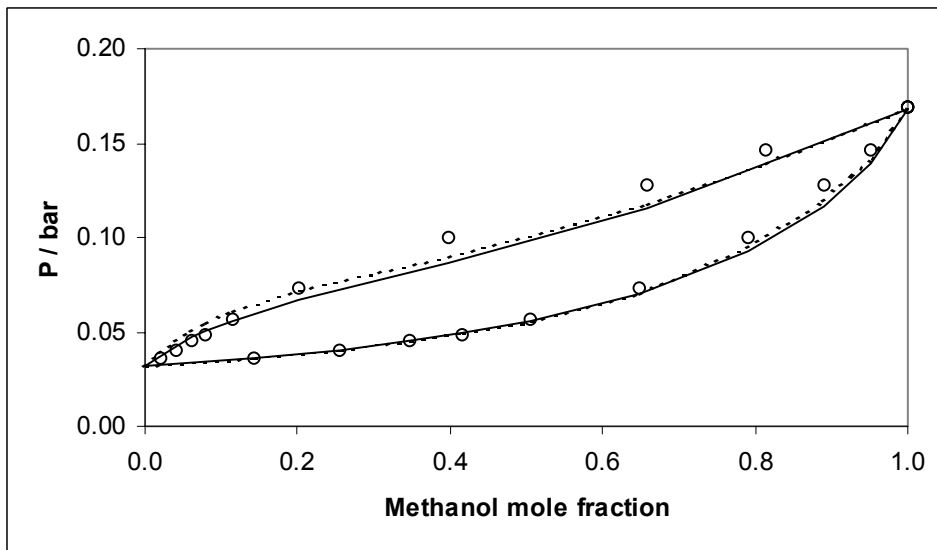


Figure 5.2 CPA-correlation and prediction of the methanol-water VLE at $T = 298.15$ K employing the CR-2 combining rule with a $k_{ij} = -0.024$ (solid line) and $k_{ij} = 0$ (dashed line).

In Figure 5.3, the VLE correlation using Elliott's rule is presented. CR-1 is equivalent to Elliott's rule and to its modification (MER), which has two adjustable parameters, k_{ij} and e_{ij} .

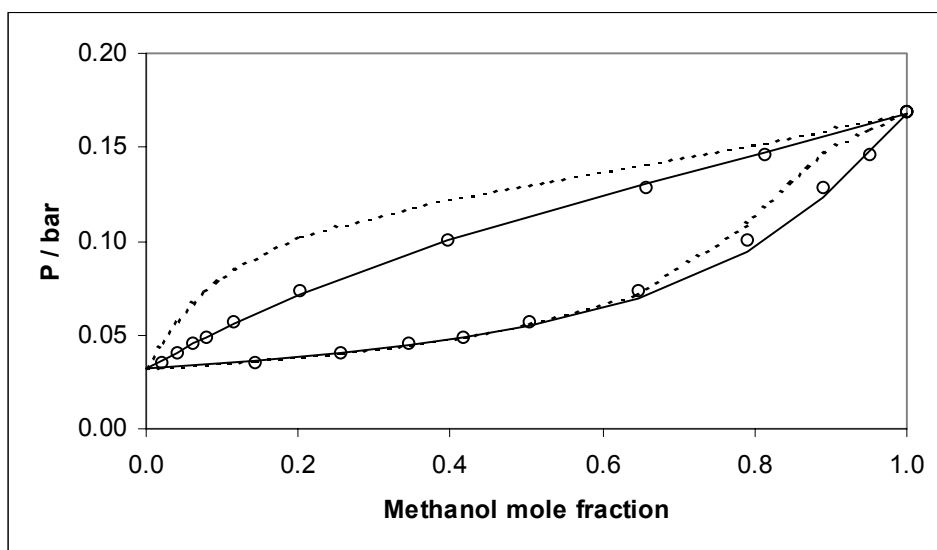


Figure 5.3 CPA-correlation and prediction of the methanol-water VLE at $T = 298.15$ K employing the Elliott rule with a $k_{ij} = -0.114$ (solid line) and $k_{ij} = 0$ (dashed line).

The MC-SRK model was able to correlate the experimental data very satisfactorily for this cross-associating system, but fails completely when a binary interaction coefficient of zero is used. Predictions ($k_{ij}=0$) yield an erroneous liquid-liquid phase split.

2. For the MEG-H₂O and DEG-H₂O systems: the CR-1 combining rule is clearly the best model. Figures 5.4 and 5.5 show the VLE correlation for the two systems using the CR-1 combining rule.

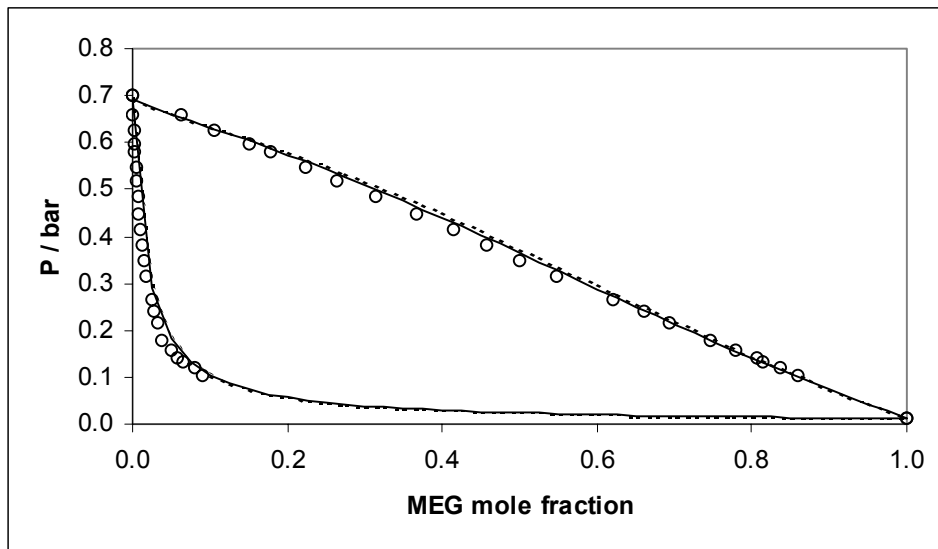


Figure 5.4 CPA-correlation and prediction of the MEG-water VLE at $T = 363.15$ K using the CR-1 combining rule with a $k_{ij} = -0.012$ (solid line) and $k_{ij} = 0$ (dashed line).

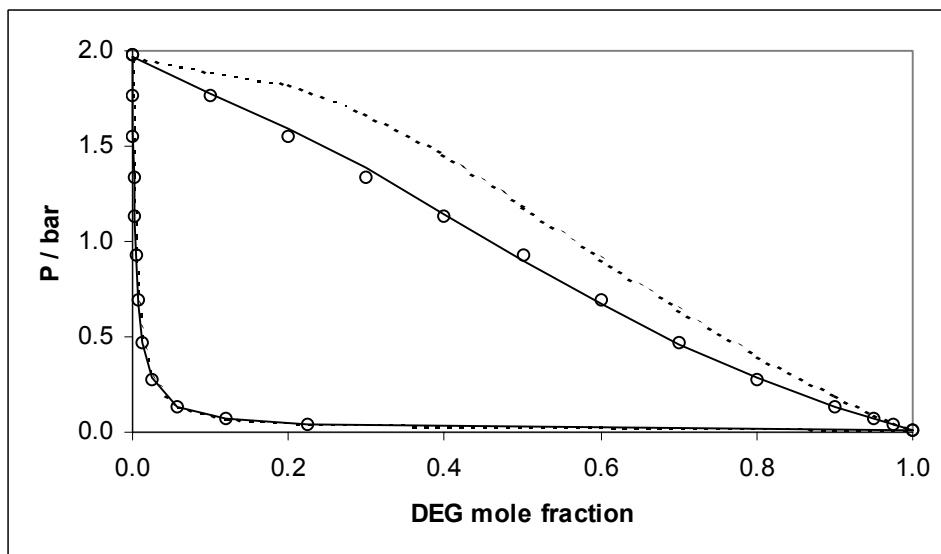


Figure 5.5 CPA-correlation and prediction of the DEG-water VLE at $T = 393.15$ K using the CR-1 combining rule with a $k_{ij} = -0.115$ (solid line) and $k_{ij} = 0$ (dashed line).

The CR-2 and CR-4 rules fail completely both in terms of the correlation and the prediction performance. Moreover, the positive k_{ij} values for CR-2 and CR-4 seem a bit surprising for these two cross-associating systems.

In Figures 5.6 and 5.7 VLE plots for the MEG-water and the DEG-water systems are shown graphically with the Elliott rule.

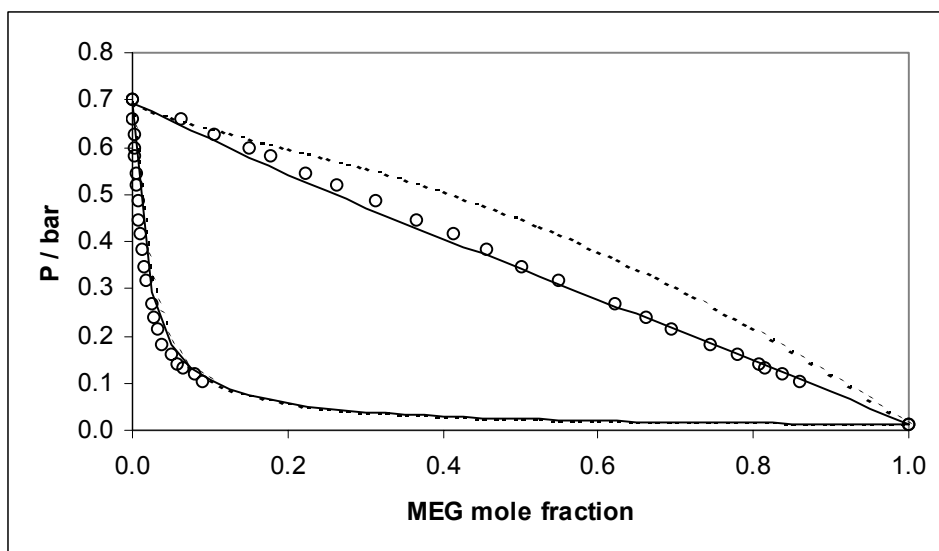


Figure 5.6 CPA-correlation and prediction of the MEG-water VLE at $T = 363.15$ K using the Elliott rule with a $k_{ij} = -0.115$ (solid line) and $k_{ij} = 0$ (dashed line).

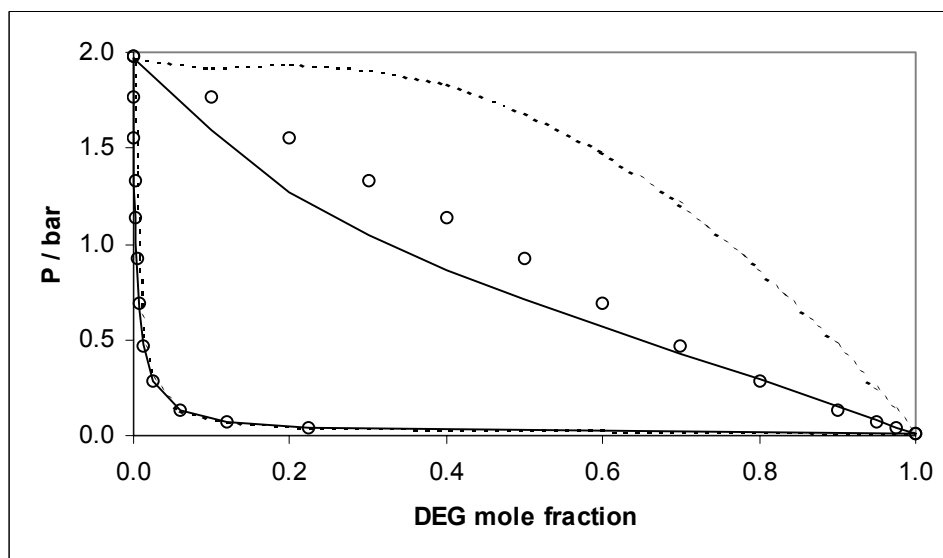


Figure 5.7 CPA-correlation and prediction of the DEG-water VLE at $T = 393.15$ K using the Elliott rule with a $k_{ij} = -0.361$ (solid line) and $k_{ij} = 0$ (dashed line).

Elliott's rule is clearly inferior to CR-1: worse correlation, especially for DEG-H₂O, very poor predictions, and high k_{ij} values are observed. The MC-SRK provides a very reasonable correlation for the data, but the prediction is very poor, especially for the heavier glycol (DEG).

3. For the TEG-water system: the CR-1 combining rule is again overall superior to all the other combining rules. However, the value of the binary interaction parameter is relatively high and the prediction performance poorer compared to the two other glycol-water systems. This may be due to the lower temperature used for the TEG-water system. Indeed at the higher temperature (332.6 K) the results are improved. The MC-SRK provides the best correlation result for this system, which may though be due to cancellation of errors since it fails for predictions. Figures 5.8 and 5.9 show these results graphically.

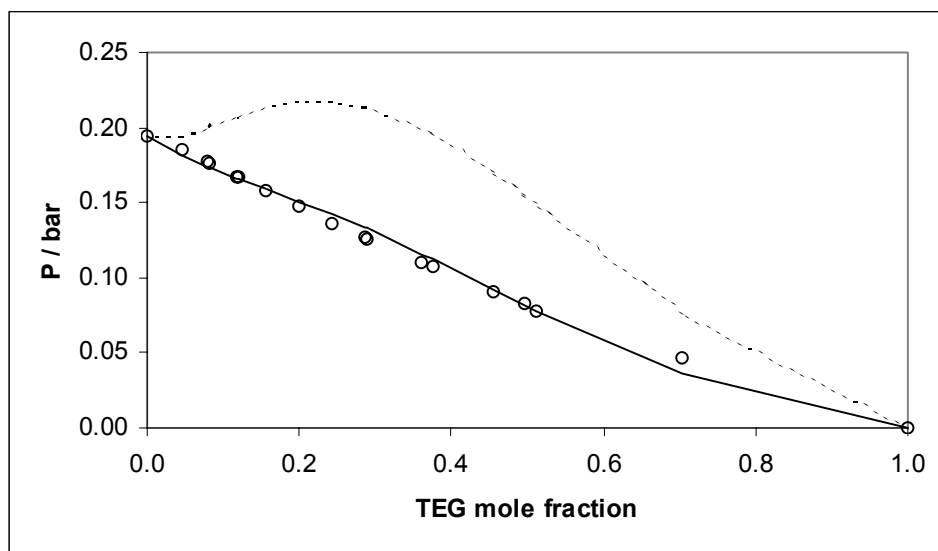


Figure 5.8 CPA-correlation and prediction of the P- x_{TEG} diagram for the TEG-water system at $T = 332.60$ K using the CR-1 combining rule with a $k_{ij} = -0.201$ (solid line) and $k_{ij} = 0$ (dashed line)..

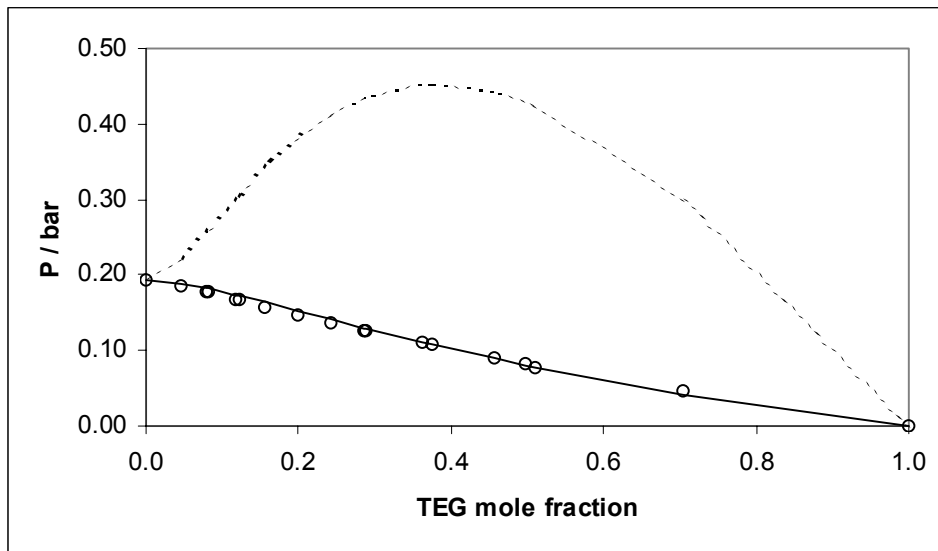


Figure 5.9 Correlation of the P - x_{TEG} diagram for the TEG-water system at $T = 332.60$ K using MC-SRK with a $k_{ij} = -0.231$ (solid line) and $k_{ij} = 0$ (dashed line).

In general, the performance of VLE is dependent on the combining rules used for the cross-association energy and volume parameters in the Wertheim expression. A single, per binary, interaction parameter has been used for the geometric mean of the energy a -parameter (Eq. 4.13) in the physical part. The best choice is the CR-1 combining rule, which includes the arithmetic mean for the ε -parameter and the geometric mean for the β -parameter.

The Elliott rule always requires higher k_{ij} values than CR-1 and the prediction is poor. The MC-SRK equation of state is extremely poor in prediction but the correlation capabilities are surprisingly good for most of the systems studied.

Overall, the results for the four cross-associating systems reveal that the combining rule for the cross-association volume parameter is the crucial one. The geometric mean (employed in CR-1 and CR-2) provides better results than the arithmetic mean for the cross-association volume.

5.4 Application of CPA to Multicomponent Associating Systems

The extension of any thermodynamic model (especially an association theory) to multicomponent mixtures is a rigorous test for its predictive capability and the various assumptions made (association scheme, combining rules for the cross-associating parameters, interaction parameters).

The CPA equation of state has been extended in this work to multicomponent multiphase equilibria, namely vapor-liquid-liquid equilibria (VLLE) of a test system: ethylene glycol (MEG), water, methylcyclohexane, and methane. The phase equilibria measurements were reported by GPA¹⁵ at 323.15 K and 70 bar in terms of mole fractions in the three phases. The components of this mixture are of great significance to the petrochemical industry where the partition coefficient of ethylene glycol and other production chemicals between an aqueous phase and a hydrocarbon phase are of vital importance for the design engineers.

The predictions with CPA are compared to the SRK equation of state with the Mathias-Copeman expression for the vapor pressure. For CPA, the CR-1 combining rule (Table 5.1), best choice for glycol-water systems, has been employed for the cross-associating system containing ethylene glycol and water. The interaction energy parameters k_{ij} for the various binary systems of the multi-component system have been calculated based on existing binary GLE, LLE, and VLE data at 323.15 K or a close temperature. The water-cyclohexane system was used to estimate the k_{ij} instead of the water-methylcyclohexane system since only one mutual solubility data point was available for the latter system. The binary interaction parameters for CPA and MC-SRK are listed in Table 5.6. Much lower k_{ij} values have been obtained with CPA for all the binary systems considered except for the methane-MEG system.

Table 5.6 Optimised binary interaction parameters with CPA and MC-SRK for the binaries of the system: ethylene glycol (MEG)/ water / methylcyclohexane (MCH) / methane

binary system	ref.	temperature range (K)	NP	type of equilibria	k_{ij} (CPA)	k_{ij} (MC-SRK)
methane-water	[16]	298.15	5	GLE	-0.045	-0.340
	[16]	313.15	5	GLE	-0.008	-0.301
	[16]	338.15	5	GLE	0.048	-0.233
		323.15			0.0088 ^a	-0.268
methane-MCH	[17]	313.15	8	GLE	0.0008	0.032
methane-MEG	[18]	323.15	7	GLE	0.124	0.049
cyclohexane-water	[19]	290.0-340.0	6	LLE	0.051	0.552
MEG-MCH	[20]	312.7-351.9	6	LLE	0.061	0.092
MEG-water	[10]	343.15	19	VLE	-0.028	-0.058
	[10]	363.15	23	VLE	-0.012	-0.054
		323.15			-0.044 ^a	-0.062

In Figures 5.10 and 5.11, the methane solubility in water and MEG is shown graphically using both the CPA and the MC-SRK models.

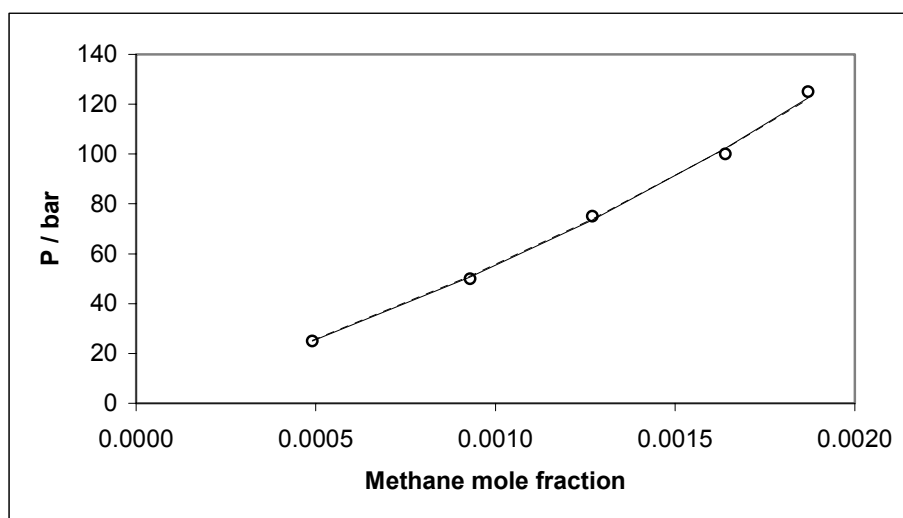


Figure 5.10 The solubility curve for the methane - water system at $T = 313.15$ K as function of pressure: o, experimental data points; solid line, CPA model with $k_{ij} = -0.008$; dashed line, MC-SRK model with $k_{ij} = -0.301$.

^a The k_{ij} at 323.15 K is obtained from a correlation based on the other temperatures

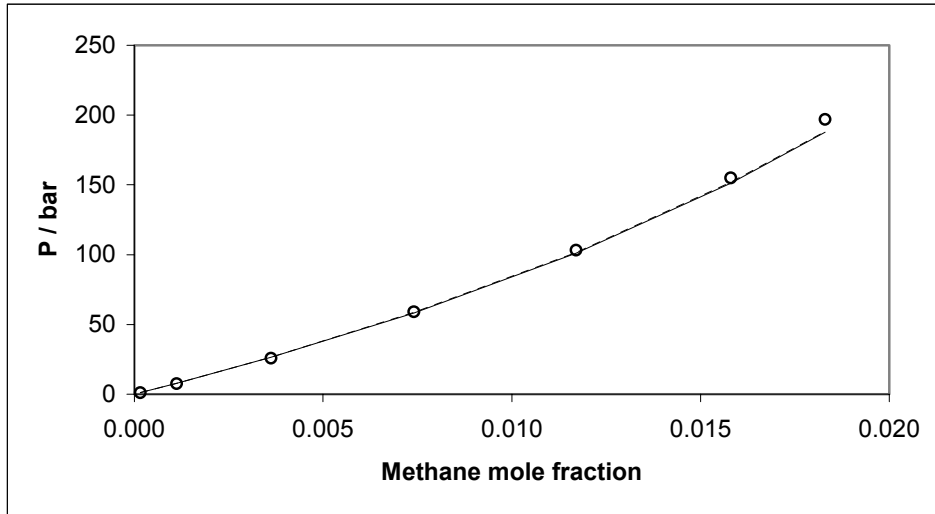


Figure 5.11 The solubility curve for the methane - MEG system at $T = 323.15$ K as function of pressure: o, experimental data points; solid line, CPA model with $k_{ij} = 0.124$; dashed line, MC-SRK model with $k_{ij} = 0.049$.

Very good correlations are obtained with both models. While the k_{ij} -value for the methane-water system is much lower for CPA, the opposite tendency is seen for the methane-MEG system. In Figure 5.12, it is seen that CPA is capable of correlating both solubility curves for the water-cyclohexane system very satisfactory with a small k_{ij} .

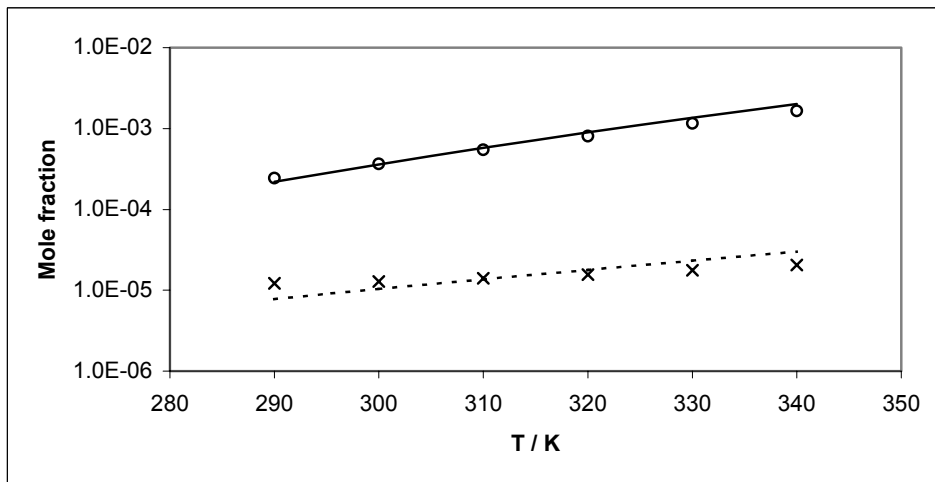


Figure 5.12 LLE for water (1) + cyclohexane (2) system with CPA with a $k_{ij} = 0.051$: \times , x_2^I , experimental; o, x_1^{II} , experimental; solid line, x_1^{II} , CPA; dashed line, x_2^I , CPA. I = Water-rich phase and II = Hydrocarbon-rich phase.

The MC-SRK fails to correlate both solubility curves at the same time. The MC-SRK can, however, fit satisfactorily one of the two solubility curves e.g. H₂O solubility in c-C6 which results in large underestimation of the other solubility by several orders of magnitude as can be seen in Figure 5.13.

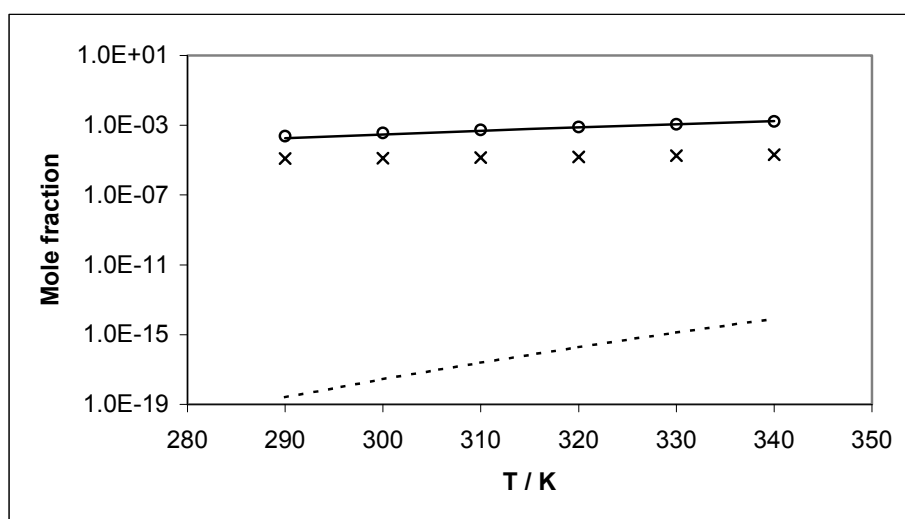


Figure 5.13 LLE for water (1) + cyclohexane (2) system with MC-SRK with a $k_{ij} = 0.552$: x, x_2^I , experimental; o, x_1^{II} , experimental; solid line, x_1^{II} , CPA; dashed line, x_2^I , CPA. I = Water-rich phase and II = Hydrocarbon-rich phase.

The phase equilibria calculations for the multicomponent system were carried with both CPA and MC-SRK with the optimised binary interaction parameters listed in Table 5.6 and with a k_{ij} value equal to zero for all the constituent binaries. No fine-tuning to the multicomponent system has been attempted and thus the calculations are pure predictions based solely on the binary interaction parameters.

In Figure 5.14, the partition coefficient of ethylene glycol between the aqueous and the organic phase is shown. It is observed, that the CPA model provides very satisfactory prediction of the partition coefficient of ethylene glycol even when all the binary interaction parameters are set to zero, while the MC-SRK underestimates the partition coefficient by two orders of magnitude.

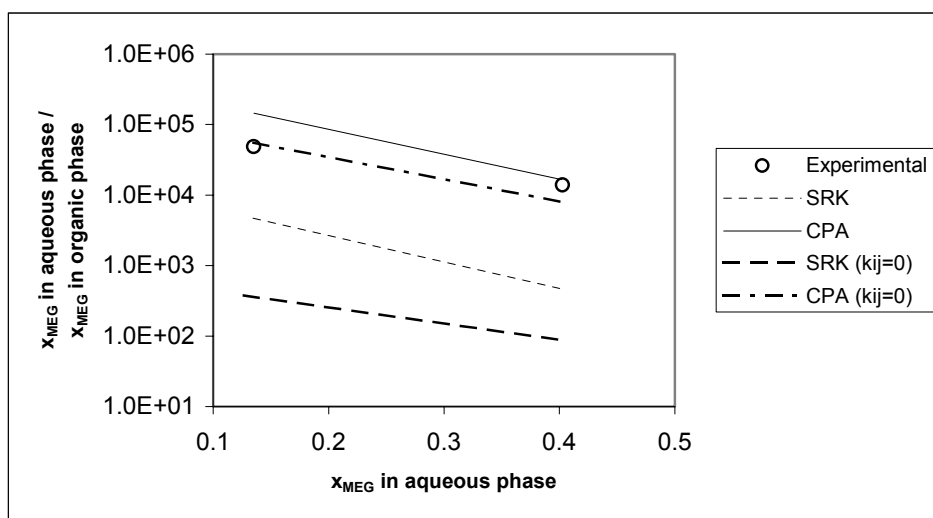


Figure 5.14 Prediction of the partition coefficient of MEG between the aqueous and the organic phase of the quaternary system ethylene glycol (MEG)/ water/ methane/ methylcyclohexane with the CPA and the MC-SRK models at 323.0 K and 70 bar.

Using all the optimised binary interaction parameters for MC-SRK improves the prediction by one order of magnitude. When k_{ij} 's are used, CPA predicts the partition coefficient at the higher concentration of ethylene glycol in the aqueous phase perfectly, but less satisfactory at the lowest ethylene glycol concentration.

5.5 Conclusions

The CPA equation of state has been extended in this work to binary methanol-water and glycol-water systems, where the species in the mixture are able to cross-associate (solvate) with each other. Combining rules for the cross-associating energy and volume parameters are required in the association term of the CPA model. Different sets of combining rules have been proposed and tested in terms of their prediction and correlation performance of isothermal VLE. It has been shown that the performance of the CPA equation of state in modeling VLE for cross-associating systems depends on the employed combining rule. It is found that the optimal combining rules are the geometric mean for the cross-associating energy parameter and the arithmetic mean for the cross-associating volume parameter (abbreviated as CR-1). The Elliott rule, which has been successfully applied previously in modeling alcohol-water VLE, requires in all cases a higher k_{ij} than the optimal combining rule for glycol-water systems. Moreover, the prediction performance is rather poor.

The Mathias-Copeman SRK model has also been tested for the glycol-water systems. This model performs very poorly in prediction i.e. $k_{ij} = 0$ but the correlation capabilities are very satisfactory for many of the systems studied.

The CPA model with its optimal combining rules provided very good results in predicting phase equilibria for a multi-component mixture based solely on binary interaction parameters. Particularly impressive are the results of the phase equilibria for the multi-component system with CPA using a zero binary interaction parameter for all the involved binaries. The MC-SRK underestimates the results using the optimized k_{ij} 's by one order of magnitude and by two orders of magnitude when $k_{ij}=0$. This verifies the importance of the use of the association term in CPA.

References

- (1) Derawi, S. O.; Michelsen, M. L.; Kontogeorgis, G. M.; Stenby, E. H. Application of the CPA equation of state to glycol/hydrocarbons liquid-liquid equilibria. (Accepted in Fluid Phase Equilibria)
- (2) Kontogeorgis, G. M.; Yakoumis, I. V.; Meijer H.; Hendriks, E. M.; Moorwood, T. Multicomponent phase equilibrium calculations for water–methanol–alkane mixtures. *Fluid Phase Equilibria*. **1999**, *158–160*, 201–209.
- (3) Huang, S. H.; Radosz, M. Equation of state for small, large, polydisperse, and associating molecules. *Ind. Eng. Chem. Res.* **1990**, *29*, 2284-2294.
- (4) Suresh, J.; Beckman, E. J. Prediction of liquid-liquid equilibria in ternary mixtures from binary data. *Fluid Phase Equilibria*. **1994**, *99*, 219–240.
- (5) Fu, Y.-H.; Sandler, S. I. A simplified SAFT equation of state for associating compounds and mixtures. *Ind. Eng. Chem. Res.* **1995**, *34*, 1897-1909.
- (6) Voutsas, E. C.; Yakoumis, I. V.; Tassios, D. P. Prediction of phase equilibria in water/alcohol/alkane systems. *Fluid Phase Equilibria*. **1999**, *158–160*, 151–163.
- (7) Suresh, S. J.; Elliott, J. R. Multiphase equilibrium analysis via a generalized equation of state. *Ind. Eng. Chem. Res.* **1992**, *31*, 2783-2794
- (8) Butler, J. A. V.; Thomson, D. W.; McLennan, W. H. *J. Chem. Soc.* **1933**, 674.
- (9) Kurihara, K.; Minoura, T.; Takeda, K.; Kojima, K. J. Isothermal vapor-liquid equilibria for methanol + ethanol + water, methanol + water, and ethanol + water. *J. Chem. Eng. Data*. **1995**, *40*, 679-684.
- (10) Chiavone-Filho, O.; Proust, P.; Rasmussen, P. Vapor-liquid equilibria for glycol ether + water systems. *J. Chem. Eng. Data*. **1993**, *38*, 128-131.
- (11) Klyucheva, E. S.; Yarym-Agaev, N. L. Experimental study of liquid-vapor equilibrium in the system diethylene glycol-water. *Zh. Prikl. Khim.* **1980**, *53(5)*, 794-796.

- (12) Herskowitz, M.; Gottlieb, M. Vapor-liquid equilibrium in aqueous solutions of various glycols and poly(ethylene glycols), 1. Triethylene glycol. *J. Chem. Eng. Data*. **1984**, *29*, 173-175.
- (13) Parrish, WM. R.; Won, K. W.; Baltatu, M. E. Phase behaviour of the triethylene glycol-water system and dehydration/regeneration design for extremely low dew point requirements. *Proceedings of the Sixty-Fifth Gas Processors Association Annual Convention*. **1986**, Mar. 10-12, 202-210.
- (14) *Simulation software & Database SPECS*, version 4.1; IVC-SEP, Department of Chemical Engineering, TU Denmark, DK-2800 Lyngby.
- (15) Chen, C. J.; Ng, H-J.; Robinson, D. B. The solubility of methanol or glycol in water-hydrocarbon systems. *Gas Processors Association (GPA) Research Report 117*. DB Robinson Research Ltd., Canada, **1988**.
- (16) Yarym-Agaev, N. L.; Sinyavskaya, R. P.; Koliushko, I. I.; Levinton, L. Ya. *Zh. Prikl. Khim. (Leningrad)*. **1985**, *58*, 165.
- (17) Richon, D.; Laugier, S.; Renon, H. High-pressure vapor-liquid equilibria for binary mixtures containing a light paraffin and an aromatic compound or a naphthene in the range 313-473 K. *J. Chem. Eng. Data*. **1991**, *36*, 104-111.
- (18) Jou, F-Y.; Otto, F. D.; Marther, A. E. Solubility of methane in glycols at elevated pressures. *The Canadian Journal of Chemical Engineering*. **1994**, *72*, 130-133.
- (19) Tsonopoulos, C.; Wilson, G. M. High-temperature mutual solubilities of hydrocarbons and water. *AIChE Journal*. **1983**, *29* (6), 990-999.
- (20) Derawi, S. O.; Kontogeorgis, G. M.; Stenby, E. H.; Haugum, T.; Fredheim, A. O. Liquid-liquid equilibria for glycols + hydrocarbons: Data and correlation. *J. Chem. Eng. Data*. **2002**, *47*, 169-173.

Chapter 6

Conclusions and Recommendations for Future Work

The primary target of this thesis was to review and develop thermodynamic models capable of describing accurately phase equilibria for multicomponent multiphase mixtures containing non-polar, polar and associating compounds.

In the first phase of this project, the partition coefficients of 115 mono-functional chemicals between an octanol and water phase have been critically evaluated by use of five UNIFAC models and the empirical AFC correlation model. This correlation model was shown to be superior to all UNIFAC models in all cases. However, the AFC correlation is limited to the octanol-water partition coefficients and cannot be employed to other partition coefficients e.g. oil/water of these chemicals, which is the primary aim of our study. Among the various more general group-contribution UNIFAC models, the *UNIFAC LLE* and the *WATER UNIFAC* are recommended to predict the partitioning of molecules between the water and octanol phase. This conclusion is also valid for the 22 multi-functional compounds investigated. Still problems are encountered for specific chemicals, which only partly could be attributed to the experimental data. Thus, we believe that the group-contribution concept has possibly exhausted its applicability to account for highly asymmetric systems, especially aqueous solutions with multi-functional chemicals.

In the second phase of this thesis, the Cubic-Plus-Association (CPA) equation of state has been applied to multiphase equilibria in mixtures containing glycols, hydrocarbons, and water. The CPA model reflects a new thermodynamic concept, which explicitly take into account for the association contribution.

Liquid-liquid equilibrium data for seven binary glycol + hydrocarbon systems were measured in the temperature range 32 °C to 80 °C using GLC (gas-liquid chromatography)

for the analysis. The measured data were successfully correlated with the temperature-dependent UNIQUAC and NRTL models. The temperature-independent UNIQUAC model was not as successful.

The CPA equation of state was successfully applied to the correlation of liquid–liquid equilibria for glycols + alkane systems with the four–site (4C) association model for the pure glycols. A single, temperature–independent binary interaction parameter was sufficient to provide a very satisfactory LLE correlation. Moreover, an excellent capability of CPA in the extrapolation of temperature has been shown based on this single binary interaction parameter.

It was necessary to consider the LLE data (though those were not directly used) in the optimization procedure in order to select the proper parameter set due to large uncertainty in the experimental pure–compound vapor pressure and liquid density data for glycols.

The comparison of CPA with the SRK model had shown that CPA performs much better than SRK in correlating LLE. This is attributed to the association term in CPA, which is based on Wertheim’s theory.

The CPA equation of state has also been extended to binary methanol–water and glycol–water systems, where the species in the mixture are able to cross-associate (solvate) with each other. Combining rules for the cross-associating energy and volume parameters are required in the association term of the CPA model. Different sets of combining rules have been proposed and tested in terms of their prediction and correlation performance of isothermal VLE. It has been shown that the performance of the CPA equation of state in modeling VLE for cross-associating systems depends on the employed combining rule. It is found that the optimal combining rules are the geometric mean for the cross-associating energy parameter and the arithmetic mean for the cross-associating volume parameter (abbreviated as CR-1). The Elliott rule, which has been successfully applied previously in modeling alcohol–water VLE, requires in all cases a higher k_{ij} than the optimal combining rule for glycol–water systems. Moreover, the prediction performance is rather poor.

The Mathias-Copeman SRK model has also been tested for the glycol-water systems. This model performs very poorly in prediction i.e. $k_{ij} = 0$ but the correlation capabilities are very satisfactory for many of the systems studied.

The CPA model with its optimal combining rules provided very good results in predicting phase equilibria for a multi-component mixture based solely on binary interaction parameters. Particularly impressive are the results of the phase equilibria for the multi-component system with CPA using a zero binary interaction parameter for all the involved binaries. The MC-SRK underestimates the results using the optimized k_{ij} 's by one order of magnitude and by two orders of magnitude when $k_{ij}=0$. This verifies the importance of the use of the association term in CPA.

The CPA equation of state is shown to be a very successful model for multiphase multicomponent mixtures containing glycols, hydrocarbons, and water. Further calculations for multicomponent systems need to be performed in the future. There is an industrial need to extend CPA further to other associating molecules such as ketones, amines, alkanolamines and organic acids. Further, CPA can also be developed for calculating the phase equilibria in mixtures containing electrolyte solutions. This needs an additional term such as Debye-Hückel to account for the ionic effects. Moreover, cubic equations of state have been successfully employed for polymer solutions. Thus, CPA could potentially be employed for such systems in the future, when hydrogen bonding solvents and polymers are present.

List of Symbols

a_{mn} (K), b_{mn} , c_{mn} (K ⁻¹)	UNIFAC group-interaction parameters between groups m and n
a_0	parameter in the energy term, bar dm ⁶ mol ⁻² (Eq. 4.8)
b	covolume parameter, dm ³ mol ⁻¹
c_1	parameter in the energy term, dimensionless (Eq. 4.8)
e_{ij} , k_{ij} , l_{ij}	binary interaction parameters
g	radial distribution function
q_i	molecule surface area parameter of component i
r_i	molecule volume parameter of component i
x_i	liquid mole fraction of component i
y_i	vapor mole fraction of component i
A_i	site A in molecule i
B_j	site B in molecule j
C_1 , C_2 , C_3	Mathias-Copeman constants for the SRK EoS
C_i^o	concentration of solute i in the octanol phase
C_i^w	concentration of solute i in the aqueous phase
H^E	excess Enthalpy
P	pressure
P_{ow}	octanol-water partition coefficient
Q_k	surface area parameter of subgroup k
R_k	volume parameter of subgroup k
R	gas constant, bar dm ³ mol ⁻¹ K ⁻¹
T	temperature
V_m	molar volume, dm ³ mol ⁻¹
X_{A_i}	mole fraction of the molecule i not bonded at site A
Z	compressibility factor
Z	coordination number

Greek Letters

α_{ij}	correction parameter in Eq. (5.2) by Suresh and Beckman
β	association volume parameter, dimensionless
γ_i	activity coefficient of component i in the liquid phase
ε	association energy parameter , bar dm ³ mol ⁻¹
η	reduced density
θ_i	UNIFAC surface area fraction of component i
ρ	molar density, mol dm ⁻³
ν_k^i	number of structural group k in molecule i
ω	acentric factor
Δ	association strength
Φ_i	UNIFAC segment fraction of component i
Ψ_{mn}	UNIFAC group-interaction parameters between group m and n

Superscripts/Subscripts

aq	aqueous
b	boiling (Table 4.8)
bub	bubble
c	critical
cal, model	calculated value
comb	combinatorial term
exp	experimental
o	octanol phase
r	reduced
res	residual term
w	water phase, weight
∞	infinite dilution

List of Abbreviations

AAD	Average Absolute Deviation
AFC	Atom & Fragment Contributions
ASOG	Analytical Solution of Group theory
c-C6	Cyclohexane
CH ₄	Methane
CPA	Cubic Plus Association equation of state
DEG	Diethylene Glycol
GC	Group Contribution
GLE	Gas-Liquid Equilibria
H ₂ O	Water
LLE	Liquid-Liquid Equilibria
LSER	Linear Solvation Energy Relationship
MCH	Methylcyclohexane
MC-SRK	Mathias-Copeman SRK
MEG	(Mono)ethylene Glycol
MOSCED	Modified Separation of Cohesive Energy Density
NP	Number of data points
OF	Objective function
PEG (300)	Polyethylene Glycol
PG	1,2-Propylene Glycol
SAFT	Statistical Associating Fluid Theory
SRK	Soave-Redlich-Kwong equation of state
TEG	Triethylene Glycol
Tetra-EG	Tetraethylene Glycol
TPT	Thermodynamic Perturbation Theory
UNIFAC	Universal Quasi Chemical Functional Group Activity Coefficient
VLE	Vapor-Liquid Equilibria

Appendices

Appendix A

Derivation of the Pressure and Chemical Potential from the Association Helmholtz Free Energy Based on Wertheim's Perturbation Theory

We consider a mixture of total composition n with total volume V at a temperature T . The association Helmholtz energy for the mixture can be expressed as

$$\frac{A^{assoc}}{RT} = \sum_i n_i \sum_{A_i} \left(\ln X_{A_i} - \frac{1}{2} X_{A_i} + \frac{1}{2} \right) \quad (\text{A.1})$$

The small letters i, j , and k are used to index the molecules, and the capital letters A and B are used to index the bonding sites on a given molecule. The fraction of non-bonded A-sites on molecule i , X_{A_i} , is calculated by solving the following nonlinear equations

$$X_{A_i} = \frac{1}{1 + (1/V) \sum_j n_j \sum_{B_j} X_{B_j} \Delta^{A_i B_j}} \Leftrightarrow \frac{1}{X_{A_i}} - 1 = \frac{1}{V} \sum_j n_j \sum_{B_j} X_{B_j} \Delta^{A_i B_j} \quad (\text{A.2})$$

The association strength between site A on molecule i and site B on molecule j , $\Delta^{A_i B_j}$, is expressed as

$$\Delta^{A_i B_j} = g \left[\exp \left(\frac{\epsilon^{A_i B_j}}{RT} \right) - 1 \right] b_{ij} \beta^{A_i B_j} = g(n, V) \lambda(T) \quad (\text{A.3})$$

where g is the radial distribution function.

The pressure contribution attributed to association can be calculated by the following expression

$$\frac{P^{assoc}}{RT} = -\frac{\partial}{\partial V} \left(\frac{A^{assoc}}{RT} \right) \quad (\text{A.4})$$

$$\frac{P^{assoc}}{RT} = -\sum_i n_i \sum_{A_i} \left(\frac{\partial \ln X_{A_i}}{\partial V} - \frac{1}{2} \frac{\partial X_{A_i}}{\partial V} \right) = -\sum_i n_i \sum_{A_i} \left(\frac{\partial \ln X_{A_i}}{\partial X_{A_i}} \frac{\partial X_{A_i}}{\partial V} - \frac{1}{2} \frac{\partial X_{A_i}}{\partial V} \right)$$

$$\frac{P^{assoc}}{RT} = -\sum_i n_i \sum_{A_i} \left(\frac{1}{X_{A_i}} - \frac{1}{2} \right) \frac{\partial X_{A_i}}{\partial V} \quad (\text{A.5})$$

and the association contribution to the chemical potential can be calculated by

$$\frac{\mu_i^{assoc}}{RT} = \frac{\partial}{\partial n_i} \left(\frac{A^{assoc}}{RT} \right) \quad (\text{A.6})$$

$$\frac{\mu_i^{assoc}}{RT} = \sum_{A_i} \left(\ln X_{A_i} - \frac{1}{2} X_{A_i} + \frac{1}{2} \right) + \sum_i n_i \sum_{A_i} \left(\frac{\partial \ln X_{A_i}}{\partial X_{A_i}} \frac{\partial X_{A_i}}{\partial n_i} - \frac{1}{2} \frac{\partial X_{A_i}}{\partial n_i} \right)$$

$$\frac{\mu_i^{assoc}}{RT} = \sum_{A_i} \left(\ln X_{A_i} - \frac{1}{2} X_{A_i} + \frac{1}{2} \right) + \sum_i n_i \sum_{A_i} \left(\frac{1}{X_{A_i}} - \frac{1}{2} \right) \frac{\partial X_{A_i}}{\partial n_i} \quad (\text{A.7})$$

In the calculation of the liquid and the vapor volumes, the Newton-Raphson iteration method needs the first and the second derivative of X_{A_i} with respect to the volume. As seen in Eq. (A.5), it is not a trivial task to calculate the first derivative of X_{A_i} with respect to the volume, and the calculation of the second derivatives will become tremendously complex. A much simpler approach was suggested by Michelsen and Hendriks¹. They introduced a function Q given by

$$Q(T, V, n, \mathbf{X}) = \sum_i n_i \sum_{A_i} (\ln X_{A_i} - X_{A_i} + 1) - \frac{1}{2V} \sum_i \sum_j n_i n_j \sum_{A_i} \sum_{B_j} X_{A_i} X_{B_j} \Delta^{A_i B_j} \quad (\text{A.8})$$

and showed that at a stationary point with respect to \mathbf{X} , Q equals the Helmholtz energy expression in Eq. (A.1)

The conditions that apply at a stationary point are

$$\frac{\partial Q}{\partial X_{A_i}} = 0, \text{ all sites}$$

By differentiating Eq. (A.8),

$$n_i \left(\frac{1}{X_{A_i}} - 1 \right) - \frac{1}{V} n_i \sum_j n_j \sum_{B_j} X_{B_j} \Delta^{A_i B_j} = 0$$

which yields

$$\frac{1}{X_{A_i}} = 1 + \frac{1}{V} \sum_j n_j \sum_{B_j} X_{B_j} \Delta^{A_i B_j}$$

i.e. Eq. (A.2) for \mathbf{X} . The value of Q at the stationary point (sp) is

$$\begin{aligned} Q_{sp} &= \sum_i n_i \sum_{A_i} (\ln X_{A_i} - X_{A_i} + 1) - \frac{1}{2} \sum_i n_i \sum_{A_i} X_{A_i} \left(\frac{1}{V} \sum_j n_j \sum_{B_j} X_{B_j} \Delta^{A_i B_j} \right) \\ &= \sum_i n_i \sum_{A_i} (\ln X_{A_i} - X_{A_i} + 1) - \frac{1}{2} \sum_i n_i \sum_{A_i} X_{A_i} \left(\frac{1}{X_{A_i}} - 1 \right) \\ &= \sum_i n_i \sum_{A_i} \left(\ln X_{A_i} - \frac{1}{2} X_{A_i} + \frac{1}{2} \right) = \frac{A^{assoc}}{RT} \end{aligned}$$

The pressure and the chemical potential can now be expressed by the Q-function as

$$\frac{P^{assoc}}{RT} = - \frac{\partial}{\partial V} \left(\frac{A^{assoc}}{RT} \right) = - \frac{\partial Q_{sp}}{\partial V} \quad (\text{A.9})$$

$$\frac{\mu_i^{assoc}}{RT} = \frac{\partial}{\partial n_i} \left(\frac{A^{assoc}}{RT} \right) = \frac{\partial Q_{sp}}{\partial n_i} \quad (\text{A.10})$$

The derivative of Q_{sp} with respect to the a variable, E, can be calculated using the chain rule

$$\frac{\partial Q_{sp}}{\partial E} = \frac{\partial Q}{\partial E} \Big|_X + \sum_i \sum_{A_i} \frac{\partial Q}{\partial X_{A_i}} \Big|_V \left(\frac{\partial X_{A_i}}{\partial E} \right)_{sp} = \left(\frac{\partial Q}{\partial E} \right)_X \quad (\text{A.11})$$

since the derivative of the Q-function with respect to \mathbf{X} is zero at the stationary point.

If E in Eq. (A.11) is the volume, the association contribution to the pressure is

$$\frac{P^{assoc}}{RT} = -\left. \frac{\partial Q}{\partial V} \right|_X = \frac{\partial}{\partial V} \left(\frac{1}{2V} \sum_i \sum_j n_i n_j \sum_{A_i} \sum_{B_j} X_{A_i} X_{B_j} \Delta^{A_i B_j} \right)_X \quad (\text{A.12})$$

and after differentiating Eq. (A.12) with respect to volume

$$\frac{P^{assoc}}{RT} = \frac{1}{2V} \left(-\frac{1}{V} \sum_i \sum_j n_i n_j \sum_{A_i} \sum_{B_j} X_{A_i} X_{B_j} \Delta^{A_i B_j} + \sum_i \sum_j n_i n_j \sum_{A_i} \sum_{B_j} X_{A_i} X_{B_j} \frac{\partial \Delta^{A_i B_j}}{\partial V} \right)$$

The first term, which is denoted r , can now be simplified using Eq. (A.2)

$$r = \sum_i n_i \sum_{A_i} X_{A_i} \frac{1}{V} \sum_j n_j \sum_{B_j} X_{B_j} \Delta^{A_i B_j} = \sum_i n_i \sum_{A_i} X_{A_i} \left(\frac{1}{X_{A_i}} - 1 \right) = \sum_i n_i \sum_{A_i} (1 - X_{A_i}) \quad (\text{A.13})$$

The derivative of $\Delta^{A_i B_j}$ with respect to V and n_i can be written as

$$\frac{\partial \Delta^{A_i B_j}}{\partial V} = \frac{\partial g}{\partial V} \lambda = \frac{\partial \ln g}{\partial V} g \lambda = \frac{\partial \ln g}{\partial V} \Delta^{A_i B_j} \quad (\text{A.14})$$

$$\frac{\partial \Delta^{A_i B_j}}{\partial n_i} = \frac{\partial g}{\partial n_i} \lambda = \frac{\partial \ln g}{\partial n_i} g \lambda = \frac{\partial \ln g}{\partial n_i} \Delta^{A_i B_j} \quad (\text{A.15})$$

and the equation for the pressure can finally be expressed as

$$\begin{aligned} \frac{P^{assoc}}{RT} &= \frac{1}{2V} \left(-r + \frac{\partial \ln g}{\partial V} \sum_i \sum_j n_i n_j \sum_{A_i} \sum_{B_j} X_{A_i} X_{B_j} \Delta^{A_i B_j} \right) \\ \frac{P^{assoc}}{RT} &= -\frac{1}{2V} \left(r - V r \frac{\partial \ln g}{\partial V} \right) = -\frac{1}{2V} \left(1 - V \frac{\partial \ln g}{\partial V} \right) \sum_i n_i \sum_{A_i} (1 - X_{A_i}) \end{aligned} \quad (\text{A.16})$$

As seen in Eq. (A.16), no derivative of X_{A_i} with respect to the volume is needed.

If E in Eq. (A.11) is the mole number, the association contribution to the chemical potential is

$$\frac{\mu_i^{assoc}}{RT} = \left. \frac{\partial Q}{\partial n_i} \right|_X = \frac{\partial}{\partial n_i} \left(\sum_k n_k \sum_{A_k} (\ln X_{A_k} - X_{A_k} + 1) - \frac{1}{2V} \sum_k \sum_j n_k n_j \sum_{A_k} \sum_{B_j} X_{A_k} X_{B_j} \Delta^{A_k B_j} \right)_X \quad (\text{A.17})$$

and after differentiating Eq. (A.17) with respect to mole number

$$\frac{\mu_i^{assoc}}{RT} = \sum_{A_k} (\ln X_{A_k} - X_{A_k} + 1) - \frac{1}{2V} \frac{\partial}{\partial n_i} \left(\sum_k \sum_j n_k n_j \sum_{A_k} \sum_{B_j} X_{A_k} X_{B_j} \Delta^{A_k B_j} \right)$$

⇔

$$\frac{\mu_i^{assoc}}{RT} = \sum_{A_k} (\ln X_{A_k} - X_{A_k} + 1) - \frac{1}{2V} \frac{\partial}{\partial n_i} \Big|_{\Delta} \left(\sum_k n_k \sum_j n_j \sum_{A_k} \sum_{B_j} X_{A_k} X_{B_j} \Delta^{A_k B_j} \right) - \frac{1}{2V} \sum_k \sum_j n_k n_j \sum_{A_k} \sum_{B_j} X_{A_k} X_{B_j} \frac{\partial \Delta^{A_k B_j}}{\partial n_i}$$

⇔

$$\frac{\mu_i^{assoc}}{RT} = \sum_{A_k} (\ln X_{A_k} - X_{A_k} + 1) - \frac{1}{2V} \left(\left(\sum_k n_k \sum_j \frac{\partial n_j}{\partial n_i} \delta_{ji} + \sum_k \frac{\partial n_k}{\partial n_i} \delta_{ki} \sum_j n_j \right) \sum_{A_k} \sum_{B_j} X_{A_k} X_{B_j} \Delta^{A_k B_j} \right) - \frac{1}{2V} \sum_k \sum_j n_k n_j \sum_{A_k} \sum_{B_j} X_{A_k} X_{B_j} \frac{\partial \Delta^{A_k B_j}}{\partial n_i}$$

⇔

$$\frac{\mu_i^{assoc}}{RT} = \sum_{A_k} (\ln X_{A_k} - X_{A_k} + 1) - \frac{2}{2V} \left(\sum_j n_j \sum_{A_k} X_{A_k} \sum_{B_j} X_{B_j} \Delta^{A_k B_j} \right) - \frac{1}{2V} \sum_k \sum_j n_k n_j \sum_{A_k} \sum_{B_j} X_{A_k} X_{B_j} \frac{\partial \Delta^{A_k B_j}}{\partial n_i}$$

By using Eq. (A.2) the above equation is simplified to

$$\frac{\mu_i^{assoc}}{RT} = \sum_{A_k} (\ln X_{A_k} - X_{A_k} + 1) - \left(\sum_{A_k} X_{A_k} \left(\frac{1}{X_{A_k}} - 1 \right) \right) - \frac{1}{2V} \sum_k \sum_j n_k n_j \sum_{A_k} \sum_{B_j} X_{A_k} X_{B_j} \frac{\partial \Delta^{A_k B_j}}{\partial n_i}$$

and after reduction of the first two terms

$$\frac{\mu_i^{assoc}}{RT} = \sum_{A_k} \ln X_{A_k} - \frac{1}{2V} \sum_k \sum_j n_k n_j \sum_{A_k} \sum_{B_j} X_{A_k} X_{B_j} \frac{\partial \Delta^{A_k B_j}}{\partial n_i}$$

By using Equations (A.13) and (A.15) we get

$$\frac{\mu_i^{assoc}}{RT} = \sum_{A_k} \ln X_{A_k} - \frac{1}{2V} \sum_k \sum_j n_k n_j \sum_{A_k} \sum_{B_j} X_{A_k} X_{B_j} \Delta^{A_k B_j} \frac{\partial \ln g}{\partial n_i}$$

$$\frac{\mu_i^{assoc}}{RT} = \sum_{A_k} \ln X_{A_k} - \frac{r}{2} \frac{\partial \ln g}{\partial n_i} \tag{A.18}$$

As seen in Eq. (A.18), no derivative of X_{A_i} with respect to the mole number is needed.

References

- (1) Michelsen, M. L.; Hendriks, E. M. Physical properties from association models. *Fluid Phase Equilibria*. **2001**, *180*, 165-174.

Appendix B

A Theoretical Justification for the CR-1 Combining Rule of CPA

The CR-1 combining rule can be expressed as follows:

$$\begin{aligned}\varepsilon^{A_i B_j} &= \frac{\varepsilon^{A_i B_i} + \varepsilon^{A_j B_j}}{2} \\ \beta^{A_i B_j} &= \sqrt{\beta^{A_i B_i} \beta^{A_j B_j}}\end{aligned}\tag{B.1}$$

According to Prausnitz et al.¹ the cross enthalpy and entropy of hydrogen bonding can be expected to follow:

$$\begin{aligned}\Delta H_{ij} &= \frac{\Delta H_{ii} + \Delta H_{jj}}{2} \\ \Delta S_{ij} &= \frac{\Delta S_{ii} + \Delta S_{jj}}{2}\end{aligned}\tag{B.2}$$

The equilibrium constant K in the chemical theory is related to the Gibbs energy, enthalpy and the entropy of hydrogen bonding as:

$$\ln K_{ij} = \left(\frac{-\Delta G_{ij}}{RT} \right) = -\frac{\Delta H_{ij}}{RT} + \frac{\Delta S_{ij}}{R}\tag{B.3}$$

Economou and Donohue² and Kontogeorgis et al.³ have established the relation between the equilibrium constant K in the chemical theory and the association strength(Δ) in the perturbation theory as:

Assumption 1: $\frac{d\Delta}{d\rho} = 0$ in the perturbation theory.

$$K_{ij} RT \propto \Delta_{ij}$$

$$\exp\left(-\frac{\Delta H_{ij}}{RT}\right) \exp\left(\frac{\Delta S_{ij}}{R}\right) RT \propto g \left[\exp\left(\frac{\varepsilon^{A_i B_j}}{RT}\right) - 1 \right] b_{ij} \beta^{A_i B_j}\tag{B.4}$$

Assumption 2: $\exp\left(\frac{\varepsilon^{A_i B_j}}{RT}\right) - 1 \approx \exp\left(\frac{\varepsilon^{A_i B_j}}{RT}\right)$. This is a very reasonable assumption

For instance: $\frac{\varepsilon(\text{MEG})}{RT} = \frac{19752 \text{ J/mol}}{8.314 \text{ J/(molK)} * 300 \text{ K}} = 7.9$

$$\exp(7.9) \approx 2750$$

Thus:

$$\exp\left(-\frac{\Delta H_{ij}}{RT}\right) \propto \exp\left(\frac{\varepsilon^{A_i B_j}}{RT}\right) \quad (\text{B.5})$$

This suggests an arithmetic mean combining rule for the cross-association energy parameter in agreement to Eq. (B.2). If we assume the proportionality of the dimensionless parameters related to association volume in Eq. (B.4), we obtain the following:

$$\begin{aligned} \beta^{A_i B_j} &\propto \exp\left(\frac{\Delta S_{ij}}{R}\right) \\ R \ln \beta^{A_i B_j} &= \Delta S_{ij} = \frac{\Delta S_{ii} + \Delta S_{jj}}{2} \\ R \ln \beta^{A_i B_j} &= \frac{1}{2} R (\ln \beta^{A_i B_i} + \ln \beta^{A_j B_j}) \\ \beta^{A_i B_j} &= \sqrt{\beta^{A_i B_i} \beta^{A_j B_j}} \end{aligned} \quad (\text{B.6})$$

Equation (B.6) is the geometric mean rule for the associating volume parameter employed in CR-1.

References

- (1) Prausnitz, J. M.; Lichtenthaler, R. N.; Gomes de Azevedo, E. *Molecular thermodynamics of fluid phase equilibria*; Prentice-Hall: New Jersey, 1999.
- (2) Economou, I. G.; Donohue, M. D. Chemical, quasi-chemical and perturbation theories for associating fluids. *AIChE Journal*. **1991**, *37* (12), 1875-1894.
- (3) Kontogeorgis, G. M.; Voutsas, E. C.; Yakoumis, I. V.; Tassios, D. P. An equation of state for associating fluids. *Ind. Eng. Chem. Res.* **1996**, *35*, 4310–4318.